Neutrophil serine proteases as triggers of inflammation and as targets of autoimmunity

Dissertation zur Erlangung des
Doktorgrades der Naturwissenschaften (Dr. rer. nat.)
der Fakultät für Biologie
der Ludwig-Maximilians-Universität München

Vorgelegt von
Kai Alexander Ulrich Kessenbrock
aus
Bad Neuenahr-Ahrweiler

München 2008

Eingereicht am: 9.9.2008.....

Mitglieder der Promotionskommission:

Erstgutachter: Prof. Dr. Elisabeth Weiß

Zweitgutachter: Prof. Dr. Harry MacWilliams

Prof. Dr. Michael Schleicher

Priv. Doz. Dr. Berit Jungnickel

Tag des Promotionskolloquiums: 07.01.2009 .....

Doktorurkunde ausgehändigt am:.....

Die Versuche zur vorgelegten Dissertation wurden in der Zeit vom Februar 2004 bis August 2008 in der Arbeitsgruppe von PD Dr. med. habil. Dieter Jenne, Abteilung für Neuroimmunologie am Max-Planck-Institut für Neurobiologie in Martinsried bei München durchgeführt.

Hiermit erkläre ich, daß ich diese Arbeit selbständig und nur unter Verwendung der angegebenen Quellen und Hilfsmittel angefertigt habe.

Martinsried, den 5. September 2008

Acknowledgements

First of all, I would like to thank my supervisor PD Dr. Dieter Jenne for his continual guidance, but also for the stimulating, scientific discussions that certainly formed the basis for our research. I am especially thankful that Dieter supported me to develop my own ideas and therefore aided me to become an independent scientist. I am also very grateful to Prof. Dr. Hartmut Wekerle for making this thesis, here at the Max Planck Institute of Neurobiology, possible and for his constant interest and support.

I am thankful to Prof. Dr. Elisabeth Weiß for her interest in the progress of my research project and for being my principal supervisor at the biological faculty of the Ludwig Maximilian University in Munich. I also kindly acknowledge the members of my thesis examination board, namely Prof. Dr. Harry MacWilliams, Prof. Dr. Heinrich Leonhardt, PD Dr. Berit Jungnickel, Prof. Dr. Hugo Scheer and Prof. Dr. Michael Schleicher.

I would also like to thank the members of my internal thesis committee, Prof. Dr. Edgar Meinl and Dr. Michael Sixt, for their helpful discussions and guidance of my research projects.

Further, I would like to acknowledge the Sonderforschungsbereich 571 (Autoimmune reactions: from manifestations and mechanisms to therapy) from the Deutsche Forschungsgemeinschaft for their financial support of my Ph.D. thesis. I thank the Böhringer Ingelheim Fonds for granting me travel allowances to visit Prof. Dr. Zena Werb´s laboratory at the University of California, San Francisco in November 2007. Along with this, I am especially grateful to Prof. Zena Werb for hosting me so nicely in San Francisco, but also for her advice and intellectual support of my Ph.D. research project.

I am very thankful to my colleagues and co-authors from our neighbor Max Planck Institute for Biochemistry: I very much enjoyed working and discussing with Julia Riedl and Dr. Roland Wedlich-Söldner from the Cellular Dynamics and Cell Patterning group. I am particularly thankful to Tim Lämmermann and Dr. Michael Sixt from the department of Molecular Medicine not only for their excellent scientific contributions to my work, but also for being good friends. Moreover, I am thankful to Prof. Dr. Markus Ollert and Bettina Maar from the GSF Neuherberg.

I have benefited greatly from the pleasant working environment and I thank each member of the Jenne group. Elisabeth Stegmann, Angelika Kuhl, Heike Reimann, Natascha Pereira, Brice Korkmaz, Florian Kurschus and Edward Fellows, it has been a pleasure working and laughing together with you and I am thankful for that. In particular, I am deeply grateful to Edward Fellows (alias “Eduardo Fellone”) for his invaluable friendship and for the unforgettable time in Munich. I am also thankful to the former mentor of my diploma thesis, Dr. Michael Mahler, for his constant support over all the past years.

I would like to dedicate this work to my loving family, especially to my mother Gisela and my father Ulrich, who have always supported me with their love, help and input into my education.

Finally, I dearly thank my girlfriend Daniela for her love throughout the years of my study and of this thesis

TABLE OF CONTENT

1 Summary

Neutrophil granulocytes form the body's first line of antibacterial defense, but also contribute to tissue injury and non-infectious, chronic inflammation. Proteinase 3 (PR3) and neutrophil elastase (NE) are two abundant neutrophil serine proteases (NSPs) with overlapping and potentially redundant substrate specificity, which are mainly implicated in anti-microbial defense. In the first part of my Ph. D. thesis, I unravelled a novel, cooperative role of PR3 and NE in neutrophil activation and non-infectious inflammation *in vivo*. PR3/NE double-deficient mice demonstrated strongly diminished immune complex (IC)-mediated neutrophil infiltration *in vivo* as well as reduced activation of isolated neutrophils by ICs *in vitro*. In contrast, neutrophil recruitment to ICs was only marginally impaired in NE single-deficient mice. The defects in PR3/NE-lacking mice were found to be directly linked to the accumulation of anti-inflammatory progranulin (PGRN). I found that both PR3 and NE cleaved PGRN during neutrophil activation *in vitro* and inflammation *in vivo*. Local administration of recombinant PGRN potently inhibited neutrophilic inflammation *in vivo* showing that PGRN represents a crucial inflammation-suppressing mediator. Taken together, I concluded that PR3 and NE enhance neutrophil-dependent inflammation by eliminating the local anti-inflammatory activity of PGRN. These data support the use of serine protease inhibitors as anti-inflammatory agents.

In the second part of this work, I examined whether a recently discovered alternative form of neutrophil cell death, namely NETosis, may play a role in autoimmune small-vessel vasculitis (SVV). SVV is a chronic auto-inflammatory condition strongly associated with circulating antineutrophil cytoplasmic autoantibodies (ANCA) directed against the neutrophil granulocyte components proteinase 3 (PR3) or myeloperoxidase (MPO). These ANCAs were previously shown to exert a pathogenic effect by binding to PR3 and MPO on the neutrophil cell surface and thus activate the cells to perform an oxidative burst, *i.e.* the production of reactive oxygen species (ROS). Here, I found that ANCA-mediated activation leads to an alternative cell death program in neutrophils called NETosis, which was previously found to be distinct from apoptosis and necrosis. NETosis involves the active and substantial release of

nuclear DNA to form neutrophil extracellular traps (NETs), which are chromatin fibers decorated with a number of granular proteins. I found that these chromatin fibers display large amounts of the targeted autoantigens PR3 and MPO, indicating that NETosis might be a pathogenic source of autoantigens to nourish the chronic autoimmune response against PR3 and MPO. In support of this view, I found prominent deposition of NETs displaying the autoantigens in the glomeruli of inflamed kidneys of SVV patients. Furthermore, I established a capture ELISA assay, with which I detected circulating complexes consisting of nucleosomes and neutrophil granular components, namely MPO, which are most likely derived from NETs. These chromatin-autoantigen complexes were especially abundant in SVV patients with active disease, while absent in sera from healthy control individuals and multiple sclerosis patients. These findings suggest that NET formation plays an essential pathogenic role in the perpetuation of the humoral autoimmune response in SVV.

2 Introduction

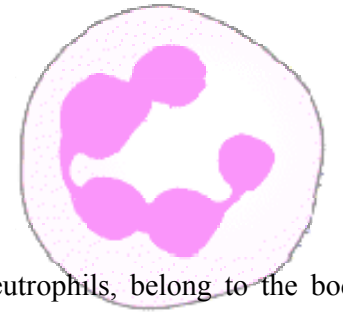

2.1 Neutrophil granulocytes

Neutrophil granulocytes, generally referred to as neutrophils, belong to the body's first line of cellular defense and respond quickly to tissue injury and invading microorganisms (Nathan, 2006). They were discovered by Ilya Metchnikoff, who inserted rose thorns into starfish larvae and then described the infiltrating phagocytic cells as macrophages and microphagocytes. The latter cell type was then called neutrophil granulocyte by Paul Ehrlich, who had already encompassed the functional significance of neutrophils in the inflammatory process. Exactly one hundred years ago, in 1908, the Nobel Prize in Medicine was awarded jointly to Metchnikoff and Ehrlich for their work that, as many scientists claim today, founded the basis for modern immunology (Kaufmann, 2008).

The name "neutrophil granulocyte" derives from their characteristic staining pattern in hematoxylin and eosin (H&E)-stained blood smears, where neutrophils are easily identified by their light pink staining of cytoplasmic compartments. As myeloid cells, neutrophils mature in the bone marrow and differentiate from myeloblasts through pro-myeloblasts to neutrophilic myelocytes. Fully differentiated neutrophils are characterized by their lobulated nucleus, hence they are also called polymorphonuclear cells (PMNs). Neutrophil granulocytes are constantly generated in the bone marrow and released into the blood stream, where they make up about 40-70% of all peripheral blood leukocytes and patrol the body to sense infection or tissue injury.

2.1.1 Neutrophils in inflammation

The function of the immune system is to protect the host from infiltration and damage by foreign genomes (Nathan, 2002). The ability to kill invading organisms is essential to this function. Since neutrophils constitute one of the major players for the

destruction of microorganisms, it is no surprise that the activation of neutrophils can also damage the host´s own cells and tissues (Weiss, 1989). In fact, neutrophil-mediated tissue damage at sites of infection constitutes a main mediator of inflammation and is important to initiate the immune reaction of the host (Nathan, 2006).

Once wounding or infection occurs in the peripheral tissue, neutrophils are rapidly recruited to the site of inflammation (**Figure 2.1**). Their emigration out of the blood stream follows a multi-step paradigm involving attachment and rolling along the endothelium, activation, adhesion and ultimately transendothelial extravasation into the interstitium (Springer, 1994). The average half-life of neutrophil granulocytes in the peripheral blood is only about 12 hours. But once they have left the bloodstream and extravasated into the interstitium, neutrophils can survive for up to two days by integrin-dependent activation (Mayadas and Cullere, 2005).

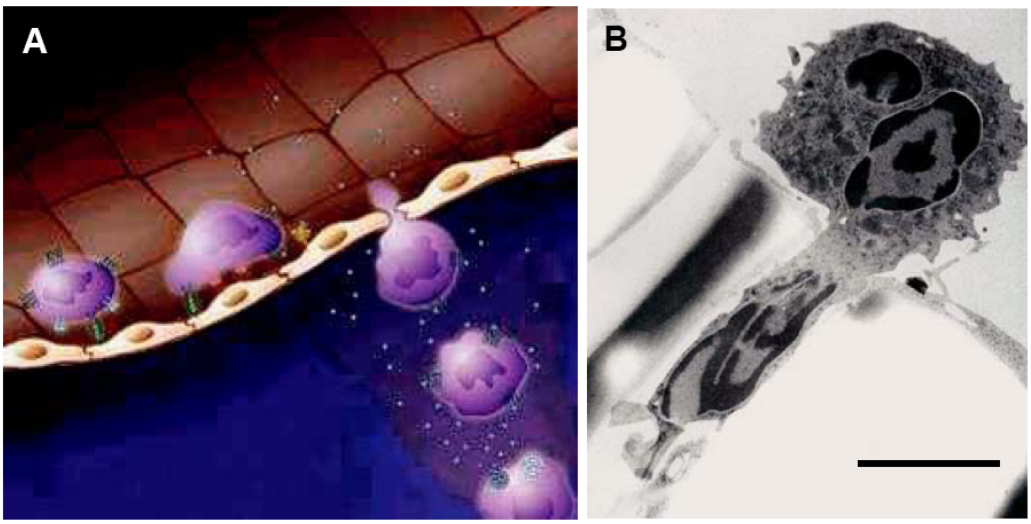

Figure 2.1 – Neutrophil extravasation. (A) The emigration of neutrophils from the blood stream to inflamed or infected peripheral tissue is guided by chemokines produced at the danger site and follows a multi-step paradigm of rolling, adhesion and transmigration. (**B**) Once stable adhesion is achieved, the neutrophil granulocyte transmigrates across the dense cellular layer of the endothelium. Electronmicroscopical picture of neutrophil transmigrating across the endothelium. Scale bar respresents 5 µm.

The key function of neutrophils is certainly antimicrobial defense, which is mainly fulfilled by the engulfment of invading pathogens into phagolysosomes, and their degradation thereafter by reactive oxygen species (ROS) and by anti-microbial proteases prestored in cytoplasmic granules (Segal, 2005). In these so-called primary or azurophilic granules of neutrophils another important anti-bacterial enzyme is stored, namely myeloperoxidase (MPO), a di-haem protein composed of two identical heterodimers, which can kill bacteria by halogenation (Klebanoff, 2005). The destruction of microbes, is also essential for the wound healing process, since neutrophils swiftly sterilize the injured tissue from pathogens and therefore allow the efficient regeneration of the wound (Singer and Clark, 1999).

However, neutrophils can also contribute to chronic inflammation in a variety of human diseases such as autoimmune disorders or hypersensitivity reactions. In many of these conditions, the underlying pathogenic mechanism is the formation of antigen-antibody complexes, or so called immune complexes (ICs), which trigger an inflammatory response by inducing the infiltration of neutrophils as depicted in **Figure 2.2** (Jancar and Sanchez, 2005). The subsequent stimulation of neutrophils by C3bi-opsonized ICs results in the generation ROS and the release of intracellularly stored proteases leading to tissue damage and inflammation (Ravetch, 1994).

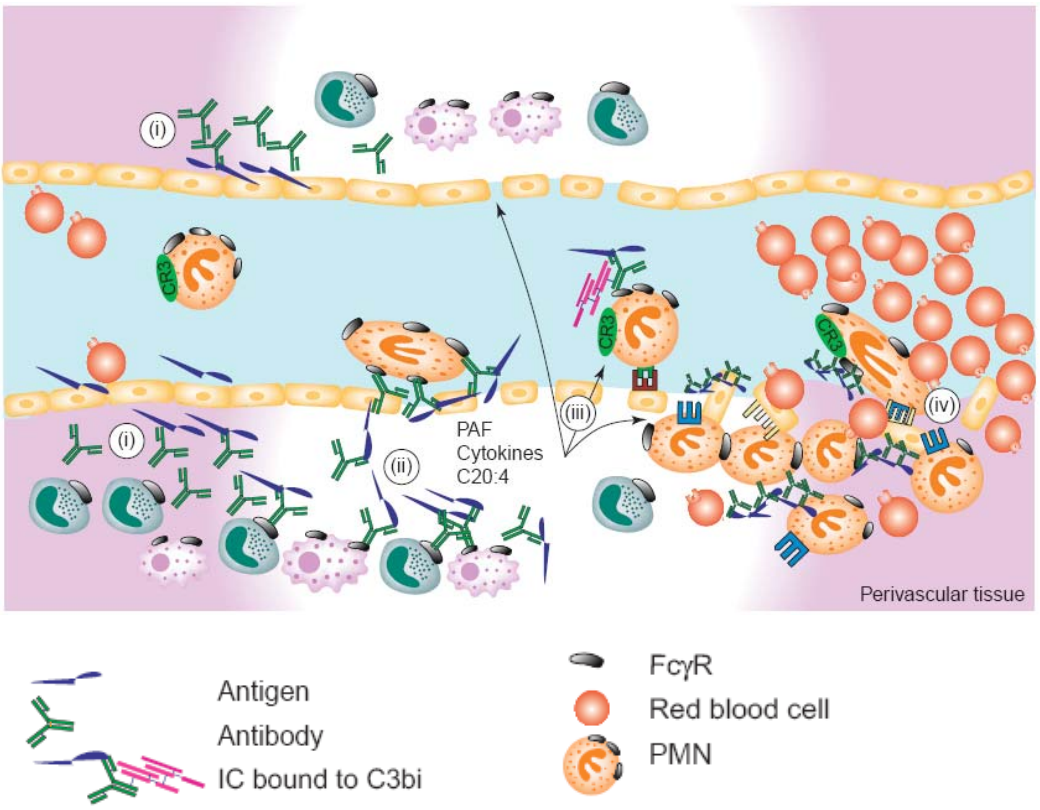

Figure 2.2 – Immune complex mediated inflammation. The formation of antigen-antibody structures (**i**), so called immune complexes (ICs), initiates a complex inflammatory reaction involving Fcγ and Mac-1 receptor-mediated recognition of ICs by mast cells and neutrophils (**ii**), which leads to substantial release of inflammatory cyto- and chemokines (*e.g.* platelet activating factor, PAF) and recruitment of neutrophils into the perivascular tissue (**iii**), where the cells release a number of inflammatory mediators such as ROS and cytokines to fully establish an inflammatory milieu including edema formation and hemorrhage, *i.e.* red blood cell release into the interstitium (**iv**).

Source: (Jancar and Sanchez, 2005)

The classic view of neutrophils as "nonspecific" killing machines has started to change in the recent years. Rather, the neutrophil granulocyte is increasingly seen as a "decision shaper" that specifically initiates and coordinates the immune response of the host (Nathan, 2006). Indeed, neutrophils can influence the function of a variety of cell types including monocytes, dendritic cells as well as T and B cells in a bidirectional manner and release cytokines and other modulators of the immune

reaction. Hence, neutrophils help the organism to decide whether to initiate and maintain an immune response.

2.1.2 Neutrophil serine proteases (NSPs)

Serine proteases are a class of proteases that have a serine residue in the active site of the enzyme. The enzymatic mechanism of serine proteases is based on the *catalytic triad* consisting of three amino acids in the active center, in which the hydroxyl group of the serine starts the reaction cascade by exerting a nucleophilic attack on the carbonyl carbon of the scissile peptide bond. This finally leads to the cleavage of the substrate polypeptide chain. The specificity of the proteases mainly depends on the amino acid residues neighboring the active center, since these residues govern the recognition and proper alignment of the substrate prior to the hydrolysis of the peptide bond.

Neutrophils abundantly express a cell-type specific set of neutrophil serine proteases (NSPs), namely cathepsin G (CG), proteinase 3 (PR3) and neutrophil elastase (NE), which are stored in the cytoplasmic, azurophilic granules. PR3 and NE are two closely related enzymes with overlapping and potentially redundant substrate specificities, which are different from that of CG. All three NSPs are implicated in anti-microbial defense by degrading engulfed microorganisms inside the phagolysosomes of neutrophils (Belaaouaj et al., 1998; Belaaouaj et al., 2000; Reeves et al., 2002; Segal, 2005; Weinrauch et al., 2002). Among many other functions ascribed to these enzymes, PR3 and NE were also suggested to play a fundamental role in granulocyte development in the bone marrow (El Ouriaghli et al., 2003; Skold et al., 1999; Bories et al., 1989).

2.1.2.1 NSPs as triggers of inflammation

While the vast majority of the enzymes is stored intracellularly in cytoplasmic granules, minor quantities of PR3 and NE are externalized early during neutrophil activation and remain bound to the cell surface, where they seem to be protected against protease inhibitors (Campbell et al., 2000; Owen et al., 1995). These membrane presented proteases were suggested to act as “path clearers” for neutrophil

migration by degrading components of the endothelial basement membrane (EBM) or the extracellular matrix to open the way for cell movement through the interstitium during inflammation (Shapiro, 2002). This notion has been addressed in a number of studies, which have, however, yielded conflicting results (Carden and Korthuis, 1996; Hirche et al., 2004; Young et al., 2004). Thus, the role of PR3 and NE in leukocyte extravasation and interstitial migration still remains controversial.

Emerging data suggest that externalized NSPs can contribute to the inflammatory response in a more complex way than by simple proteolytic tissue degradation, namely as specific regulators of inflammation (Pham, 2006). For instance, recent observations using CG/NE double-deficient mice indicated that CG directly regulated the receptor-mediated interaction of neutrophils with ICs (Adkison et al., 2002; Raptis et al., 2005). Neutrophils recognize ICs via Fcγ receptors (FcγR) binding to the Fc part of the antibody and integrin CD11b/CD18 (Mac-1) interacting with C3bi (**Figure 2.3**). This leads to neutrophil activation and integrin clustering on the outer membrane as well as ROS production and rearrangement of the actin cytoskeleton inside the cell (Yamada and Miyamoto, 1995). More recently, Raptis et al. have now shown that CG enhanced IC-mediated neutrophil activation and inflammation by modulating integrin clustering on the neutrophil cell surface (Raptis et al., 2005). Yet, the substrate(s) cleaved by CG in this reaction could not be identified.

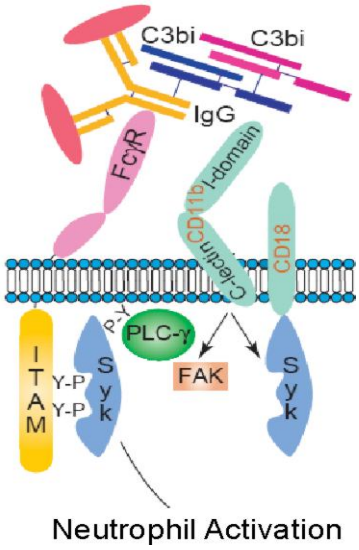

Figure 2.3 – Receptor-mediated recognition of ICs. ICs consist of antigens bound by IgG antibodies and C3bi opsonization. Neutrophils recognize ICs via surface receptors FcγR (binding to IgG antibody) and integrin CD11b/CD18 (binding to C3bi). This initiates a complex outside-in signaling cascade, which involves intracellular signaling via immunoreceptor tyrosine-based activation motif (ITAM), focal adhesion kinase (FAK), spleen tyrosine kinase (Syk) leading to neutrophil activation involving integrin clustering on the cell surface and cytoskeletal rearrangement and ROS production intracellularly.

Source: (Jancar and Sanchez, 2005)

The role of the other two NSPs in IC-mediated inflammation has not yet been addressed. Since PR3-deficient mice have not been analyzed in this context, the role of PR3 in inflammatory processes remains to be deciphered. Also, important NE-dependent effects, which can be compensated by the highly similar enzyme PR3 in NE single-deficient animals, are still elusive. Based on *in vitro* studies many potential substrates have been suggested for NSPs (Pham, 2006) but, until now, the relevance of these candidates could not be clarified *in vivo*.

2.1.2.1.1 Progranulin - an important substrate for NSPs?

A mechanism by which NSPs could up-regulate the inflammatory response has recently been suggested. The ubiquitously expressed progranulin (PGRN) is a growth factor implicated in tissue regeneration, tumorigenesis and inflammation (He et al., 2003; He and Bateman, 2003; Zhu et al., 2002). PGRN was shown to directly inhibit adhesion-dependent neutrophil activation by suppressing the production of ROS and the release of neutrophil proteases *in vitro* (Zhu et al., 2002). This anti-inflammatory activity was degraded by the NE-mediated proteolysis of PGRN to granulin (GRN) peptides (Zhu et al., 2002). Conversely, the resulting GRN fragments are thought to enhance inflammation (Zhu et al., 2002) and have been detected in neutrophil-rich peritoneal exudates (Bateman et al., 1990). In short, recent studies proposed PGRN as a regulator of the innate immune response, but the factors that control PGRN function are still poorly defined and its relevance to inflammation needs to be elucidated *in vivo*.

2.1.2.2 NSPs as targets in autoimmunity

The function of the immune system is to fight infections using multiple mechanisms that evolved to recognize and neutralize pathogens. Therefore, the immune system needs to detect a variety of different structures and – at the same time – differentiate between *self* and *non-self*. Autoimmunity occurs when the organism fails to recognize its *self* constituents and thus raises an immune response against its own cells and tissues.

Surprisingly, all three NSPs present in azurophilic granules have been reported as targets of autoantibodies in certain pathological situations. While the occurrence of

autoantibodies against NE and CG appears to be a concomitant phenomenon of diseases such as cocaine-induced midline lesions (Wiesner et al., 2004) and ulcerative colitis (Halbwachs-Mecarelli, 1994), respectively, the development of anti-PR3 autoantibodies represents a characteristic feature for a systemic, autoimmune vasculitis called Wegener´s granulomatosis (Jenne et al., 1990). Interestingly, myeloperoxidase, which is stored together with the NSPs in the azurophilic granula, is the principal autoantigen of a related autotimmune vasculitis called microscopic polyangiitis.

2.1.2.2.1 Small-vessel vasculitis

Wegeners´ granulomatosis (WG) and microscopic polyangiitis (MPA) are systemic autoimmune conditions leading to strong inflammation of small blood vessels, hence they are termed small-vessel vasculitides or shortly SVV (Kallenberg et al., 2006). Both WG and MPA are strictly associated with the development of anti-neutrophil cytoplasm autoantibodies (ANCAs), which are directed against abundant intracellular proteins in the cytoplasmic, azurophilic granules of neutrophils. As already mentioned above, ANCAs against PR3 represent a hallmark for WG, while MPA is directly associated with the occurrence of anti-MPO ANCAs (Bosch et al., 2006; Kallenberg et al., 2006).

Wegener´s disease typically starts with disease symptoms in the upper airway, such as the nose and lungs. In later the stages of the disease, the symptoms become more systemic with affection of the kidneys (glomerulonephritis) as well as the skin and the nervous system. Glomerulonephritis is a common feature of both WG and MPA. In severe cases, the patients develop rapidly progressing, necrotizing glomerulonephritis that may lead to death due to renal failure (**Figure 2.4**).

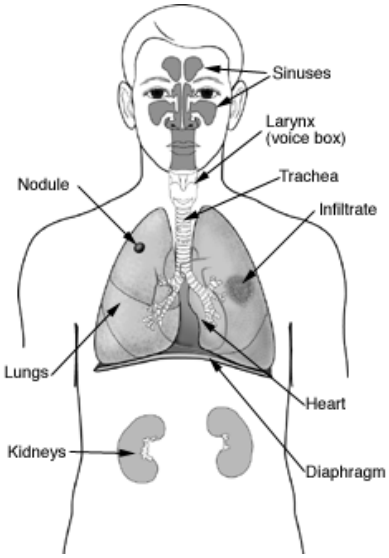

Figure 2.4 – Affected organs in small-vessel vasculitides. WG is a systemic autoimmune disease that mostly starts with chronic inflammation with perivascular infiltrates in the small and medium-sized blood vessels in the upper respiratory tract (Sinuses, Larynx and trachea). Advanced stages of the disease are characterized by increased involvement of the lungs. The cellular infiltrates can form large clusters, also called nodules, for instance in the lungs. At later stages, the patients suffer from multiple and systemic symptoms such as strong affection of the kidneys (glomerulonephritis), but also the heart and the skin can be affected.

Source: www.clevelandclinics.org

Recent findings indicate that ANCAs are not only a useful serological marker for the diagnosis of small-vessel vasculitides, but are also main players in the pathogenesis of these diseases. For instance, recently established animal models of the diseases support a pathogenic effect of these autoantibodies (Pfister et al., 2004; Xiao et al., 2002). The pathogenicity of ANCAs was linked with their potential to activate tumor necrosis factor α (TNFα)-primed neutrophils to produce ROS and release granular proteases (Falk et al., 1990). Subsequent studies showed that this effect was dependent on Fcγ receptor (FcγR) RIIa and RIIIb function (Kocher et al., 1998; Porges et al., 1994). According to the current view (displayed in **Figure 2.5**), ANCA-activated neutrophils readily extravasate, damage endothelial cells and thus cause perivascular inflammation (Heeringa et al., 2005). Despite this knowledge, the mechanisms that drive the development and the perpetuation of the chronic

autoimmune response against the neutrophil autoantigens MPO and PR3 remain largely unknown.

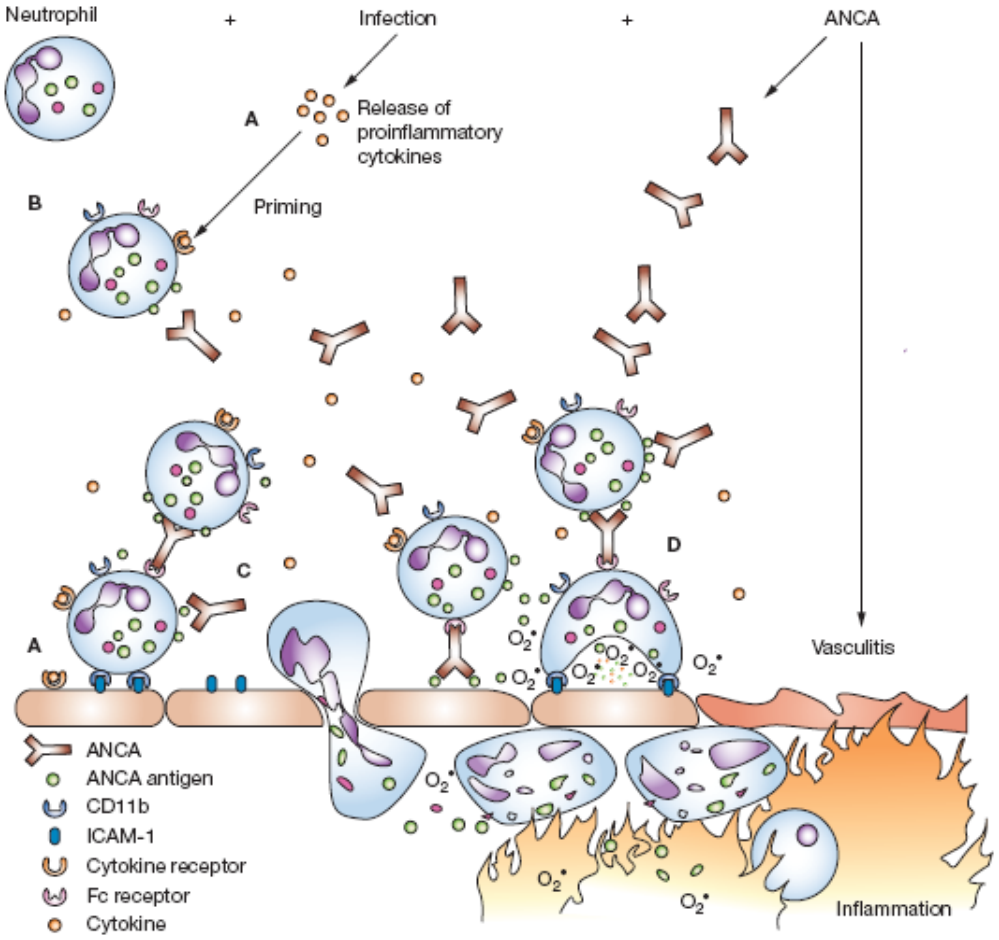

Figure 2.5 – Current view of pathogenis of ANCA-mediated disease. During infections the human body reacts with production of pro-inflammatory cytokines such as TNFα (**A**), which "primes" neutrophils and leads to increased surface expression of the autoantigens PR3 and MPO on the neutrophil cell surface (**B**). Anti-PR3 and –MPO ANCAs, present in the sera of patients with small-vessel vasculitides, bind to "primed" neutrophils and trigger neutrophil activation and ROS formation (**C**). This leads to increased adhesiveness and transmigration of neutrophils across the endothelium into the perivascular tissue, where the neutrophils finally cause strong inflammation of the blood vessel (**D**).

Source: (Kallenberg et al., 2006)

2.1.2.2.2 Neutrophil extracellular traps (NETs)

Recently, it has been found that neutrophils not only kill pathogens intracellulary in the phagolysosome after receptor-mediated engulfment, but are also able spill out their own DNA into the extracellular space to trap and kill bacteria outside the cell.

These structures were termed **N**eutrophil **E**xtracellular **T**raps (NETs) and are composed of chromatin attached with specific bactericidal proteins from neutrophilic granules (Brinkmann et al., 2004).

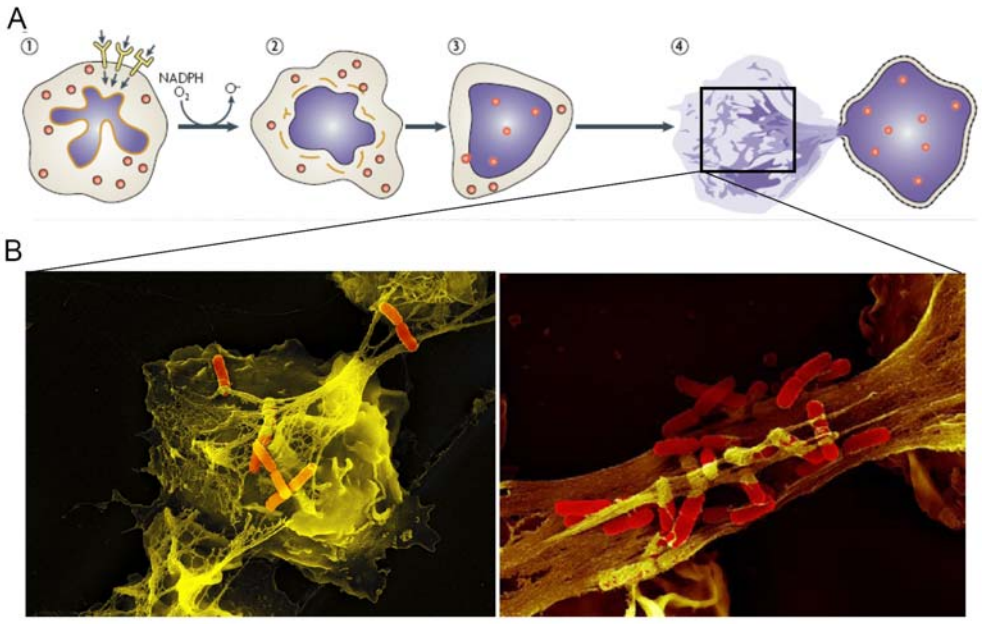

Figure 2.6 – NETs trapping bacteria. (**A**) NETs are the product of an unusual cell death pathway of neutrophils. Activation of neutrophils (1) leads to an oxidative burst and the production of reactive oxagen species. Then the nuclear membrane disintegrates (2) and cytoplasmic granula components are fused with nuclear chromatin inside the cell (3). Finally, the cell membrane opens and the chromatin fibers of NETs decorated with anti-microbial granular proteins is released into the extracellular space (4). (**B**) Colored electronmicroscopic picture of extracellular chromatin fibers of NETs (yellow) trapping shigella bacteria (red), depicting the extracellular trapping and killing of pathogens by NETs.

Source: Max Planck Institute of Infection Biology

NETs are complex structures of smooth "threads", approximately 15 nm in diameter, which are likely to represent a chain of nucleosomes from unfolded chromatin. Upon activation by interleukin (IL)-8, lipopolysaccharide (LPS) or phorbol-esters, neutrophils initiate an alternative cell death program that leads to the formation of NETs. This novel form of cell death was found to be distinct from apoptosis and necrosis, and consequently it was called NETosis (Fuchs et al., 2007). In a first step of this process, the nuclear membrane begins to disintegrate so that the nuclear material fills the whole cytoplasm. At this stage, the granular components are mixed and fused with the chromatin inside the cell. Finally, the cells release the chromatin fibers fused

with granular proteins to produce NETs. Interestingly, Fuchs et al. have provided evidence that NETosis is critically dependent on ROS formation by the phagocyte oxidase (phox), since both treatment with ROS scavengers as well as genetic deficiency of phox in patients with chronic granulomatous disease (CGD) rendered the neutrophils unable to form NETs (Fuchs et al., 2007). This cellular suicide of neutrophils has been clearly shown to be beneficial during microbial infections (Brinkmann and Zychlinsky, 2007), but it remains unclear whether NET formation can also play a role in the pathogenesis, for instance, of autoimmune disorders.

2.1.2.2.3 Self DNA as an adjuvans in autoimmunity

Proteins that form complexes with nucleic acids are remarkably frequent targets of autoantibodies in a variety of autoimmune diseases such as systemic lupus erythematosus (SLE). In the recent years, it has become increasingly evident that this observation is linked to the potential of nucleic acids to activate toll-like receptors (TLRs) in immune cells such as B cells or dendritic cells (Marshak-Rothstein and Rifkin, 2007). TLRs are innate pattern recognition receptors that normally sense the presence of microbial or viral components, including their lipopolysacchararide (LPS), RNA or DNA (Janeway and Medzhitov, 2002). However, also self DNA/chromatin was recently found to activate the TLR9 pathway leading to the activation of autoreactive B cells (Leadbetter et al., 2002). Therefore, the release of substantial amounts of chromatin, in the form of NETs, could be a highly immunostimulatory process.

Interestingly, LL37, a 37 amino acid long antimicrobial peptide expressed by neutrophils, was recently shown to be the key factor in converting self-DNA into an activator of immune cells in an autoimmune disease of the skin called psoriasis (Lande et al., 2007). The authors showed that LL37 directly interacts with DNA and enables its entry into dendritic cells, therefore allowing activation of the TLR9 pathway by self-DNA. As LL37 is produced by PR3-mediated processing of its precursor CAP-18 (Sorensen et al., 2001), it would be interesting to test if LL-37 is also a component of NETs.

2.2 Aim of the project

In the first part of this Ph.D. thesis, my aim was to clarify the role of the highly related neutrophil serine proteases PR3 and NE in non-infectious inflammation. To this end, the *in vivo* function of PR3 and NE was studied using mutant mice that lack both PR3 and NE (PR3/NE-/-). In these mice, I induced different models of neutrophilic inflammation in the absence of infection, for instance by applying phorbol-esters or inducing immune complex formation in the skin. I then compared the function of neutrophil granulocytes during the inflammatory response between PR3/NE double-deficient, NE single-deficient and wildtype (WT) mice. Furthermore, I employed cell based *in vitro* assays using isolated murine neutrophils to examine the role of PR3 and NE on the cellular level. These assays included neutrophil chemotaxis analysis by live microscopic imaging, neutrophil activation by immune complexes, but also bio-imaging of cytoskeletal rearrangements and integrin-clustering of activated neutrophils. Moreover, I analyzed the proteolytic cleavage of PGRN by PR3 and NE on the molecular level using recombinant, purified proteins and evaluated the role of PGRN as a crucial substrate for both PR3 and NE during non-infectious inflammation. These studies provided further insight in the regulation of neutrophil function during inflammatory processes and may provide the rationale basis for the development of novel anti-inflammatory drugs.

In the second part of my work, I analyzed the role of a recently discovered, alternative form of neutrophil cell death (NETosis) in the autoimmune response against PR3 and MPO. It was previously shown that autoantibodies, so called ANCAs, can bind to PR3 and MPO on the neutrophil cell surface and trigger an oxidative burst. Since the oxidative burst appears to be crucial for the formation of NETs, I examined whether neutrophils undergo NETosis when stimulated with anti-PR3 and –MPO ANCAs isolated from autoimmune vasculitis patients. Furthermore, I determined by immunofluorescence if the targeted autoantigens PR3 and MPO are components of the extracellular chromatin fibers of NETs. As the immunostimulatory peptide LL37 is known to be produced by neutrophils, I also tested if LL37 is found on NETs. Kidney biopsies from patients with autoimmune vasculitis and renal involvement

were dissected by *in situ* immunofluorescence to determine whether NET formation actually occurs in the patients. As extracellular is swiftly degraded to nucleosomes by DNAses in the body, I also measured nucleosome levels in serum and urine samples from SVV patients and analyzed whether neutrophil granular marker proteins were attached to circulating nucleosomes. These studies shed more light on the development of autoimmunity towards neutrophil components in ANCA-associated vasculitis.

3 Methods

3.1 General Methods

3.1.1 Cloning in plasmid vectors

3.1.1.1 Plasmid DNA purification

DNA from *E. coli* was purified using the Qiagen mini and maxiprep systems to prepare up to 20/500 µg of plasmid DNA from 5/500 ml bacterial overnight cultures of in Luria-Bertani (LB) medium (Bacto trypone 10 g, yeast extract 5 g, NaCl 5 g and deionized H_2O, 1 litre) containing the appropriate selective antibiotic. The desired plasmids were isolated using the appropriate Qiagen kits, mentioned above, according to the provided protocols. The resulting plasmid DNA was then used for sequence verification or for further cloning procedures after transformation into the *E. coli* host strain DH5α (Birnboim, 1983; Birnboim and Doly, 1979).

3.1.1.2 Polermerase chain reaction (PCR)

The PCR was performed using a thermocycler ("Trio-Thermobloc"; Biometra) to amplify short target sequences (100-500 bp) of a longer DNA molecule. A typical amplification reaction includes the sample of template DNA, two oligonucleotide primers, deoxynucleotide triphosphates (dNTPs), reaction buffer, magnesium and a thermostable DNA polymerase, here the PfuTurbo-DNA polymerase (Stratagene Kit with supplied 10x Pfu-buffer). All PCR reactions were started with a pre-incubation step termed "Hot Start", which denatures the template DNA at 95-100°C so that the primers can anneal after cooling. The second step, otherwise referred to as "touchdown", allows the oligonucleotide primers to anneal to the denatured template by lowering the temperature to 37-65°C depending on the annealing temperature of the primers. The reaction proceeds with the extension, or elongation of the primers at 72°C, the optimal temperature for PfuTurbo-DNA polymerase. The duration of the

extension steps can be increased if longer templates are being amplified. Usually, the elongation time of the final cycle is longer (up to 10 minutes) to ensure that all product molecules are fully extended. Steps 1-3 constitute one cycle of the PCR. The whole PCR reaction is usually carried out in 25-30 cycles. Higher cycle numbers may result in an increase of unwanted artifacts, while no increase in the desired product is achieved.

Typical amplification reaction:

50 ng Template DNA
5 µl 10x Pfu-buffer (Stratagen kit)
5 µl 2 mM dNTP-Mix
10 µM forward primer
10 µM reverse primer
2.5 U PfuTurbo-DNA polymerase (Stratagen kit)
Add H_2O to 50 µl

3.1.1.3 DNA restriction digestion

Restriction digestion of plasmid DNA was performed following a standardized protocol for the use of one or more endonucleases. The definition of 1 Unit (U) of restriction enzyme activity is the amount needed to completely digest one microgram of substrate DNA (often Lambda DNA) in one hour at the optimal temperature (usually 37°C). Additionally, each reaction is carried out with a buffer that ensures 100% activity of the respective endonuclease. As a rule of thumb, the total volume of restriction enzyme in the digest should not exceed 10% of the total digest volume, which also ensures that the glycerol concentration in the reaction mixture remains below 5%. Once all the components, DNA, H_2O and buffer, have been added to the reaction mix, the endonulease is applied, so it enters optimal reaction conditions. Under non-standard conditions, restriction endonucleases are capable of cleaving sequences, which are similar but not identical to their defined recognition sequence. This process is termed “star” activity, and is completely controllable in the vast majority of cases when the enzymes are used under the recommended conditions. Cleaving plasmid DNA with two restriction endonucleases simultaneously (double digestion) is achieved by selecting a buffer that provides reaction conditions that are amenable to both restriction endonucleases. Choosing the optimal buffer for both

enzymes should be done carefully under the guidelines supplied by the manufacturer (New England Biolabs). Alternatively, if no single buffer is available to satisfy the buffer requirements of both enzymes, the reactions should be done sequentially; the salt conditions adjusted in between digestions using a small volume of a concentrated salt solution to approximate the reaction conditions of the second restriction endonuclease. Reactions were stopped by thermal inactivation or by the addition of loading-buffer in preparation for gel electrophoresis.

3.1.1.4 Agarose gel electrophoresis

Agarose gel electrophoresis enables the user to monitor restriction digestion or PCR procedures, but also to size fractionate DNA molecules in order to purify these from the gel. Prior to gel casting, dried agarose is dissolved in buffer by heating and is then poured into a self assembled mold, into which a comb is fitted while the mixture is still wet. The percentage of agarose in the gel varies. In this work, 0.8% agarose was used, 1% agarose gels being necessary for the accurate size fractionation of DNA molecules smaller than 1 kb. Ethidium bromide (EtBr) (end concentration: 1 µg/ml) was included in the gel matrix to enable fluorescent visualization of the DNA fragments under UV light. The gels were then submerged in electrophoresis buffer (TAE) in a horizontal electrophoresis apparatus. After the samples were mixed with gel loading dye and loaded into the sample wells, the electrophoresis was initiated by applying 60 mV for 30 minutes to 1 hour at RT. Size markers are co-electrophoresed with DNA samples for fragment size determination. Two size markers, 1 kb and 50 bp, were used from Peqlab. After electrophoresis, the gel was placed on a UV light box and the fluorescent ethidium bromide-stained DNA pictured using the thermal imaging system FTI-500 from Pharmacia Biotech.

TAE buffer (10 fold):

242 g Tris
57.1 ml Acetic acid
100 ml 0.5 M EDTA, pH 8.0
Add H_2O to 1 litre

3.1.1.5 DNA purification from agarose gels

After electrophoresis, DNA fragments were visualized on a UV light box before being removed from the gels by the use of scalpels. Once captured, the DNA was eluted from the jellified agarose following the instructions of the "QIAquick Gel Extraction Kits" from Qiagen.

3.1.1.6 Determination of DNA concentration

DNA concentration and purity was determined by using the Eppendorf spectrophotometer "BioPhotometer". The concentration was determined by measuring the absorbance at 260 nm and purity was measured by calculating the ratio of absorbance at 260 versus 280 nm.

3.1.1.7 DNA ligation

Purified and restriction enzyme-treated DNA fragments (PCR product) were cloned into the desired plasmid vectors, which also have been treated with the respective endonucleases producing compatible overhangs. After the vector and insert DNA have been prepared and their concentration determined, various vector to insert DNA ratios were tested in order to determine the optimum ligation ratio. In most cases a 1 to 3 molar ratio of vector and insert proved successful. All ligations were performed with ATP-dependent T4 DNA ligase and the provided buffer (Boehringer) overnight at 16°C or for 3 hours at RT. Following the reaction, the ligated DNA was transformed into an appropriate host strain, here the *E. coli* stain DH5α.

3.1.1.8 DNA sequencing

The sequencing of plasmids and PCR products was performed by Toplab (Martinsried, Germany) using fluorescently labeled nucleotides as described by Sanger and colleagues (Sanger et al., 1977).

3.1.2 Protein separation and analysis

3.1.2.1 SDS-PAGE

Gel electrophoresis is a useful method to separate and identify proteins. In **s**odium **d**odecyl **s**ulphate (SDS) **p**oly**a**crylamide **g**el **e**lectrophoresis (PAGE) or SDS-PAGE, proteins are separated on the basis of polypeptide length, therefore allowing their molecular weight to be estimated. Our protocol uses Laemmli buffer (a denaturing buffer) and a discontinuous gel system composed of both a stacking and separating gel. The stacking gel is slightly acidic (pH 6.8) and has a low acrylamide concentration to make a porous gel. Under these conditions, proteins separate poorly but form thin, sharply defined, bands. The separating gel is more basic (pH 8.8) and has a higher polyacrylamide content (in our case mostly 15%), which causes the gel to have narrower channels. As the protein of interest travels through the separating gel, the narrower pores have a sieving effect on the proteins, allowing smaller proteins to travel more easily and hence rapidly through the matrix (Laemmli, 1970).

SDS polyacrylamide gels (15%): Eight-gel assembly

Stacking Gel (20 ml)		**Separating Gel** (40 ml)
d H_2O	13.6 ml	9.4 ml
30% acrylamide	3.32 ml	20 ml
1 M Tris HCl, pH 6.8	2.56 ml	-
1.5 M Tris HCl, pH 8.8	-	10 ml
20% SDS	100 µl	200 µl
10% APS	200 µl	400 µl
TEMED	20 µl	16 µl
Bromophenol blue	5 µl	-

Once polymerized, the polyacrylamide gels were next mounted in a Mini-protean II apparatus (Bio-Rad) and covered with 1x running buffer based on glycine (10x running buffer: 250 mM Tris, 1.92 M glycine and 1% SDS in an aqueous solution). The low molecular weight protein marker, Roti-Mark prestained (Roth) was loaded (3 µl for silver staining and 5 µl for coomassie staining) in one of twelve wells during sample preparation. Concentrated Laemmli buffer ((4x denaturing buffer: 200 mM

Tris HCl, pH 6.8, 40% Glycerol (denser than water, makes the sample fall to the bottom of the well), 30% β-mercaptoethanol (disulphide bridge reduction), 10% SDS (confers negative charge) and 0.2% bromophenol blue (visualisation)) was added to the samples which were then boiled (95°C, 5 minutes) and loaded. For the best results all samples should be in identical, low ionic strength buffers and should be loaded in equal volumes. The protein amount per well should not exceed 30-40 µg. Finally, gels were run at a constant voltage (200 mV/s) using a Bio-Rad electrophoresis apparatus.

3.1.2.1.1 Silver nitrate staining

After the separation of proteins comes their detection. One of the most popular detection methods is silver staining, which can detect as little as 3-10 ng of loaded protein. In fact, while a 100 fold more sensitive than Coomassie blue staining, silver staining comes close to the sensitivity provided by Western Blot analysis. Following electrophoresis, polyacrylamide gel plates were disassembled and briefly washed in H_2O. Next, the gels are soaked, while shaking, in a fixing solution composed of 50% Methanol, 12% acetic acid and 0.5 ml 37% formaldehyde (topped up to 1 litre with H_2O) for 1 hour after which 3 baths of 10 minutes in 50% ethanol are required. Thereafter, the gels were introduced into a sodium thiosulphate solution (0.2 g $Na_2S_2O_3$ x 5 H_2O per litre) for 1 minute before being washed 3 times for 20 seconds in H_2O. A freshly made silver nitrate solution (2 g $AgNO_3$ and 750 µl 37% formaldehyde per litre) was then exposed to the gels. After 30 minutes the staining solution was removed by several washing steps in H_2O. A developing solution (60 g/L Na_2CO_3, 4 mg/L $Na_2S_2O_3$ x 5 H_2O, 0.5 ml 37% formaldehyde per litre) was then applied and eventually stopped by thorough washing with H_2O. Two methanol based washes follow, first 10 minutes incubation in 50% methanol, 12% acetic acid and then 20 minutes bath in 50% methanol. Both solutions were brought to 1 litre with H_2O. The gels were finally stored in H_2O.

3.1.2.1.2 Coomaassie blue staining

Coomassie blue staining is much less sensitive than silver staining as described above. Following SDS-PAGE, the gel was incubated for 1 hour in Coomassie blue solution (25% isopropanol, 10% acetic acid and 0.05% Coomassie Brilliant Blue G per litre), after which it was heated to 60°C, with lid, for 1 minute in a microwave oven. After careful removal, the gel was left to shake in the solution for 5-10 minutes. The

Coomassie solution was then removed (back into original bottle) and the gel was bathed in de-staining solution (10% ethanol, 10% acetic acid) until bands appear. For the efficient removal of excess coomassie staining, absorbing paper can be used along with the exchange of destaining solution. If proteins bands take time to appear, further heating in a microwave can help accelerate development (Meyer and Lamberts, 1965).

3.1.2.2 Western Blot

Western Blot analysis is a very sensitive technique used for the identification of specific proteins in a mixture of different proteins, but also for the determination of relative amounts of proteins from different samples, which have been previously separated by SDS-PAGE and thereafter blotted onto a "Hybond ECL" (nitrocellulose) membrane (Amersham-Pharmacia) again by electrophoresis. These membranes can then be probed with a specific primary antibody following incubation with a labeled secondary antibody directed against the species immunoglobulins of the specific first antibody. An often used label of the secondary antibody is the enzyme horseradish peroxidase (HRP), which can be visualized by enhanced chemiluminescence (ECL) using a peroxidase substrate.

In this work, both Wet-Transfer (Bio-Rad apparatus) and Semi-Dry (Biometra) Western blotting (WB) was performed. As a rule of thumb, Semi-Dry WB was used for low molecular weight proteins up to 30-35 kDa. Wet-Transfer WB on the other hand was chosen for proteins exceeding 35 kDa in size. Fresh transfer buffer was made before both procedures and although the Wet Transfer WB also worked well for proteins of low molecular weight, Semi-Dry WB was often the method of choice as much less transfer buffer (25 mM Tris HCl, 200 mM glycine, 20% methanol, 0.1% SDS) is needed along with less Whatman 3 mm paper.

Before the Wet Transfer run was carried out, the SDS polyacrylamide gel and both Whatman and membrane of choice were equilibrated in transfer buffer. Then, after assembly and correct set up of the Bio-Rad Protean apparatus (filled with transfer buffer and containing an ice pack) the transfer was initiated and run for 1 hour at 100 V. Constant stirring was applied during the transfer.

The Semi-Dry procedure differs in a number of aspects. Apart form being preferred for low molecular weight proteins, as noted above, the quantity of buffer is largely

reduced. Secondly, the sandwich assembly is horizontal, the bottom surface being the cathode. Further differences include the use of fewer Whatman sheets (3 each side as opposed to 5 in Wet-Transfer WB) and importantly, depending on the surface area with the membrane, an increasing surface requires a higher voltage applied.

Once the run of choice was through, the transfer was verified by checking the presence of a similarly sized pre-stained marker bands (Roth). Thereafter, the membrane was washed three times in PBS-T (1x PBS, 0.05% Tween) and blocked in a milk solution (PBS-T, 5% non-fat-powered-milk (NFPM)) for 1 h at RT (shaking). The membrane was then washed three times in PBS-T with shaking before being exposed overnight to the desired primary antibody, diluted appropriately in PBS-T containing 5% NFPM, at 4°C with rotation. To save antibody, the membrane was sealed within a tight, special plastic poach. Again, the membrane was washed three times, with shaking in PBS-T. The PBS-T was then drained off before the ECL substrate solution (Amersham Pharmacia), 1 ml of both solutions mixed for a membrane of 5x10 cm in size, was added for 1 min. Finally, the membrane was exposed to light-sensitive ECL film (Amersham Pharmacia) for 20 seconds to 30 minutes until the expected bands developed.

3.2 Antibody list

3.2.1 Primary antibodies

Antigen (species)	Species	Clonality	Provider	Cat. No.
Actin	Mouse	m	Calbiochem (clone JLA-20)	CP01
Cathepsin G (mouse)	Rabbit	p	A. Belaaouaj, France	-
CD11b (mouse)	Rat	m	BD Pharmingen	553310
Elastase (mouse)	Rabbit	p	A. Belaaouaj, France	-
Gr-1 / Ly-6G (mouse)	Rat	m	BD Pharmingen	RB6-8C5
Histone (Pan)	Mouse	m	Chemicon International	MAB3422
Laminin (mouse)	Rabbit	p	Sigma	L9393
LL37 (human)	Mouse	m	HyCult Biotech	HM-2070

Myeloperoxidase (human)	Mouse	m	ABD Serotec	0400-0002
Myeloperoxidase (mouse)	Rabbit	p	A. Belaaouaj, France	-
Ovalbumin	Rabbit	p	Sigma	C6534
Progranulin (human)	Rabbit	p	A. Bateman, Canada	-
Progranulin (mouse)	Sheep	p	R&D Systems	MAB2420
Proteinase 3 (human)	Mouse	m	Wieslab	Clone 4A5
Proteinase 3 (mouse)	Rabbit	p	A. Belaaouaj, France	-

3.2.2 Secondary antibodies

Antigen	Species	label	Provider	Cat. No.
Human IgG	goat	AP	Sigma	A-3188
Mouse IgG	rat	FITC	BD Pharmingen	553443
Mouse IgG+M	goat	HRP	BD Pharmingen	555988
Rabbit IgG	donkey	HRP	JacksonImmuno	731-035-152
Rabbit IgG	goat	FITC	JacksonImmuno	111-095-045
Rabbit IgG	goat	Alexa-488	Molecular Probes	A11008
Rat IgG	goat	biotin	Biogenex	GP220-OT
Rat IgG	goat	PE	JacksonImmuno	112-116-071
Rat IgG	goat	Cy3	Dianova	112-165-003
Sheep IgG	donkey	HRP	JacksonImmuno	713-035-003

3.3 Analysis of PR3 and NE as triggers of inflammation

3.3.1 Recombinant and purified proteins

Recombinant mouse PR3 was produced and expressed in *E. coli* and purified from inclusion bodies as previously described (Pfister et al., 2004).

Human NE was purchased from Elastin products (Owensville, Missouri, USA).

Recombinant human PGRN was a kind gift from Prof. Andrew Bateman (McGill University, Montreal, Canada) and was prepared as previously reported (He et al., 2003).

Recombinant mouse PGRN (aa18-589) was produced with an N-terminal S-tag by transient expression in H5 insect cells using a modified pIEx-5 vector (Novagen/Merck). The mouse PGRN expressing pIEx-5 vector was kindly prepared by Miriam Urscher in our lab. Secretion of recombinant PGRN was driven by the secretion signal of the adipokinetic hormone (AKH). Transfection of H5 insect cells cultured in TC-100 medium (Gibco/Invitrogen) was done using the Fugene HD transfection reagent (Roche) according to the manufacturer´s instuctions, and positive transfection was controlled using a pIEx-5 vector expressing green-fluorescent protein. Six days upon transfection, the supernatant was harvested and recombinant mouse PGRN was purified using S-protein agarose column (Novagen/Merck). Following extensive washing of the column with phosphate-buffered saline (PBS), the bound protein was eluted by 3 M magnesium chloride. Immediately thereafter, fractions were dialyzed against PBS and analyzed by silver-stained SDS-PAGE. Pure fractions were pooled and dialyzed against 20 mM ammonium bicarbonate, lyophilized and stored at -80°C until use. For experiments, lyophilized protein was reconstituted in sterile PBS (Gibco/Invitrogen).

3.3.2 Measurement of PR3/NE enzyme activity

Enzymatic activity of the proteases PR3 and NE in lysates from WT, NE-/- and PR3/NE-/- neutrophils was determined using Boc-Ala-Pro-Nva p-chlorothiobenzylester (BAPN-TBE; Sigma), a chromogenic substrate widely used to

monitor both NE and PR3 activity due to their similar specificity. Lysates of neutrophils purified from the casein-inflamed peritoneum were prepared as described in 3.3.3.3 and PR3/NE activity in the lysate of 8 x 10^4 neutrophils was measured in 50 mM Hepes, 0.75 M NaCl, 0.05% Nonidet containing 1 mM BAPN-TBE and 0.5 mM DTNB. The OD_{405} was measured at 37°C over time using FLUOstar Optima (BMG Labtech).

3.3.3 Mouse experiments

3.3.3.1 Mice

Simultaneous deficiency of the PR3/NE gene cluster in 129S6/SvEv mice was generated by homologous recombination in embryonic stem cells as detailed in the Ph. D. thesis written by Dr. Leopold Fröhlich in our laboratory (2001). NE-/- mice on the 129S6/SvEv genetic background were previously generated (Tkalcevic et al., 2000) and were obtained as frozen embryos from the Medical Research Council (Harwell, Oxford, UK). These and WT control mice were kept under pathogen-free conditions at the GSF Neuherberg (Munich, Germany). For most experiments mice at the age of 5 to 8 weeks of age were used. All animal experiments were performed with approval by the Institutional Animal Care and Use Committee.

To control normal neutrophil differentiation in PR3/NE-deficient mice, peripheral blood neutrophils were characterized by flow cytometry using fluorescently-labeled Gr-1 and CD11b specific antibodies (Pharmingen/BD Bioscience) as previously described (Fleming et al., 1993; Hestdal et al., 1991). Moreover, blood smears were prepared and stained on glass slides according to the "Diff-Quick" protocol (Dade-Behring) to monitor the cellular morphology of PR3/NE-lacking neutrophils, which were analyzed by light microscopy. Differential blood leukocytes were identified by morphology and counted under the microscope to determine the percentage of each population. The cell count per milliliter blood of each leukocyte population was determined using a hemocytometer (improved Neubauer chamber).

3.3.3.2 Skin inflammation models

3.3.3.2.1 Croton oil-induced inflammation

Croton oil (Sigma; C6719) was diluted to 1% in acetone and each 20 µl of this dilution was topically applied to the ventral and the dorsal side of the ear of WT (n = 4) and PR3/NE-/- mice (n = 4). After 4 hours, mice were sacrificed by CO_2 inhalation. The earlap was split into two halves by carefully separating the dorsal and ventral skin. For histological analysis dorsal and ventral halves of ears were subjected to whole mount immunostaining. After fixation in 3% paraformaldehyde (PFA), ear halves were blocked with 1% bovine serum albumin (BSA; PAA, Pasching, Austria) in PBS for 1 hour at room temperature (RT), probed with biotin labelled anti-Gr-1 (RB6-8C5, Pharmingen) to identify neutrophil granulocytes and anti-pan-laminin (Sigma; L9393) to visualize the EBM diluted in 1% BSA in PBS overnight at 4°C (while shaking) and washed with 1% BSA in PBS. Antibodies were detected with a repeated cycle of staining with anti-rabbit Alexa-488 (Molecular Probes) and anti-rat Cy3 (Dianova; Hamburg, Germany) before tissue was embedded in elvanol and representative images taken with a Zeiss Axio Imager (Zeiss, Jena, Germany) equipped with the Apotome®. Location of neutrophils was analyzed in detail for potential accumulation at the basement membrane. For quantification of neutrophil influx, at least three pictures of the inflamed skin were taken using a 10x objective to quantify total neutrophil infiltrates as the percentage of Gr-1 signal per microscopic field using Metamorph software (Molecular devices), while intravascular signal was excluded.

3.3.3.2.2 Immune complex-mediated inflammation

The reverse passive Arthus reaction (RPA), a widely used model of IC-mediated inflammation, was induced in the skin of mice using ovalbumin grade-V (OVA; Sigma) as the antigen and purified rabbit anti-OVA antibodies of the IgG class (Rockland Immunochemicals Inc) as depicted in **Figure 3.1**. Initially, the hair was removed from the ventral skin and the area was cleaned with 70% alcohol. Anti-OVA IgG (2 µg/µl) was deposited intradermally in a volume of 30 µl using a 27-gauge needle. Intradermal injection of 30 µl unspecific polyclonal rabbit IgG (2 µg/µl; Sigma) served as a negative control in the same animal. Without delay, the antigen

(20 mg OVA per kg body weight diluted in 100 µl sterile PBS) solution was injected intravenously (*i.v.*). After 4 hours, mice were sacrificed by CO_2 asphyxiation and the inflammatory response was assessed by histology. Paraffin-sections of the specimens were processed for H&E staining and analyzed by light microscopy for inflammatory cellular infiltrates. Neutrophils were additionally identified using Gr-1 immunohistochemistry. Briefly, deparaffinized tissue sections were incubated with a rat anti–Ly-6G antibody (BD PharMingen, Heidelberg, Germany) followed by a biotinylated goat anti-rat antibody (BioGenex, San Ramon, CA). Bound antibodies were labeled with streptavidin-alkaline phosphatase and visualized with fast red (BioGenex). Sections were counterstained with Mayer hematoxylin solution (Merck Eurolab, Darmstadt, Germany). Random high power fields (HPF) of the respective lesion were photographed using a Leica DFC320 CCD camera (Leica, Wetzlar, Germany) attached to a Zeiss Axioplan 2 microscope (Zeiss, Jena, Germany) with a 10x objective. Digitized images were used to enumerate neutrophils as average per HPF in lesions from WT (n = 12), NE-/- (n = 13) and PR3/NE-/- mice (n = 12).

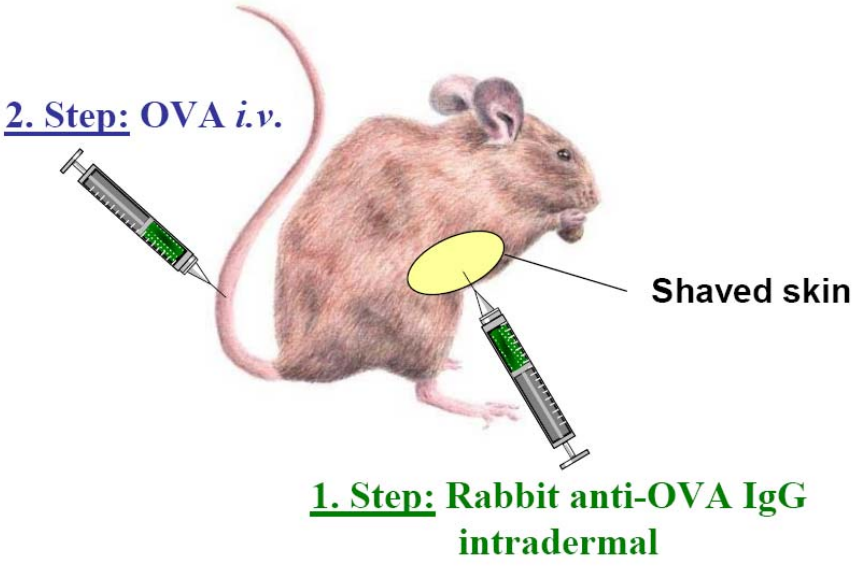

Figure 3.1 – Immune complex-mediated inflammation. Cutaneous inflammation mediated by the formation of immune complexes, *i.e.* the reverse, passive Arthus reaction (RPA), was induced in mice. After removing the hair at the ventro-lateral skin area, rabbit anti-OVA antibodies were deposited intradermally and, immediately afterwards, the RPA was started by systemically applying the antigen OVA *i.v.* via the tail vein.

3.3.3.2.2.1 Administration of PGRN to immune complex inflammation

To study the inhibitory capacity of PGRN on IC-stimulated inflammation, I deposited 2 µg recombinant mouse PGRN by intradermal injection together with 30 µl anti-OVA solution as detailed above. In the same mouse at different sites of the ventral skin, I intradermally applied anti-OVA alone and control rabbit IgG as a positive and negative control, respectively. The RPA was started by *i.v.* administration of OVA. Four hours after initiation, mice were sacrificed and biopsies were taken to histologically quantify neutrophil infiltrates per HPF in PGRN-treated and non-treated lesions from WT (n = 5) and PR3/NE-/- mice (n = 5).

3.3.3.3 Isolation of mouse neutrophils

Mouse neutrophils were purified from the bone marrow using a discontinuous percoll® gradient (Amersham Bioscience) as previously described (Lowell et al., 1996). In brief, the bone marrow was flushed out of the tibiae bones using RPMI medium, rinsed through cell strainer (40 µm; BD Bioscience) to get rid of large cell aggregations. Red blood cells were lysed using ammonium chloride. Finally, neutrophils were separated using a discontinuous percoll gradient (81/62/50/45%; Amersham Bioscience) centrifuged at 1200 g at RT without break for 30 min and harvested from the 81/62% interface. Neutrophil preparations were characterized by Gr-1 and CD11b (Mac-1) double immunostaining using flow cytometry and were found at least 80% pure.

To isolate murine neutrophils *ex vivo* from an inflammatory environment, I injected 1 ml of a 9% sterile casein solution in PBS to induce peritonitis. Four hours after injection, cells were harvested by peritoneal lavage using sterile PBS without Ca^{2+}/Mg^{2+} (Gibco). Peritoneal cells were layered on a discontinuous histopaque® 1119-1077 gradient (Sigma) and after centrifugation for 30 min at 700 g, neutrophils were isolated from the 1.119-1.077 kg/L interphase. For anti-PGRN Western blots and PR3/NE activity assays, neutrophil lysates were prepared. In brief, neutrophils were lysed in 50 mM Tris/HCl (pH 7.4), 150 mM NaCl, 0.5 mM EDTA and 0.5% nonidet by mechanical disruption using syringes with 27-gauge needles. Cell debris was pelleted by centrifugation. All steps were carried out at 4°C and supernatant was frozen until used.

3.3.3.4 Neutrophil 3D collagen chemotaxis assay

For migration assays, PureCol™ (INAMED, Fremont, USA) in 1x minimum essential medium eagle (MEM, Sigma) and 0.4% sodium bicarbonate (Sigma) was mixed with cells in RPMI (Invitrogen), 10% fetal calf serum (FCS, Invitrogen) at a 2:1 ratio, resulting in gels with a collagen concentration of 1.6 mg/ml. Neutrophils were "primed" by 10 ng/ml mouse TNFα (Biosource; PMC3016) for 15 min at 37°C. Final cell concentrations in the assay were 1.6 Mio granulocytes per ml gel. Collagen-cell mixtures were cast in custom-made migration chambers with a thickness of 0.5-1.0 mm. Thirty minutes after the assembly of the collagen fibres at 37°C, the gel surface was covered with 50 µl of 0.1 µg/ml C5a (R&D Systems) solution. Pictures of migrating cells were taken every 20 sec using a Zeiss Axioplan 2 lightfield microscope (Zeiss, Jena, Germany) and stacks of images were used to generate time-lapse movies in avi-format using Metamorph (Molecular devices). Chemotactic parameters were calculated and visualized as plots by analyzing the acquired data with a Chemotaxis and Migration Tool plug-in (http://www.ibidi.de/applications/ap_chemo.html).

3.3.3.5 Neutrophil oxidative burst *in vitro*

To test neutrophil activation by ICs *in vitro*, I prepared immobilized IC using a OVA/anti-OVA system as described previously (Raptis et al., 2005). Isolated neutrophils were resuspended at a density of 2 x 10^6 cells/ml in phenol red free RPMI (Gibco) containing 10 ng/ml recombinant mouse TNFα (Biosource; PMC3016) and added to immobilized ICs in 96-well microtiter plates. Activation by 25 nM PMA (Sigma; P1585) without TNFα served as a positive control. I also determined the oxidative burst of neutrophils as a function of increasing PMA concentrations (0.1 nM to 50 nM) in order to define the concentrations that yielded submaximal responses in mouse neutrophils. ROS production as the read-out for neutrophil activation was detected using dihydrorhodamine 6G (Molecular Probes; D633) according to the manufacturer´s instructions and the increase in fluorescence was measured over time with the fluorometer FLUOstar OPTIMA (BMG Labtech, Offenburg, Germany) at 37°C. For each time point, the IC-specific oxidative burst was determined by subtracting the mean fluorescence read on negative control coating from that on IC

coating. To compare independent experiments, I calculated the relative oxidative burst as ratio vs. maximum ROS production by WT neutrophils.

3.3.3.5.1 Administration of PGRN to neutrophil oxidative burst

To examine the effect of PGRN on the neutrophil activation *in vitro*, I first approximated the concentration of cell-associated and secreted PGRN in the absence of PR3/NE during IC-mediated neutrophil stimulation by comparison with the positive control band in anti-PGRN Western blot to be ~100 nM (data shown in **Figure 4.12**). I then added recombinant PGRN at a final concentration of 100 nM to isolated WT stimulated by ICs or PMA. I compared the oxidative burst between PGRN-treated and non-treated cells as detailed above.

3.3.3.6 Neutrophil adhesion assay to ICs

Isolated neutrophils were labeled with Calcein AM (Molecular Probes) according to the manufacturer´s instructions and plated on ICs in microtiter plates (96 well) in the presence of 10 ng/ml TNFα as previously described (Raptis et al., 2005). In brief, wells were three times washed with PBS at indicated time points, adhering cells were determined using a fluorescence reader (BMG Fluostar Optima) and the percentage was calculated.

3.3.3.7 Immunofluorescence of neutrophils interacting with ICs

Bone marrow-derived mouse neutrophils from WT and PR3/NE-deficient mice were allowed to settle on IC-coated glass slides in the presence of 10 ng/ml TNFα for one hour at 37°C in a 5% CO_2 incubator. ICs on glass slides were prepared as described above for microtiter plates (3.3.3.5). Immediately thereafter, the cells were fixed using 4% PFA for 15 min and, after extensive washing in PBS, unspecific binding sites were blocked using PBS containing 5% goat serum and 5% fetal calf serum (= blocking buffer; BB) for one hour. The specimens were stained for Mac-1 using anti-mouse CD11b antibody (Pharmingen) or stained for F-actin using fluorescently-labeled phalloidin (Molecular Probes) according to the manufacturer´s instructions. Immunofluorescence microscopy was done using a Zeiss Axioplan fluorescence microscope (Zeiss Microimaging GmbH).

3.3.3.8 Analysis of PGRN degradation *in vitro* and *in vivo*

PGRN processing activity was tested with recombinant mouse PR3 and human NE each at a molar enzyme to substrate ratio of 1:10 according to the buffer conditions described by Zhu et al. (Zhu et al., 2002). 2.5 µg of recombinant human PGRN (kind gift from Andrew Bateman, Montreal, Canada) was added to enzymes and incubated at 37°C. At the time points indicated in the figures, samples were placed on ice and the pattern of cleavage products was analyzed by reducing SDS-PAGE and subsequent silver nitrate staining carried out as detailed above.

To test if other PGRN-degrading enzymes besides PR3 and NE existed in neutrophils, I incubated recombinant mouse PGRN with lysates from 3 x 10^4 WT, NE-/- and PR3/NE-/- neutrophils for one hour at 37°C. Samples were separated by SDS-PAGE and transferred onto nitrocellulose membranes. After incubation for two hours in blocking buffer (BB; 5% fat-free dry milk in PBS/0.2% TWEEN-20), recombinant mouse PGRN was detected by Western blotting with sheep anti-mouse PGRN antibody (R&D Systems) at a concentration of 0.4 µg/ml and unspecific sheep IgG as a negative control (1 µg/ml; Sigma I5131), respectively. Bound antibodies were visualized using peroxidase-conjugated donkey anti–sheep immunoglobulins (1:10,000; JacksonImmuno) and enhanced chemiluminescence (ECL) reagents (Amersham/Pharmacia). For actin detection the membranes were incubated in a 1:5,000 dilution of anti-actin mouse monoclonal antibody (clone JLA-20; Calbiochem) followed by peroxidase conjugated goat anti-mouse IgG+M incubation (1:10,000; Pierce) and subsequent ECL detection.

For detection of PGRN from neutrophils activated by ICs *in vitro*, I harvested the supernatant as well as the cellular pellet of isolated TNFα-primed neutrophils after 3 hours of IC-stimulation. The concentrated supernatant and the cellular pellet of 2 x 10^5 IC-activated neutrophils was separated by reducing SDS-PAGE and subjected to anti-PGRN Western blotting as described above.

To analyze if PGRN was cleaved by PR3/NE during inflammation *in vivo*, I harvested neutrophils from the inflamed peritoneum of WT and PR3/NE-/- mice. Lysates were prepared from these cells as described above, but in the presence of 75 µg/ml PMSF and protease inhibitor cocktail (Calbiochem; 218739). Total lysates from 8 x 10^5 cells

were subjected to anti-PGRN Western blotting, which was carried out as detailed before.

3.4 Analysis of PR3 as target in autoimmunity

3.4.1 Isolation of human neutrophils

Human peripheral blood neutrophils were isolated by density centrifugation using a Pancoll® gradient. Briefly, 10 ml blood containing EDTA was diluted in 10 ml phosphate buffered saline (PBS) and layered on 10 ml Pancoll (PAN Biotech GmbH, Cat.No: P04-60500). After 30 min centrifugation at 500 g at RT without brake, granulocytes were further purified from the cellular pellet by dextran sedimentation (Dextran T500, Pharmacia Biotech, Cat.No: 17-0320-01). Residual erythrocytes were removed by hypertonic lysis in 0.2% and 1.6% NaCl each for one min on ice and, after washing, neutrophil granulocytes were resuspended in RPMI (Gibco, Cat.No: 61870). Neutrophil purity as assessed by forward and side scatter with flow cytometry was routinely ~95%. Human granulocytes were subjected to autoantibody and PMA activation to subsequently determine NET formation.

3.4.2 NETs immunofluorescence

NET release by isolated neutrophils seeded on lysinated glass slides was triggered by 25 nM PMA as described elsewhere (Brinkmann et al., 2004). After two hours, the cells were fixed using 4% PFA. Unspecific binding sites were blocked in PBS containing 5% goat serum and 1% BSA (Blocking buffer; BB). To test whether PR3 is a component of NETs, the specimens were incubated with anti-PR3 mouse mAb (clone 4A5; Wieslab) in BB. LL37 on NETs was identified using mouse mAb anti-LL37 (HBT biotechnology). Positive mAb binding was visualized using FITC labeled rat anti-mouse IgG (Pharmingen). DNA was stained using Hoechst 33352.

3.4.2.1 Autoantibody-mediated NET formation

To test if autoantibodies, so called ANCAs, from patients with small-vessel vasculitis (SVV) trigger the formation of NETs, isolated neutrophils were primed for 30 min with 10 ng/ml TNFα, seeded on lysinated glass slides and treated with purified IgG from SVV patients (microscopic polyangiitis: n = 2; Wegener´s granulomatosis: n = 2) and from healthy control individuals (n = 2), and with 25 nM PMA as a positive control. After 90 and 180 min time points, cells were fixed with 4% PFA and DNA was stained using Hoechst 33352. The percentage of neutrophils releasing DNA fibers in random microscopic fields (20x objective) was determined.

3.4.3 DNA binding ELISA

Human DNA was purified from peripheral blood cells of a healthy donor using human DNA extraction Kit (Quiagen) according to the manufactur´s instructions. DNA was coated to 96 well microtiter plates (NUNC) at 2.5 µg/ml over night at 4°C. The plate was washed with PBS and blocked with BSA for four hrs at 4°C. After another washing step, the coated surfaces were incubated with a dilution series of purified PR3 ranging from 0.5 to 0.0625 µg/ml in PBS for two hrs at RT. Subsequently, PR3 binding after stringent washing with PBS was detected using an immunoassay. Briefly, the surfaces were probed with 1:500 dilution of mouse mAb anti-human PR3 (clone 4A5; Wieslab) following incubation with HRP-labeled anti-mouse IgG rabbit antibody 1:2000 both in PBS. Binding was finally quantified by incubation of the samples with the TMB substrate and colorimetric measurement, after stopping the development by adding 10 µl 1 M HCl, at 405 nm wavelength in an ELISA-reader (FluoOptima). DNA binding was determined by direct comparison of DNA-BSA to only BSA coated wells in triplicates.

3.4.4 *In situ* immunofluorescence analysis of kidney biopsies

Kidney needle biopsies from SVV patients with glomerulonephritis (kindly provided by Dr. Walter Back) were fixed and embedded in paraffin. Five µm sections were prepared and mounted on glass slides. After antigen retrieval with citrate buffer, sections were treated with blocking buffer and reacted with primary antibodies

followed by species-specific secondary antibodies. Specimens were analyzed on a Leica SP5 confocal microscope and confocal stacks were modelled using Volocity software. Wide field images were recorded using a Nikon DXM 1200 camera on a Leica DMR microscope equipped with band pass filters. These analyzes were carried out at the Max Planck Institute for Infectious Biology in Berlin, Germany, in collaboration with Dr. Volker Brinkmann.

3.4.5 Measuring nucleosome levels in the urine

The chromatin fibers of NETs would be swiftly degraded to nucleosomes by DNAses present in the kidney tissues. Interestingly, a previous study showed increased nucleosome concentrations in the sera from patients with SVV (Holdenrieder et al., 2006). In collaboration with Prof. Samtleben from the Klinikum Großhadern in Munich, I collected urine and sera from patients suffering from Wegener´s granulomatosis with active disease (n = 2) and compared to patients in remission (n = 6). To test for nucleosomes in these specimens, the commercially available cell death detection ELISA^{PLUS} (Roche, Cat. No: 11774425001) was used. This test is based on the "sandwhich ELISA" principle using two different mouse monoclonal antibodies directed against histones and DNA, respectively. The test was carried out according to the manufacturer´s instructions.

3.4.6 Measuring MPO-nucleosome complexes in the serum

To show that the increased levels of circulating nucleosomes in patients suffering from SVV are – at least in part – derived from NETosis, I sought to identify granular components of neutrophils in association with circulating nucleosomes. As MPO was found to be a prominent constituent of NETs, I chose to test for MPO attached to nucleosomes. To this end, I established two different assays.

In the first assay, I identified MPO via its enzymatic activity. 5 µg/ml anti-histone monoclonal antibody (Chemicon International) was coated to microtiter plates (75 µl per well) overnight at 4°C. After blocking with 1% BSA (125 µl per well), wells were washed with PBS, and incubated with 40 µl per well of patient and control sera, supernatants from PMA-activated neutrophils as the positive control for NETs, and supernatant from non-activated neutrophils as the negative control. Samples were

diluted in incubation buffer (component of the cell death detection ELISA, Roche) to 100 µl final volume per well, incubated for 2 hours at RT while shaking (320 rpm) and washed for three times in 200 µl PBS per well. To identify MPO, I added TMB as widely used chromogenic substrate for MPO that can be measured via absorbance at 620 nM wavelength, and, after stopping the reaction by the addition of 20 µl 1 M HCl per well, at 450 nm.

In the second assay, MPO-DNA complexes were identified using a capture ELISA. As the capturing antibody, 5 µg/ml anti-MPO monoclonal antibody was coated to microtiter plates (75 µl per well) overnight at 4°C. After blocking in 1% BSA (125 µl), the specimens were added as described above, but this time in combination with the peroxidase-labeled anti-DNA monoclonal antibody (component No.2 of the commercial cell death detection ELISA kit; Roche, Cat. No: 11774425001) according to the manufacturer´s instructions. After two hours of incubation at RT on a shaking device (320 rpm), the samples were washed with 200 µl PBS per well and the peroxidase substrate (ABTS) of the kit (Roche) was added. The increase in absorbance was measured over time at 405 nm wavelength using Fluostar Optima (BMG Labtech).

3.5 Statistics

All results are given as the average with standard error of the mean (SEM) for data derived from different *in vivo* experiments or as the mean with standard deviation (SD) for data resulting from triplicate *in vitro* assays using isolated cells or cell lysates. Normal distribution of datasets was determined by the Kolmogorov-Smirnov test before I applied an unpaired t-test to compare two groups. I regarded $p<0.05$ as statistically significant. Calculations were done using GraphPad Prism software.

4 Results

4.1 PR3 and NE as triggers of inflammation

4.1.1 Characterization of PR3/NE double-deficient mice

To study the function of the highly similar serine proteases PR3 and NE *in vivo*, I used a previously generated mouse strain that lacks both PR3 and NE (Fröhlich, Ph.D thesis). The PR3/NE double-deficient mouse line was established by targeted gene disruption in embryonic stem cells as depicted in **Figure 4.1**. Previous characterization experiments proved the positive recombination of the PR3/NE locus by Southern blotting of embryonic stem cell clones (Fröhlich, Ph.D. thesis): PR3/NE-depleted mice showed no expression of mRNA for PR3 and NE in bone marrow cells as assessed by RT-PCR.

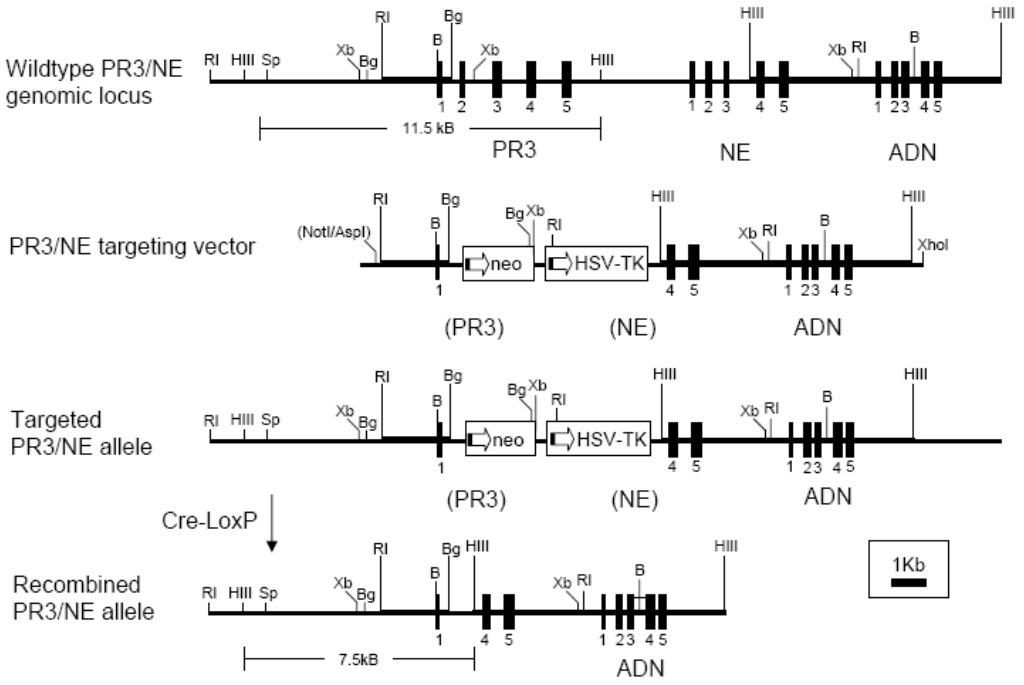

Figure 4.1 – Gene-targeting approach for the generation of PR3/NE double-deficient mice. Schematic representation of the wildtype PR3/NE locus, gene-targeting vector, targeted allele and the correctly recombined PR3/NE knockout allele. Gene-targeting results in deletion of exons 2-5 of the PR3 gene as well as exons 1-3 of the NE gene leaving the neighbored adipsin (ADN; also called complement factor D) gene unchanged.

Figure adapted from Leopold Fröhlich, Ph.D thesis (2001)

In my work, the simultaneous knockout of both serine proteases PR3 and NE was further substantiated at the level of proteolytic activity in neutrophil lysates using the PR3/NE-specific chromogenic substrate AAPV-pNA (**Figure 4.2**). This was in unison with subsequent Western blot analyses of neutrophil granule components using specific polyclonal rabbit sera (kind gift from Azzaq Belaaouaj, Reims, France), which revealed that PR3/NE-deficient neutrophils showed normal levels of CG and MPO expression, while they totally lacked PR3 and NE (**Figure 4.3A**). This clearly confirmed the successful and selective knockout of PR3 and NE in these mutant mice.

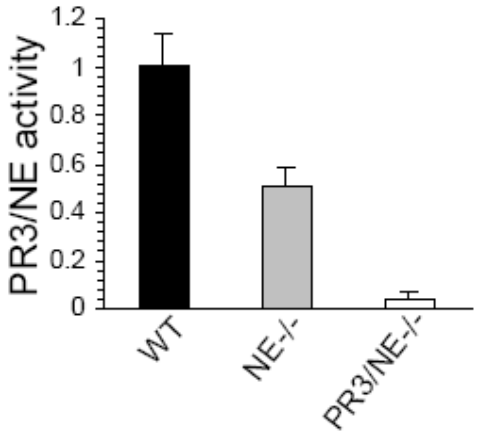

Figure 4.2 – PR3/NE-null neutrophils completely lack PR3/NE enzymatic activity. PR3/NE enzyme activity of the neutrophil lysates was measured in triplicates using a PR3/NE specific chromogenic substrate (BAPN-TBE) after 15 min incubation. The measured OD values were normalized by the average OD produced by WT neutrophil lysates. Data is shown as mean +/- SD of triplicates. Compared to WT lysates, NE-/- neutrophils show ~50% residual activity. No activity was observed in PR3/NE-negative neutrophils.

A number of previous studies suggested that PR3 and NE may play an important role in neutrophil development in the bone marrow (El Ouriaghli et al., 2003; Skold et al., 1999; Bories et al., 1989), hence I further evaluated neutrophil maturation in PR3/NE-deficient mice. In contradiction to these reports, I found unchanged neutrophil morphology with normally lobulated nuclei in the absence of PR3/NE (**Figure 4.3B**). Moreover, regular $CD11b^{+}/Gr\text{-}1^{hi}$ neutrophil populations were revealed by flow cytometry in the peripheral blood of the mutant mice (**Figure 4.3C**). Hence, the proteases are not crucially involved in granulopoiesis and ablating PR3 and NE in the germ line represents a valid approach to assess their biological significance *in vivo*.

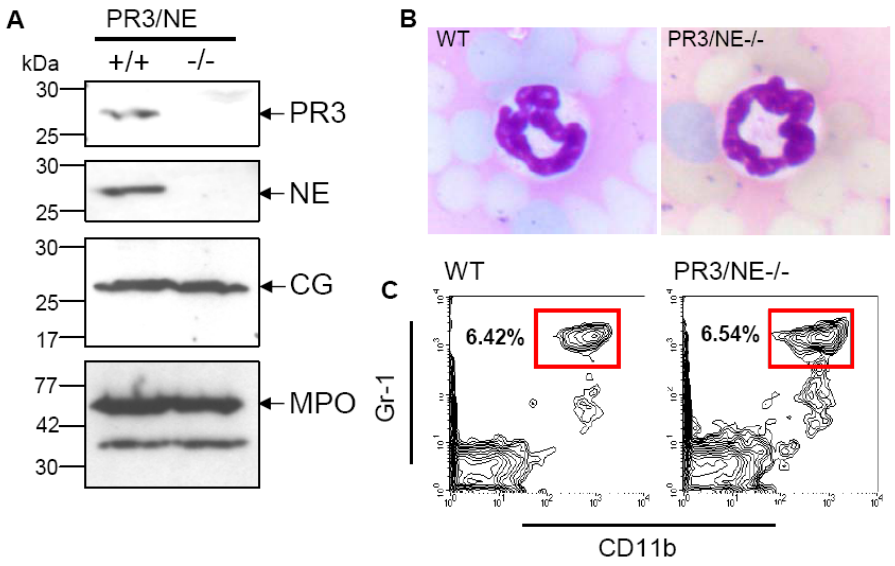

Figure 4.3 – Normal neutrophil maturation in the absence of PR3 and NE. (**A**) Neutrophils isolated from WT (+/+) and PR3/NE-deficient mice (-/-) were lysed and subjected to Western blot analysis. While no band was detected for PR3 or NE in the mutant mice, normal expression of CG and MPO was found in PR3/NE -/- mice. Molecular weight marker sizes are indicated in kDa on the left side. (**B**) Blood smears were prepared from WT and PR3/NE-deficient mice and analyzed by light microscopy using a 20x objective. Normal neutrophil morphology (lobulated nucleus) was observed in PR3/NE-deficient mice. (**C**) Neutrophil maturation was evaluated by flowcytometry of peripheral blood leukocytes by double staining of the Gr-1 marker in combination with CD11b. Neutrophil locate to the $CD11b^{+}/Gr1^{hi}$ population (red box). No difference was observed between WT and mutant mice regarding the percentage of the $CD11b^{+}/Gr1^{hi}$ population.

4.1.2 Normal extravasation of PR3/NE-deficient neutrophils

To examine neutrophil infiltration into the perivascular tissue, I applied croton oil, a natural source of phorbol-esters, to the mouse ears of WT (n = 4) and PR3/NE-depleted (n = 4) mice. Phorbol-esters are strong activators of the protein kinase C (PKC) pathway in, for example, immune cells, which trigger rapid recruitment of neutrophils to the site of application. Four hours post croton oil application, the mouse ear tissue was subjected to a whole mount immunofluorescence staining for laminin (LN) as a major component of the endothelial basement membrane (EBM), and Gr-1 to identify neutrophils. I assessed the neutrophil distribution in relation to the EBM by immunofluorescence microscopy of fixed whole mount specimens (**Figure 4.4A**). If PR3 and NE were necessary to open the EBM for extravasation, I would have

expected an accumulation of neutrophils (red) inside the EBM (green) of the blood vessels. However, I found that PR3/NE-deficient neutrophils had transmigrated into the interstitium without retention at the EBM (**Figure 4.4B**) resulting in quantitatively normal and widespread neutrophil influx compared to WT mice (**Figure 4.4C**). Based on this observation, I concluded that PR3 and NE are dispensable for the extravasation of neutrophils.

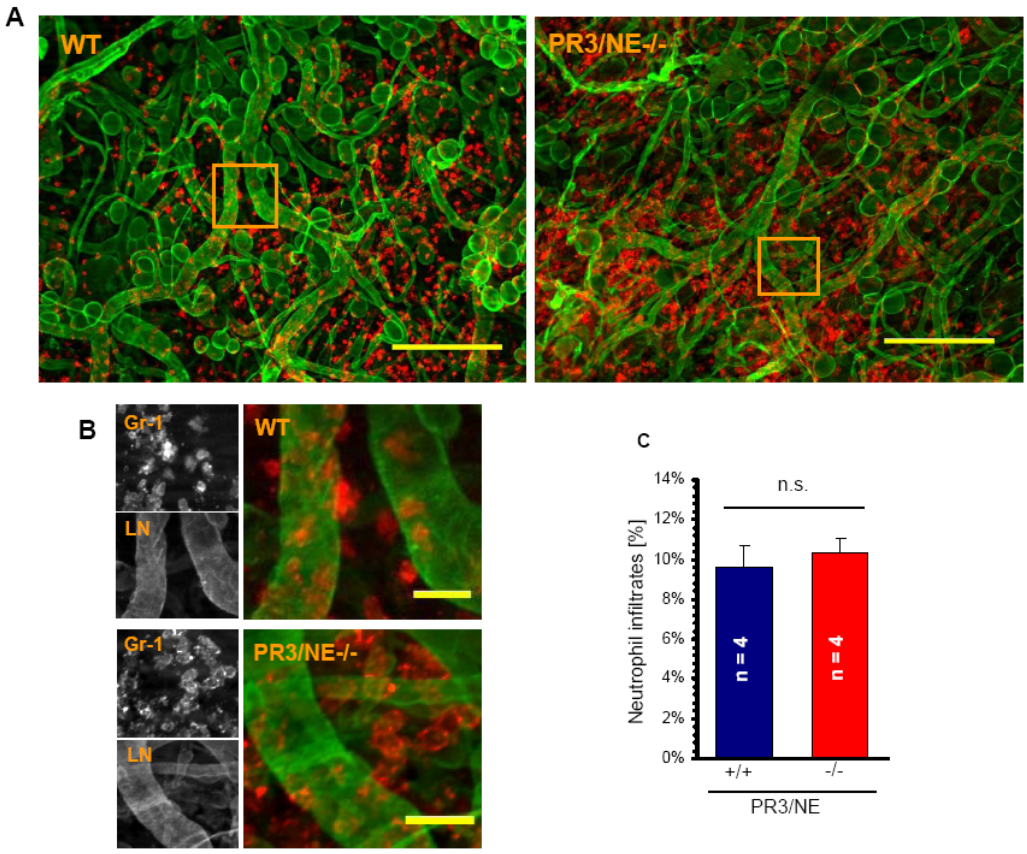

Figure 4.4 – PR3 and NE are dispensable for neutrophil extravasation. Inflammation was triggered in the ears of WT (n = 4) and PR3/NE-deficient mice (n = 4) using croton oil (phorbol-esters). After four hours, the ear tissue was subjected to immunofluorescence staining for laminin (LN; green) to stain EBM and for Gr-1 (red) to identify neutrophils. Both genotypes developed strong and widespread neutrophilic inflammation. Scale bar represent 200 µm (**A**). No retention of neutrophils inside the EBM was observed in PR3/NE-deficient mice when analyzed in higher magnification; scale bar = 25 µm (**B**). Overall neutrophil infiltrates were quantified as percentage of Gr-1 positive cells per microscopic field, while the intravascular signal was excluded. Data are mean +/- SEM. No difference was found between WT and PR3/NE-deficient mice (**C**).

4.1.3 Neutrophil chemotaxis is independent from PR3 and NE

The data presented in **Figure 4.4** showed widespread neutrophil infiltrations at the site of inflammation even in the absence of PR3 and NE suggesting that the proteases were not required for interstitial cellular migration. I further addressed this suggestion and analyzed a potential role of PR3 and NE in neutrophil chemotaxis and migration through the extracellular matrix of the interstitium using an *in vitro* approach. Therefore, isolated neutrophils were embedded in three dimensional collagen matrices. To induce chemotaxis, I placed C5a on top of the matrix and analyzed neutrophil chemotaxis by light microscopy. Neutrophils from both WT and PR3/NE-null mice readily migrated towards the C5a gradient (**Figure 4.5A**). I observed unhampered chemotactic migration of isolated PR3/NE-negative neutrophils through a three-dimensional collagen meshwork *in vitro* regarding directionality (**Figure 4.5B**) as well as velocity (**Figure 4.5C**) of the cells. These findings indicated that PR3 and NE are not principally required for interstitial migration.

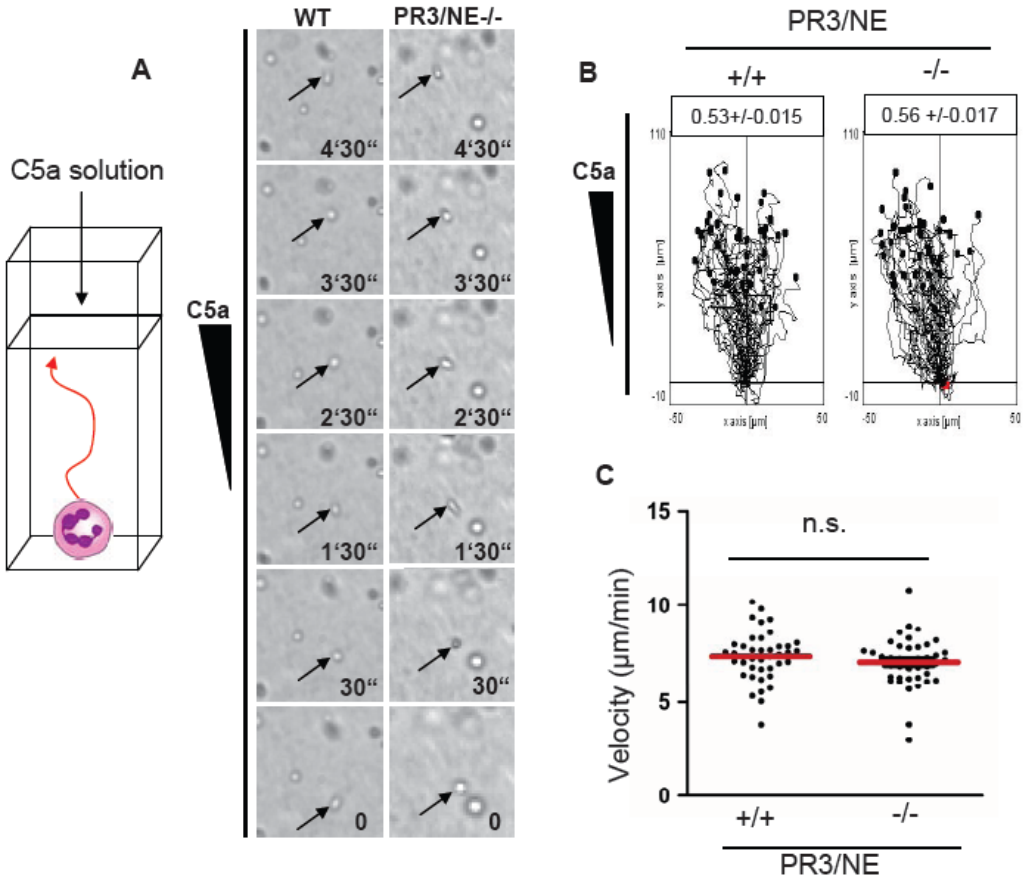

Figure 4.5 – Normal neutrophil chemotaxis in the absence of PR3 and NE. (**A**) Scheme depicts experimental procedure: neutrophils were embedded in three-dimensional collagen gel and chemotactic C5a was applied in solution on top of the matrix. *In vitro* migration of WT and PR3/NE-deficient neutrophils directed by C5a through collagen matrices was analyzed by time-lapse video microscopy and migrating neutrophils (arrow) were tracked (**D**) The tracks of WT (n = 41) and PR3/NE-deficient (n = 42) neutrophils are shown, and the factor for directionality +/- SEM is indicated. No impairment was observed regarding chemotactic directionality of PR3/NE-deficient versus WT neutrophils (P = 0.19). (**E**) Velocities of single cells (individual points) were calculated and averaged (red bar). PR3/NE-/- neutrophils showed no significant difference versus WT cells (P = 0.30).

4.1.4 Impaired IC-mediated inflammation in PR3/NE-null mice

The formation of immune complexes (ICs) represents an important trigger of neutrophil-dependent inflammation in many human diseases (Jancar and Sanchez, 2005). To determine the role of PR3 and NE in this context, a classical model of

subcutaneous IC-mediated inflammation, namely the reverse passive Arthus reaction (RPA; see (Arthus and Breton, 1903), was induced in WT and PR3/NE-deficient mice. To this end, anti-ovalbumin (OVA) antibodies were deposited intradermally and subsequently the antigen OVA was applied systemically via the tail vein. At the site of antibody deposition in the skin, ICs are formed and the inflammatory reaction occurs.

Four hours after RPA induction by applying the OVA solution, I assessed the cellular inflammatory infiltrates by histology using H&E-stained skin sections (**Figure 4.6A;** upper panel). Neutrophils, which were additionally identified by Gr-1 immunohistochemistry, made up the vast majority of all cellular infiltrates at the relatively early four hours time point (**Figure 4.6A**; lower panel). However, I found that neutrophil infiltration to the sites of IC-formation was severely diminished in PR3/NE-null mice. Histological quantification revealed a significantly reduced neutrophil influx in PR3/NE double-deficient mice compared with WT mice, while NE single-deficient mice showed only marginally reduced neutrophil counts (**Figure 4.6B**). Together, these results indicate that PR3 and NE fulfill an important pro-inflammatory function during IC-mediated inflammation.

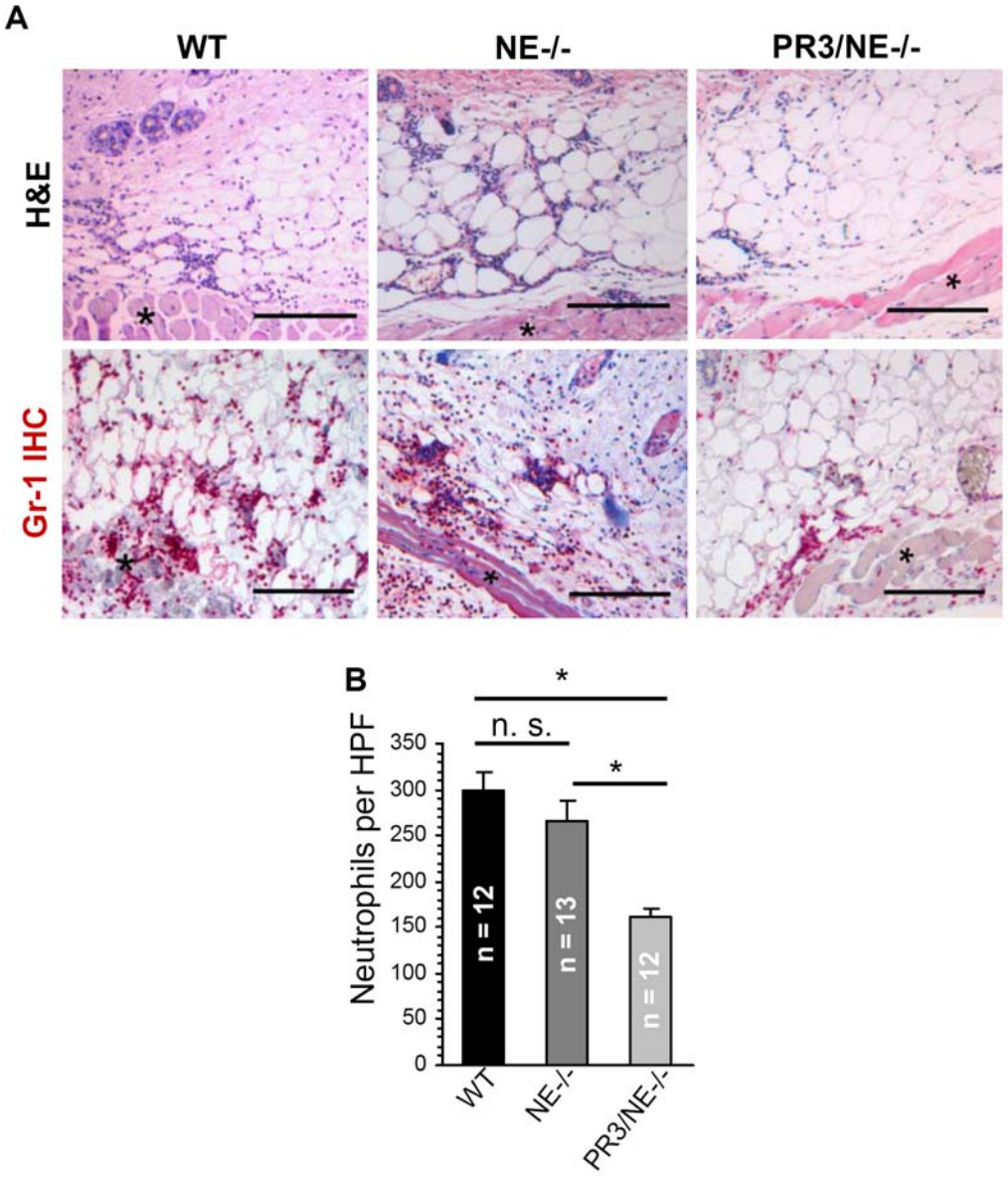

Figure 4.6 – Reduced neutrophil infiltration to the sites of IC-deposition in PR3/NE-deficient mice. (**A**) Representative photomicrographs of inflamed skin sections 4 hours after IC formation. Neutrophils were identified morphologically (polymorphic nucleus) in H&E stainings and by Gr-1 staining (red). The cellular infiltrates were located to the adipose tissue next to the panniculus carnosus muscle (asterisks) and were primarily composed of neutrophil granulocytes. Scale bars: 200 µm. (**B**) Neutrophil infiltrates in lesions from PR3/NE-deficient mice were significantly diminished compared with NE single-deficient and WT mice. Neutrophil influx in NE-deficient mice was marginally, but not significantly diminished compared with WT mice. Results are mean +/- SEM infiltrated neutrophils per high power field (HPF). *$P < 0.05$.

4.1.5 PR3 and NE enhance neutrophil activation by ICs *in vitro*

As I found in my work, PR3 and NE were required for the inflammatory response to ICs (**Figure 4.6**), but not to phorbol esters (**Figure 4.4**). Hence, I considered the enzymes as direct regulators of the neutrophil response to ICs. To test this consideration, the oxidative burst as a read-out for cellular activation was determined using dihydrorhodamine (DHR), a dye that becomes fluorescent upon oxidation. Based on a previously described procedure (Raptis et al., 2005), I set up an *in vitro* assay for the activation of neutrophils by ICs. To this end, ovalbumin (OVA) was coated on microtiter plates and treated with anti-OVA rabbit serum. Neutrophils recognize ICs via specific surface receptors (**Figure 2.3**) leading to activation of phagocyte oxidase (phox) as the downstream effect of a signal transduction cascade. Therefore, the activity of the phagocyte oxidase, *i.e.* oxidative burst, was measured over time by detecting ROS using the DHR dye. I measured the ROS production of isolated, TNFα-primed neutrophils in the presence of ICs *in vitro*. The IC-specific burst was determined by subtracting the background response of TNFα-stimulated neutrophils on only OVA-coated surfaces from the oxidative burst exhibited on Ova/anti-Ova ICs (**Figure 4.7**).

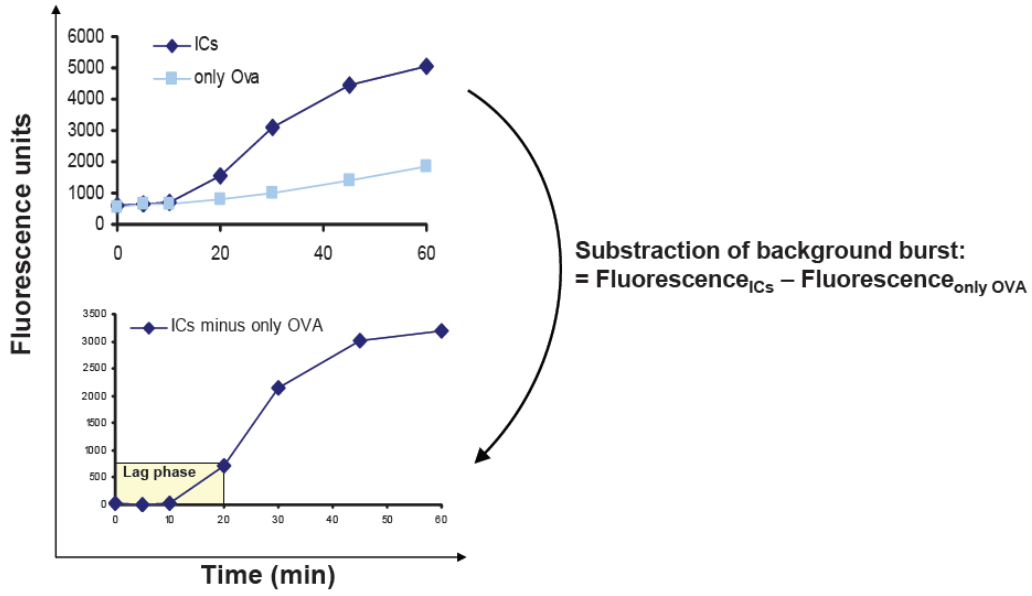

Figure 4.7 – Measurement of the IC-specific oxidative burst of neutrophils. Neutrophils isolated from the mouse bone marrow were TNFα-primed and subjected to ICs (dark blue curve) and only Ova (light blue curve) as a negative control. The IC-specific burst was determined by subtracting the fluorescence on ICs from the fluorescence on only Ova for each time point. This results in an oxidative burst curve (lower graph) that shows an initial lag phase of ~20 min until the burst commences.

Using this setup, the oxidative burst was compared between WT and PR3/NE-deficient neutrophils. While both WT and PR3/NE-deficient neutrophils showed a similar lag phase before the oxidative burst commenced (~20 min), the ROS production over time was markedly reduced by 30-40% in the absence of PR3 and NE (**Figure 4.8A**). By contrast, oxidative burst triggered by 25 nM phorbol-ester (PMA) was unhindered in PR3/NE-/- neutrophils (**Figure 4.8B**), indicating that there was no general defect in producing ROS. I also performed a titration series ranging from 0.1 to 50 nM PMA and found no reduction in oxidative burst activity in PR3/NE-deficient neutrophils irrespective of the PMA concentration used (**Figure 4.8C**). These data are consistent with our *in vivo* experiments showing that neutrophil influx to ICs was impaired (**Figure 4.6**), whereas the inflammatory response to phorbol esters was normal in PR3/NE-null mice (**Figure 4.4**).

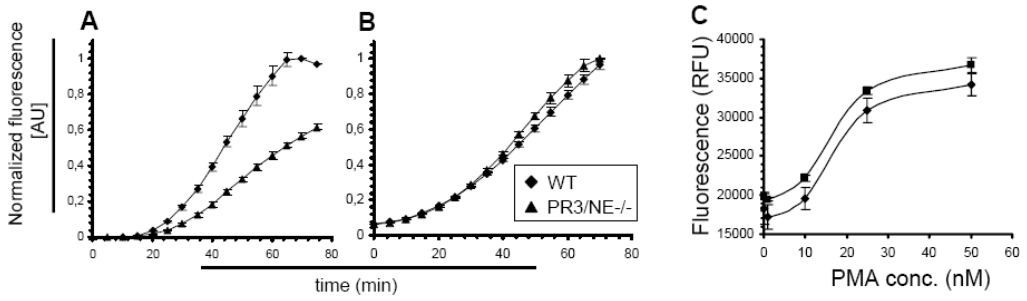

Figure 4.8 - Impaired oxidative burst by IC-activated PR3/NE-deficient neutrophils. Oxidative burst as the readout for neutrophil activation by ICs was measured over time. (**A**) While no difference was observed during the initial 20-min lag phase of the oxidative burst, PR3/NE–/– neutrophils exhibited diminished ROS production over time compared with WT neutrophils. (**B**) Bypassing receptor-mediated activation using 25 nM PMA restored the diminished oxidative burst of PR3/NE–/– neutrophils. Results are presented as normalized fluorescence in AU (arbitrary units relative to maximum fluorescence produced by WT cells). Data (mean ± SD) are representative of 3 independent experiments each conducted in triplicate. (**C**) Neutrophils were activated by PMA at concentrations ranging from 0.1 to 50 nM. After one hour of stimulation, no difference of ROS production was detected between WT and PR3/NE-deficient neutrophils. Data is representative of 3 independent experiments and SD of triplicates is shown.

4.1.6 PR3 and NE are not involved in neutrophil priming or adhesion to ICs

One explanation for the reduced oxidative burst in the presence of ICs could be that TNFα priming of neutrophils was defective when PR3 and NE are lacking. TNFα triggers the rapid transport of Mac-1 (CD11b/CD18) receptor from secretory granules to the cell surface, where it then recognizes the C3bi part of the ICs (**Figure 2.3**). To compare neutrophil priming in WT and PR3/NE-deficient neutrophils, the cell surface expression of CD11b after 30 min of incubations at various concentrations of TNFα was analyzed. No difference was observed between WT and PR3/NE-null neutrophils (**Figure 4.9A**) indicating that TNFα-mediated priming is independent from PR3/NE function. I also considered impaired adhesion of neutrophils to IC-coated surfaces in the absence of PR3 and NE. Therefore, Calcein AM-labeled neutrophils were incubated on IC-coated microtiter plates and stringently washed after several time points and the residual fluorescence was determined using a fluorescence reader. I

observed normal neutrophil adhesion to IC-coated surfaces (**Figure 4.9B**) showing that the initial interaction and binding of neutrophils to ICs is not influenced by PR3/NE.

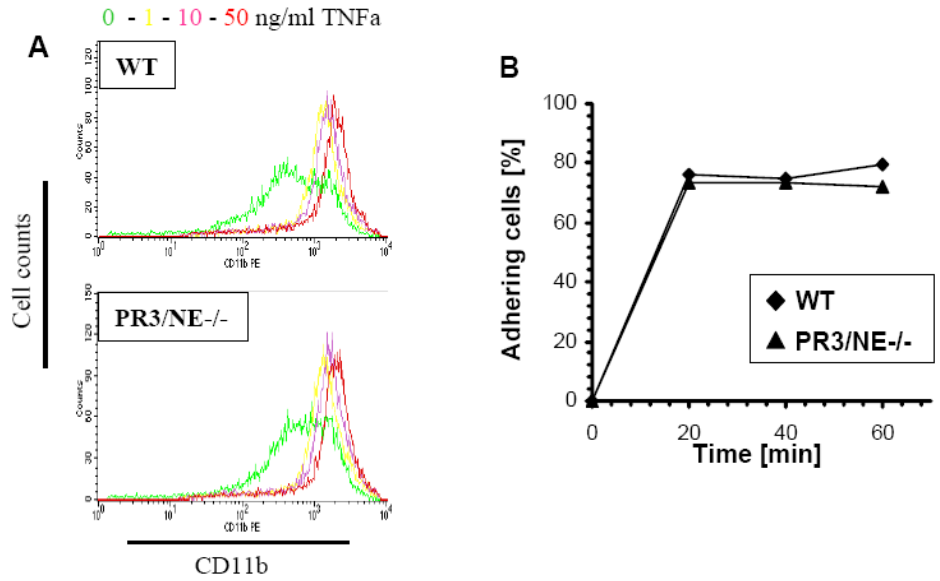

Figure 4.9 – Unaltered TNFα-priming and neutrophil adhesion to ICs of PR3/NE-deficient neutrophils. (**A**) Neutrophils were incubated with increasing concentrations of TNFα and the "priming" response was measured via the surface upregulation of CD11b using FACS. Both WT and PR3/NE-depleted neutrophils displayed a comparable upregulation of CD11b on the cell surface after 30 min indicating a normal "priming" response in the absence of PR3 and NE. **(A)** Calcein AM-labeled neutrophils were incubated on ICs in the presence of TNFα and the percentage of adherent cells was measured after washing at indicated time points. PR3/NE-/- neutrophils adhered normally to ICs. Data is representative of three independent experiments.

4.1.7 Integrin clustering and cytoskeletal reorganization

Neutrophil activation by ICs rapidly triggers integrin clustering on the cell surface as well as cytoskeletal reorganization inside the cells. Hence, I next dissected the IC-triggered Mac-1 integrin (CD11b/CD18) clustering on the cell surface as well as reorganization of the actin cytoskeleton by immunofluorescence microscopy and compared between WT and PR3/NE-deficient neutrophils. Indeed, the pattern of CD11b at the interface between neutrophils and IC-coated surfaces was found to be less clustered in PR3/NE-lacking neutrophils (**Figure 4.10A**). In addition, the actin cytoskeleton was analyzed using phalloidin-TRITC, which binds to filamentous (F)-

actin with high affinity and therefore allows to visualize the cytoskeleton in fixed cells. The actin cytoskeleton showed altered reorganization in response to IC encounter, when PR3 and NE were lacking (**Figure 4.10B**).

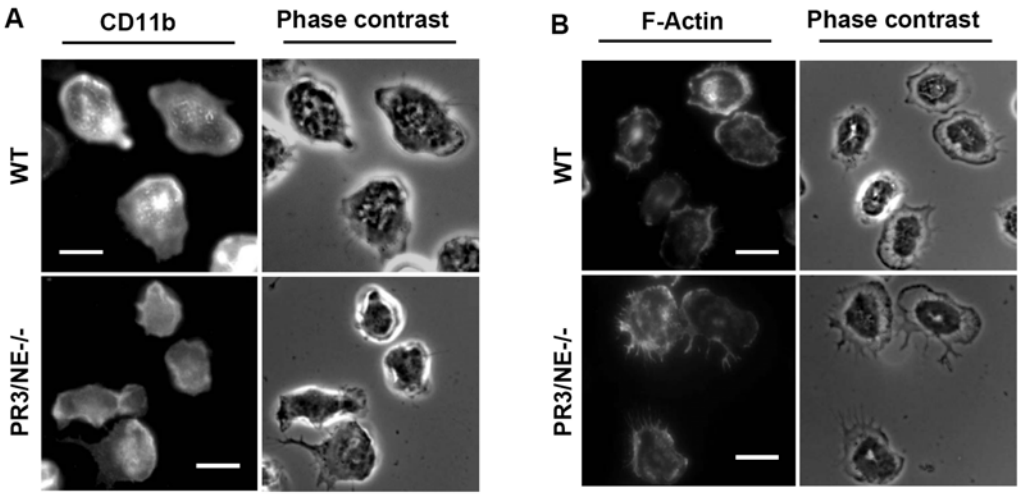

Figure 4.10 – Integrin clustering and actin reorganization on ICs is altered in the absence of PR3 and NE. Isolated, bone marrow-derived neutrophils from WT and PR3/NE-lacking mice were primed with TNFα, fixed after one hour incubation on IC-coated glass and immunostained for CD11b (**A**) and F-actin (**B**). Representative pictures were taken with 40x objective and show defective integrin clustering (**A**) and altered cytoskeletal reorganization (**B**) in PR3/NE-/- neutrophils. Scale bar represents 5 µm.

These observations support the hypothesis that PR3 and NE enhance early events of adhesion-dependent neutrophil activation that occur after TNFα priming and binding of ICs but before or during integrin clustering and cytoskeletal reorganization events. It is important to note, that NE single-deficient neutrophils were previously shown to react normally in the same setup (Raptis et al., 2005). Regarding the highly similar cleavage specificities of both proteases, I expected that PR3 and NE complemented each other during the process of neutrophil activation and inflammation.

4.1.8 PGRN is a crucial substrate of PR3 and NE

This reasoning prompted me to search for substrates that are processed by both PR3 and NE and, thereby, are able to enhance neutrophilic activation. In a previous study, PGRN has been described as a potent inhibitor of the adhesion-dependent oxidative

burst of human, TNFα-primed neutrophils *in vitro*, which can be inactivated by NE (Zhu et al., 2002). In the following paragraphs, I addressed the question whether PGRN may be a critical substrate of both PR3 and NE during neutrophil activation and inflammation.

4.1.8.1 Production of recombinant mouse PGRN

In these studies, I used both human PGRN (kindly provided by Prof. Andrew Bateman, Canada) as well as mouse PGRN. The murine variant of PGRN was produced recombinantly by transient expression in H5 insect cells (kind gift from Dr. M. Sixt, Max Planck Institute of Biochemistry) as detailed in the methods section (**3.3.1)**. The transfection efficiency was controlled by the co-transfection of the same vector (pIEx5) expressing GFP (**Figure 4.11A**). FACS analysis of tranfected insect cells revealed an approximate transfection rate of 50% (data not shown). Using peroxidase-coupled S-protein, which specifically interacts with the N-terminal S-tag of recombinant mouse PGRN, I detected substantial amounts of mouse PGRN in the supernatant of transfected, but not of untransfected cells or supernatant after S-protein treatment (**Figure 4.11B**). By silver nitrate-stained SDS-PAGE, I found only albumin contamination (~60 kD) in the PGRN purification using the S-protein column (**Figure 4.11C**). Albumin is a very abundant protein in all serum-containing cell media. In the following PGRN reconstitution experiments, I used serum-containing RPMI medium. Thus the albumin contamination in the PGRN preparation can be completely tolerated. By Western blot analysis using a sheep anti-mouse PGRN antibody, a prominent band was readily detected in the supernatant (SN) of transfected insect cells, while no signal was obtained in the SN of untransfected cells (**Figure 4.11D**). Western blot with control antibody, unspecific sheep IgG, yielded no signal, showing that the anti-mouse PGRN detection antibody was specific.

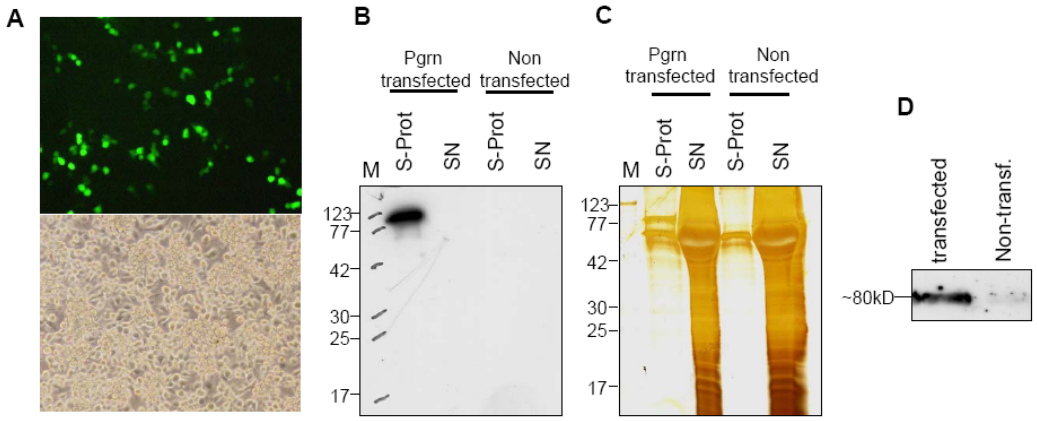

Figure 4.11 – Recombinant mouse PGRN production in H5 insect cells. (**A**) Transfection efficiency was monitored by positive control transfection of the same vector containing a GFP-expressing gene resulting in approximately 50% of green fluorescent insect cells. (**B**) Mouse PGRN expression was controlled using S-Protein-HRP detection by Western blot resulting in a clear band at ~80 kD equivalent with the calculated molecular weight of mouse PGRN. (**C**) Silver-stained SDS-PAGE showed enrichment of a band at around 80 kD most likely depicting recombinant mouse PGRN. (**D**) Mouse PGRN expression was proven using anti-mouse PGRN Western blot of cell culture supernatants, which revealed a positive signal only in the samples harvested from transfected cells.

4.1.8.2 PGRN degradation is defective during IC-activation in PR3/NE-null neutrophils

Since I observed a significant reduction of oxidative burst activity in PR3/NE-deficient neutrophils compared to WT cells (**Figure 4.8**), I evaluated a potential link between PGRN cleavage and oxidative burst of neutrophils activated by ICs. To corroborate this, I analyzed the culture supernatant (SN) as well as the cellular pellet of IC-activated neutrophils for the presence of PGRN by Western blot (**Figure 4.12**). Indeed, the inhibitory, intact form of PGRN was detected only in the SN of PR3/NE-/- neutrophils. I also found a cellular pool of PGRN in all genotypes, which was more abundant in PR3/NE-/- cells than in WT and NE-/- neutrophils. This led me to conclude that PGRN was released and degraded by PR3 and NE during neutrophil activation in WT neutrophils, while this process was defective when PR3 and NE were both lacking.

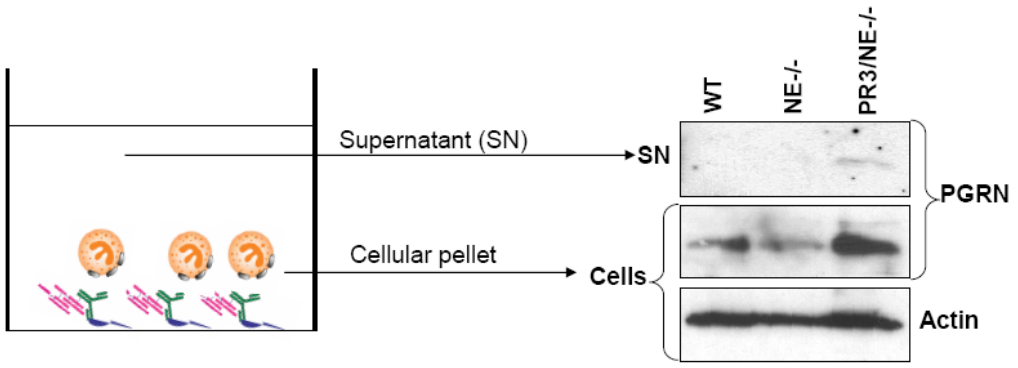

Figure 4.12 – PGRN-degradation is defective during IC-activation, when both PR3 and NE are absent. Isolated mouse neutrophils were activated by ICs *in vitro* and tested for PGRN degradation by Western blot. In the cellular fraction, the PGRN (~80 kDa) signal was markedly increased in PR3/NE-lacking cells compared with WT and NE single-deficient neutrophils. Intact PGRN was present in the supernatant (SN) of IC-activated PR3/NE-/- neutrophils only, not of WT or NE-/- cells.

4.1.8.3 PGRN inhibits neutrophil activation by ICs *in vitro*

To test if the reduced oxidative burst of PR3/NE-negative neutrophils can be caused by defective PGRN-degradation, I approximated the amount of cell-associated and secreted PGRN detected by Western blot (**Figure 4.12**). I tested whether these concentrations inhibited the IC-mediated oxidative burst of WT neutrophils, when added exogenously to the cells *in vitro*. Indeed, when 100 nM PGRN was applied to WT granulocytes activated by ICs, the ROS response was markedly decreased (**Figure 4.13A**). In positive control experiments, neutrophil activation was unaffected by PGRN-application when stimulated with PMA (**Figure 4.13B**). These data endorse the inhibitory effect of intact PGRN on innate immune cell activation and prove that defective PGRN-degradation can cause the reduced activation of PR3/NE-deficient neutrophils by ICs.

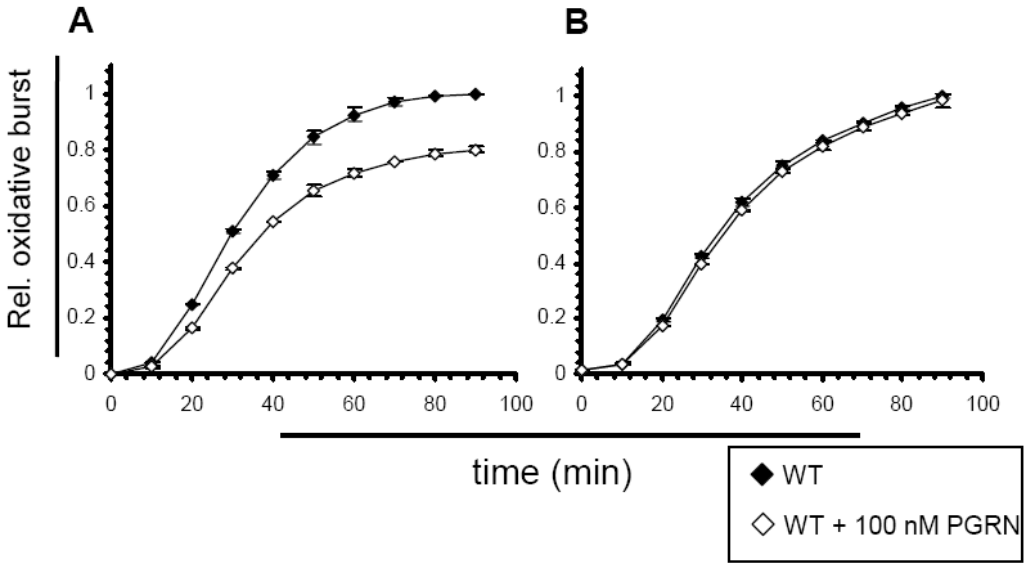

Figure 4.13 – PGRN inhibits neutrophil activation by ICs, but not by PMA. Exogenous administration of 100 nM PGRN significantly reduced ROS production of neutrophils activated by ICs (**A**), but not when activated by PMA (**B**). Data (mean ± SD) are representative of 3 independent experiments each conducted in triplicates.

4.1.8.4 Both PR3 and NE cleave PGRN *in vitro*

In previous studies, NE was proposed as the principle PGRN-converting protease. My experiments revealed an equally important role of PR3 in this pathway, since NE single-deficient neutrophils were not impaired to degrade PGRN (**Figure 4.12**). I further substantiated this concept by incubating recombinant PGRN with the purified proteases *in vitro*. Indeed, both enzymes completely degraded PGRN as early as 5 min after incubation, although the pattern of lower molecular cleavage products analyzed by silver-stained SDS-PAGE was not completely identical for both proteases (**Figure 4.14**). Hence, both PR3 and NE represent potent converters of PGRN indicating biological redundancy of the proteases in this process.

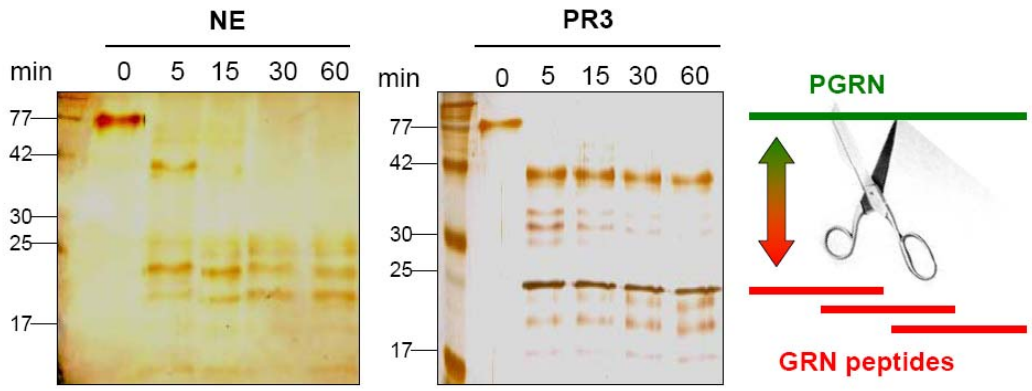

Figure 4.14 – Both PR3 and NE are PGRN-converting enzymes. Silver-stained SDS-PAGE analysis of recombinant human PGRN incubated at a 1:10 enzyme/substrate ratio with purified human NE and recombinant mouse PR3. Both NE and PR3 completely cleaved ~80-kDa PGRN to smaller molecular GRN peptides within 5 min of incubation.

4.1.8.5 PR3 and NE are the major PGRN-degrading enzymes of neutrophils

To evaluate the significance of PR3 and NE as PGRN-degrading enzymes, I next incubated recombinant mouse PGRN with neutrophil lysates from WT and protease-deficient mice. Anti-PGRN Western blot revealed that PGRN-degradation was only minimally reduced in the absence of NE, but strongly impaired when both PR3 and NE were lacking (**Figure 4.15**). This demonstrated that PR3 and NE are the major PGRN-converting enzymes of neutrophils, which is supported by previous experiments showing that CG, the third NSP of primary granules, does not cleave PGRN (Zhu et al., 2002).

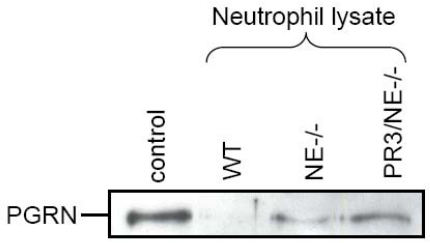

Figure 4.15 – PR3 and NE are the major PGRN degrading enzymes of neutrophils. Recombinant mouse PGRN was incubated with neutrophil lysates from WT, NE-/- and PR3/NE-/- mice for one hour at 37°C and analyzed by anti-mouse PGRN Western blot. Compared with untreated PGRN (control), WT neutrophils completely degraded PGRN. In NE-null neutrophils, a faint band of intact PGRN was detected, while in PR3/NE-deficient neutrophils, a distinct PGRN band remained, comparable to control.

4.1.8.6 PGRN inhibits IC-mediated inflammation *in vivo*

In search for *in vivo* evidence for the relevance of PGRN as an anti-inflammatory mediator, I exogenously administered 2 µg recombinant PGRN to the reverse, passive Arthus reaction. PGRN-treated lesions were directly compared to non-treated lesions in the same mouse (**Figure 4.16**). In both WT and PR3/NE-/- mice, neutrophil accumulation was significantly diminished at the PGRN-treated sites of IC-mediated inflammation, demonstrating that PGRN is a crucial inhibitory factor for neutrophilic inflammation. Neutrophil infiltration was reduced by a greater extent in the PR3/NE-deficient animals (by 40%; $p<0.01$; **Figure 4.16C**) than in WT mice (by 25%; $p<0.05$; **Figure 4.16B**), which likely reflected the impact of the PGRN-degrading proteases in this pathway.

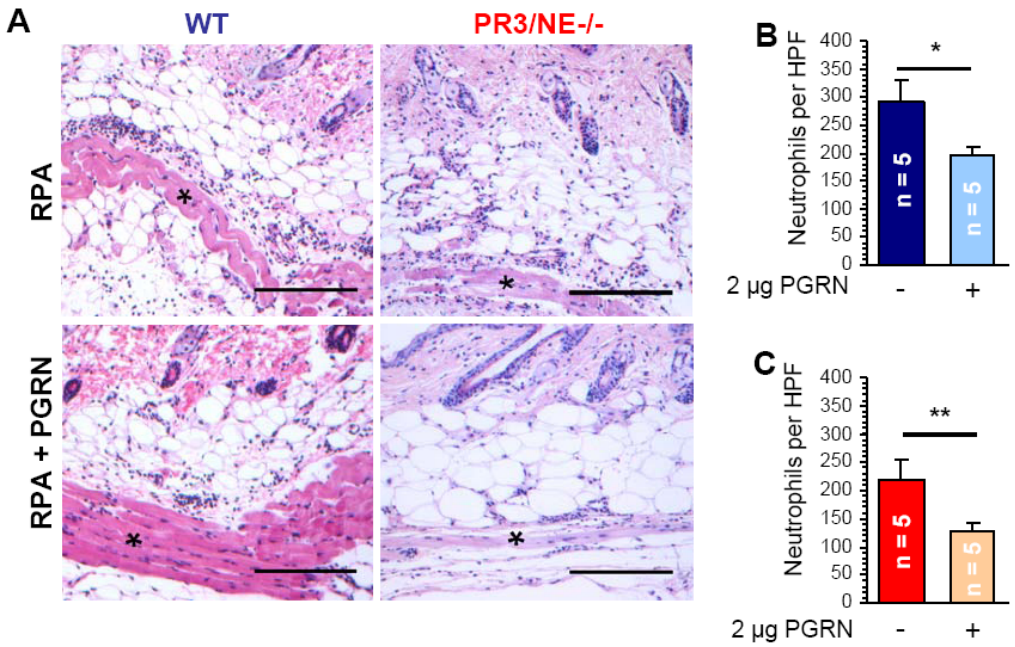

Figure 4.16 – PGRN is a potent inhibitor of IC-mediated inflammation *in vivo*. Recombinant mouse PGRN (2 µg) was intradermally applied with anti-OVA IgG, and the RPA was started in WT and PR3/NE-null mice (n = 5 per group). (**A**) After four hours, the effect of PGRN application was evaluated by histological analyses. Representative images show neutrophil infiltrates at the panniculus carnosus muscle (asterisks). Scale bars: 200 µm. (**B** and **C**) Effect of PGRN administration on neutrophil influx. In both WT (**B**) and PR3/NE-deficient (**C**) mice, neutrophil infiltration was significantly diminished at PGRN-treated sites compared with untreated sites. This effect appeared to be more pronounced in the protease-deficient mice. Data are mean ± SEM infiltrated neutrophils per HPF. *P < 0.05; **P < 0.01.

4.1.8.7 PR3 and NE cleave PGRN during inflammation *in vivo*

Finally, I aimed to analyze PGRN-degradation in PR3/NE-null mice during neutrophilic inflammation *in vivo*. For practical reasons, I harvested infiltrated neutrophils from the inflamed peritoneum four hours after casein injection and subjected the lysates of these cells to anti-PGRN Western blot. Intact, inhibitory PGRN was only found in PR3/NE-/- neutrophils, while it was not detectable in WT cells (**Figure 4.17**). These data proved that neutrophilic inflammation was accompanied by proteolytic removal of anti-inflammatory PGRN and that the process of PGRN-degradation is essentially impaired *in vivo* in the absence of PR3 and NE.

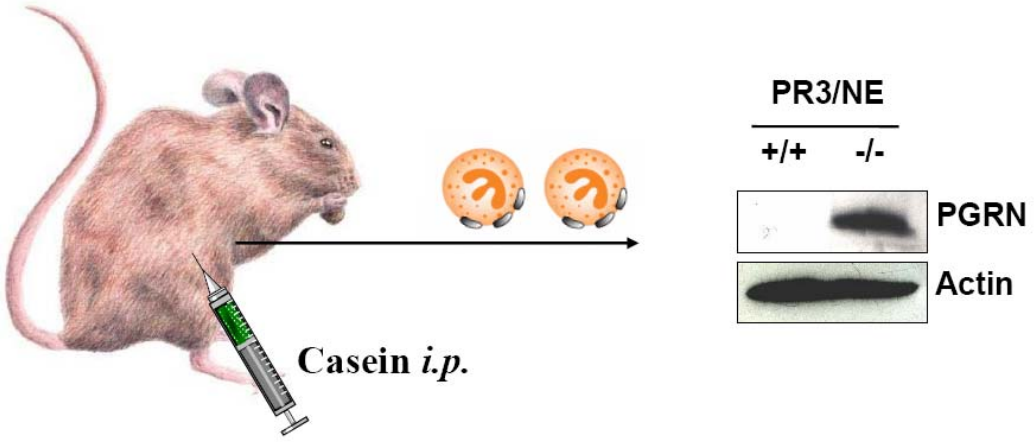

Figure 4.17 – PGRN-degradation is defective in PR3/NE-deficient mice during inflammation *in vivo*. Peritoneal inflammation was induced by *i.p.* injection of 9% casein in PBS and, after four hours, neutrophils isolated *ex vivo* from inflamed peritoneum of WT and PR3/NE-/- mice were analyzed by anti-mouse PGRN Western blot of concentrated neutrophil lysates. Intact PGRN was found abundantly in PR/NE-deficient, but not in WT neutrophils. Loading was controlled using anti-actin Western blot.

4.2 Autoimmunity against PR3 in small-vessel vasculitis

The small-vessel vasculitides (SVV) Wegener´s granulomatosis (WG) and microscopic polyangiitis (MPA) are autoimmune diseases associated with autoantibodies, so called ANCAs, directed against the neutrophil antigens PR3 and MPO, respectively. Although known for many decades, the chronic autoimmune response against these neutrophil components is puzzling to the many scientists working on autoimmunity. In my studies, I analyzed whether a recently discovered, alternative cell death program of neutrophils, namely NETosis (Brinkmann et al., 2004), might be implicated in the development and perpetuation of the humoral autoimmune response against PR3 and MPO.

4.2.1 Autoantibodies from SVV patients trigger NETosis

ANCAs can bind to PR3 or MPO on the neutrophil cell surface and trigger profound ROS formation in neutrophils (Falk et al., 1990). As ROS production was shown to be necessary for NET formation by activated neutrophils (Fuchs et al., 2007), I asked whether ANCA-activation of neutrophils may result in NETosis. To this end, isolated human neutrophils from the peripheral blood of healthy donors were primed with TNFα and were incubated with purified IgG from WG patients and from healthy donors as a negative control according to a widely used procedure established previously (Falk et al., 1990). After several time points, NET formation was determined by fluorescence microscopy analysis on the basis of morphological criteria such as faint and enlarged nuclei, colocalization of granular markers with nuclear DNA as well as extracellular DNA fiber production (Brinkmann et al., 2004; Fuchs et al., 2007). Using a DNA staining approach, I observed robust NET formation in ANCA-treated (**Figure 4.18A**), but not in control IgG-treated specimen, where the most of the nuclei still showed lobulated shape (**Figure 4.18B**), after 180 min of incubation. Quantitative analyzes of the samples revealed that ~13% of ANCA-treated neutrophils underwent NETosis, while in control IgG-treated specimen DNA release could only be detected in ~6% of neutrophils (**Figure 4.18C**). When immunostained for PR3, I observed the typical colocalization of granular proteins with the DNA of

NETs, but also inside the cell before NETs are released (**Figure 4.19D**). The effect was comparable between PR3 and MPO specific ANCAs. These observations are in line with previous reports of ANCA-induced neutrophil cell death, which was at that time interpreted as a dysregulated form of apoptosis (Harper et al., 2000). These findings that ANCAs actually trigger NETosis are consistent with previous studies showing increased levels of circulating nucleosomes in ANCA-associated SVV (Holdenrieder et al., 2006) and suggested that NETs may play a role in SVV.

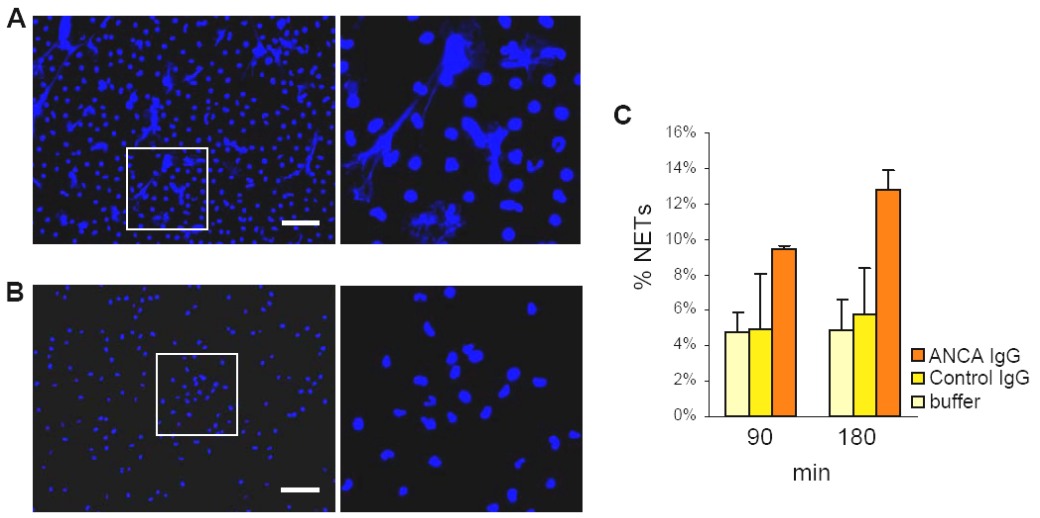

Figure 4.18 – ANCA-IgG trigger the formation of NETs. Isolated TNF-primed neutrophils analyzed by fluorescence microscopy for NET formation by DNA staining with Hoechst 33352 after treatment with IgG purified from patients with ANCA-associated SVV (n = 2; **A**) and from healthy individuals (n = 2; **B**). Scale bars represent 50 µm. The number of cells producing extracellular DNA fibers were quantified per microscopic field. ANCA-treated cells demonstrated robust NET formation after 180 min incubation while control treatment only caused background levels of cells externalizing DNA (**C**).

4.2.2 NETs display the autoantigens PR3 and MPO

It has already been shown that the anti-microbial serine protease neutrophil elastase (NE), which is stored together with and PR3 and MPO in the primary granules of neutrophils, are associated with NETs (Brinkmann et al., 2004). Indeed, by *in vitro* immunofluorescence analysis of PMA-induced NETs, I detected substantial amounts of both PR3 and MPO on the extracellular chromatin fibers (**Figure 4.19A-B**). This indicates that both autoantigens PR3 and MPO are components of NETs and that

ANCA-induced NETosis results in the release of even more of the targeted autoantigens into the extracellular environment.

Just recently, LL37 was shown to be the key factor in the autoimmune skin disease psoriasis that binds to self DNA and converts it into a dendritic cell stimulating mediator (Lande et al., 2007). Since LL37 also belongs to the neutrophilic arsenal of anti-microbial peptides and is stored in cytoplasmic granules that are known to fuse with the chromatin during NET formatin, I next tested whether LL37 is also present on NETs. By immunofluorescence, I found that LL37 is released during the process of NET formation and remains bound to the chromatin fibers (**Figure 4.19C**). However, the LL37 immunostaining revealed a punctual, rather than a homegenous, co-localization with NETs suggesting that LL37 may bind to NETs after the release of the chromatin fibers.

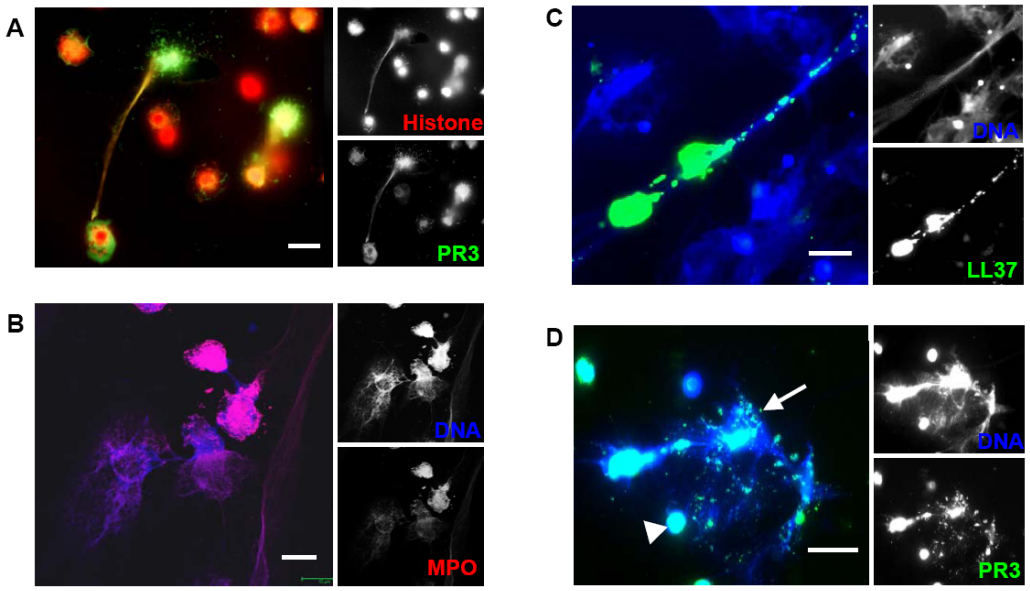

Figure 4.19 – NETs display autoantigens PR3 and MPO as well as immunostimulatory LL37. NET formation by isolated neutrophils was induced using PMA (**A-C**) or using TNFα plus PR3-ANCA (**D**). Specimens were fixed and PR3 (**A**), MPO (**B**) and LL37 (**C**) were identified by immunofluorescence. PR3 (green) was found abundantly and strongly colocalized with the chromatin of NETs as identified using histone H2a:H2b:DNA immunostaining (red) (**A**). Large amounts of MPO (red) were found in strict colocalization with extracellular DNA fibers (blue) of NETs (**B**). LL37 immunostaining (green) revealed a more punctual colocalization pattern with extracellular DNA (blue) of NETs (**C**). Co-localization of the granular marker PR3 with DNA. After 3 hours of ANCA exposure in the presence of TNFα, typical NETs were formed by neutrophils. Granular markers, here PR3 (green) as detected using the mouse anti-PR3 monoclonal antibody 4A5, colocalized with the extracellular DNA (blue) of NETs (white arrow), but also inside the cells that did not undergo NETosis (white triangle) (**D**). Scale bar equals 10 µm.

Moreover, using an ELISA approach I found that PR3 significantly bound to DNA coated but not to control protein (BSA) coated wells (**Figure 4.20**), indicating that PR3 on NETs can directly interact with DNA. This is in unison with previous results demonstrating that also NE and MPO can bind to DNA (Belorgey and Bieth, 1995; Murao et al., 1988). Hence, the granule proteins seem to associate with NETs by direct interaction with the high DNA content.

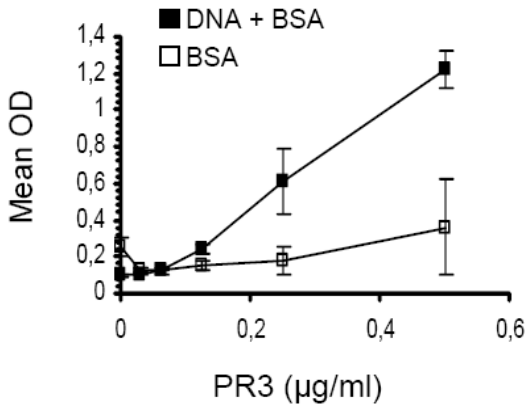

Figure 4.20 – PR3 binds to DNA. DNA was coated to microtiterplates and incubated with increasing PR3 concentrations to test DNA binding capacity of PR3. After washing, bound PR3 was identified by a specific immunoassay. PR3 demonstrated significant binding to DNA-containing wells, but not to only bovine serum albumin (BSA) coated wells, indicating that PR3 directly binds to DNA.

4.2.3 ANCAs bind to NETs

The experiments presented above clearly indicated that the autoantigens PR3 and MPO are constituents of NETs. The next question was whether the epitopes targeted by ANCAs were still accessible to autoantibodies when PR3 is bound to the DNA of NETs. Therefore, I prepared NETs *in vitro* using isolated human neutrophils stimulated by 25 nM PMA, fixed the specimen and performed an immunofluorescence staining using anti-PR3 monoclonal antibodies, a rabbit serum raised against PR3 as well as anti-PR3 containing ANCA sera from patients with Wegener´s disease. A DNA counterstaining identified the extracellular DNA fibers of the NETs. As depicted in **Figure 4.21**, all antibodies used in this assay showed reactivity with the extracellular DNA fibers, while no reactivity was observed when control sera from healthy individuals or mouse IgG isotype controls were used as the first antibody (data not shown). This indicated that the targeted epitopes are accessible to ANCAs when PR3 was bound to NETs.

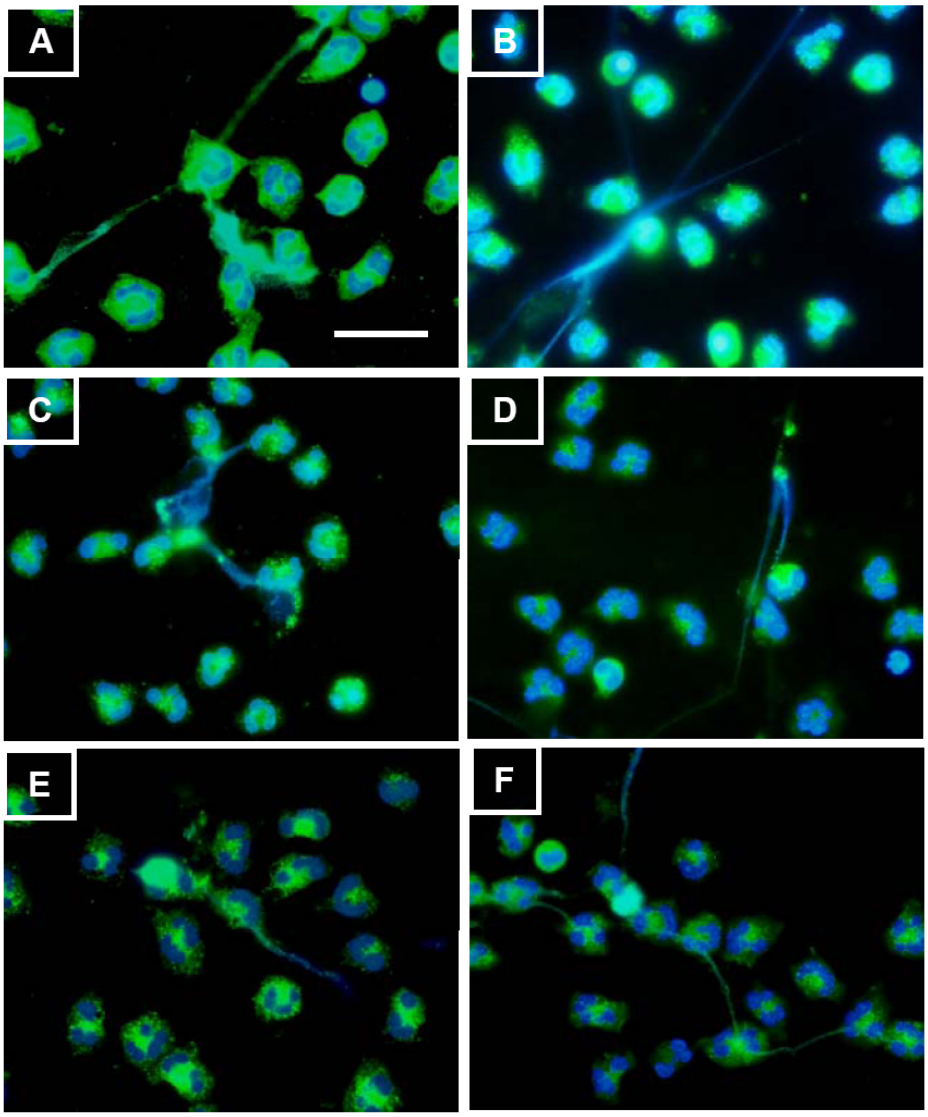

Figure 4.21 – Anti-PR3 monoclonal antibodies, rabbit sera and ANCAs bind to NETs. Immunofluorescence analysis of NETs using rabbit anti-PR3 serum (**A**), anti-PR3 mouse mAbs clones 6A6 (**B**), 3A6 (**C**) and 4A5 (**D**) as well as the ANCA sera from two WG patients (**E-F**) bind to PR3 on PMA-induced NETs to a comparable degree. Scale bar represents 25 µm.

4.2.4 Identification of NETs displaying autoantigens in patients with autoimmune SVV

To find evidence that NETosis actually occurs in autoimmune vasculitis patients, I next analyzed kidney biopsies from SVV patients that suffer from glomerulonephritis, *i.e.* non-infectious inflammation of the kidneys with profound neutrophil infiltration,

which is a common hallmark of both WG and MPA (Kallenberg et al., 2006). Needle biopsies from affected kidneys of five patients with WG and two patients with MPA (kindly provided by Dr. Walter Back, Pathology Department of the Klinikum Mannheim) were analyzed by *in situ* immunofluorescence microscopy at the Max Planck Institute of Infectious Biology in Berlin in collaboration with Dr. Volker Brinkmann. NETs were defined by co-localization of histone protein, DNA and granular markers using antibodies for histone protein, MPO or NE and DNA dyes. This allows for differentiating NETs from extracellular DNA formed by necrotic cells, which would not display granular markers. Indeed, NET structures were found both in patients with WG and MPO (**Fig. 4.22A-B**). The chromatin fibers co-localizing with granular markers were mostly present in close proximity to infiltrated neutrophils inside the glomeruli of the kidney. NETs displaying the targeted autoantigens were especially abundant in cases with severe glomerulonephritis lesions and were located inside glomeruli with strong neutrophil infiltration (**Figure 4.22C-D**).

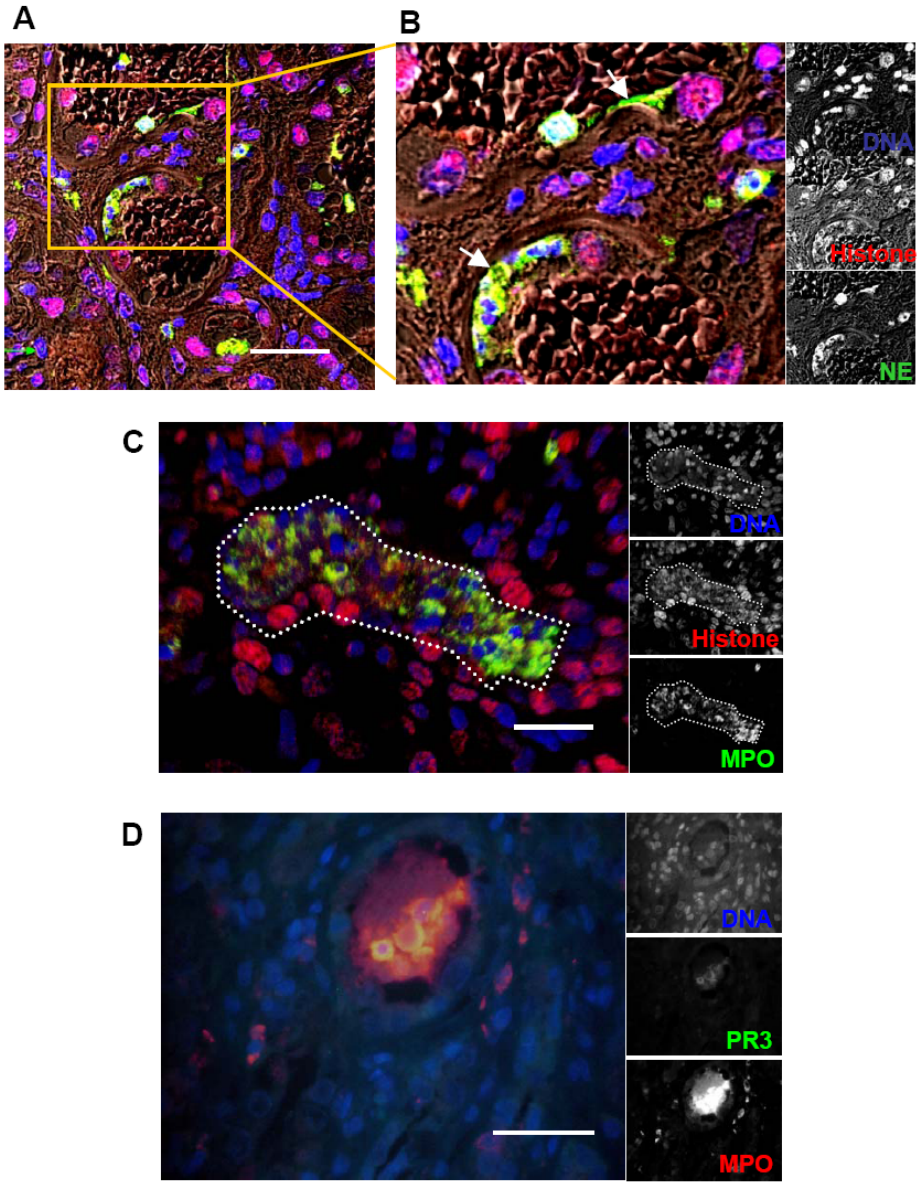

Figure 4.22 - NETs deposition in the inflamed kidney of patients with autoimmune SVV. Biopsies from the inflamed kidneys of SVV patients were subjected to immunofluorescence analysis. (**A**) NETs were identified by colocalization of DNA (blue), histone (red) and the granular marker neutrophil elastase (NE; green). Tissue structure was visualized by differential interference contrast (DIC). (**B**) Higher magnification of boxed area revealed co-localization of all three markers (white arrows) indicating the formation of NETs in the inflamed kidney. (**C**) Immunostaining of MPO (green) as one of the principle autoantigens in SVV on NETs *in situ*. An extented area showing colocalization of DNA, histone and MPO (white dotted area) indicating that NETs display the targeted autoantigen extracellularly in the inflamed kidneys of patients suffering from SVV. Colocalization of MPO (red), PR3 (green) and DNA (blue) identifies these antigen deposits as components of NET structures inside the glomerulus (**D**). Scale bars equal 25 µm.

As depicted in **Figure 4.19C**, I found that LL37 partially co-localized with NETs *in vitro*. Importantly, the immunostimulatory peptide LL37 was also found by *in situ* immunofluorescence in the inflamed kidney, where it was located to neutrophil-enriched sites and partially colocalized with NETs (**Figure 4.23**).

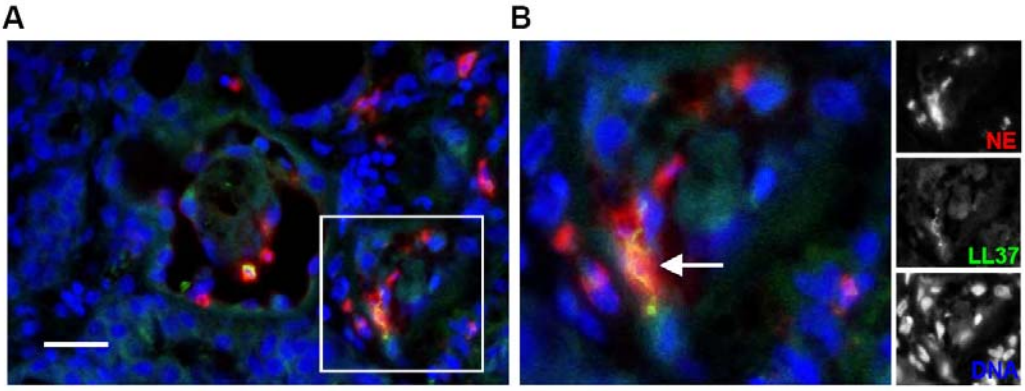

Figure 4.23 – LL37 is present on NETs in the affected kidney. Immunostaining *in situ* revealed the presence of LL37 (green) in the affected glomeruli of SVV patients (**A**). Blow up of boxed area shows extracellular colocalization of LL37 (green), DNA (blue) and NE (red) indicating NET (white arrow) that are coated with LL37 and other granular components (**B**). Scale bar equals 25 µm.

4.2.5 Increased levels of nucleosomes in urine during active disease

In a previous study, strongly increased levels of circulating nucleosomes were detected in sera from patients with ANCA-associated vasculitis (Holdenrieder et al., 2006). As I observed NET formation in the affected kidney, I assumed that some of the NET-derived nucleosomes may locate into the urine due to leakiness of the inflamed kidney. I detected NET formation especially in association with strong neutrophil infiltration in the kidney. Therefore, I presumed that nucleosomes might be detectable also in the urine of patients with active disease rather than during remission. In collaboration with Prof. Samtleben from the Klinikum Großhadern in Munich, urine and serum samples from one patient suffering from Wegener´s granulomatosis with active disease and one with partial remission and compared to patients in remission (n = 6) were collected. In support of my hypothesis, nucleosome levels were increased in the urine from an untreated patient with active disease and a patient in partial remission, while normal levels nucleosomes were found in the urine

of six patients in remission (**Figure 4.24A**). However, it was not evident whether these nucleosomes actually derive from NETs, as they may also be produced by inflammation associated necrosis of tissue cells. Therefore, I applied a nucleosome-capturing approach using an anti-histone antibody and tested for MPO activity associated with the nucleosomes using the TMB substrate. I found nucleome-associated MPO activity only in the plasma from one untreated patient with active WG (**Figure 4.24.B**). This was the first prove of principle that nucleosomes attached with granular proteins can circulate during the active phase of the disease. These complexes may be derived from NETs that were digested by DNAses present in the blood and tissue.

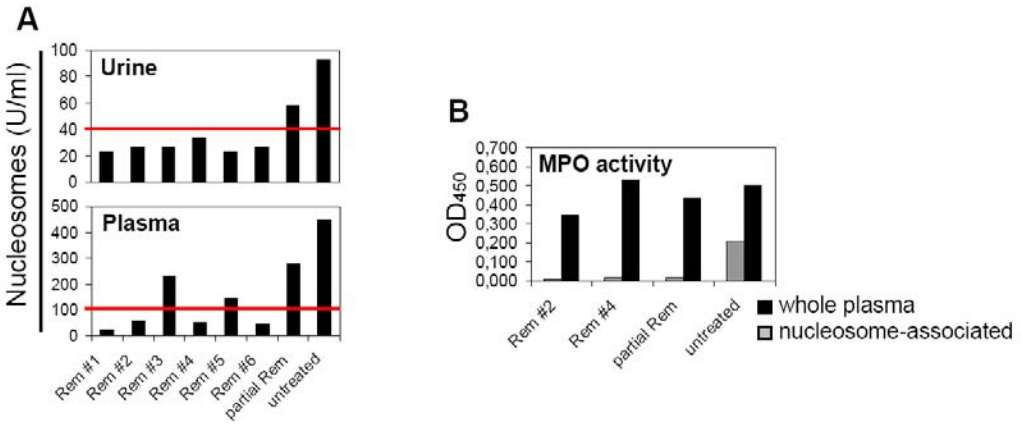

Figure 4.24 – Nucleosome levels in the urine of patients with ANCA-associated vasculitis. Nucleosomes were measured using the cell death detection ELISA (Roche) in urine samples of Wegener´s granulomatosis patients in remission (Rem; n = 6), in partial remission (n = 1) and an untreated patient with active disease (n = 1). Samples from healthy donors are below the cut-off (red line). In the urine, all six samples from patients in remission yielded negative results (below cut-off), while both samples from an untreated patient and a patient in partial remission showed increased nucleosome levels (**A**). In the plasma samples, some of the remissioned patients showed increased nucleosomes, but the highest values were found in the samples from the untreated patient and the patient in partial remission (**B**). When MPO activity was measured in the whole plasma using TMB substrate, all of the sera showed comparable levels of peroxidase activity, while only in plasma from an untreated patient, nucleosome-associated MPO activity was found (**B**).

4.2.6 Circulating MPO-DNA complexes are increased during active disease

The half-life of the activity of MPO in the serum is difficult to estimate, and I reasoned that measurement of MPO enzymatic activity attached to nucleosomes may not be a procedure that yields optimal sensitivity. Therefore, I applied another capture ELISA approach, which immobilizes MPO from patient sera using an anti-MPO monoclonal antibody as the capture antibody and subsequently, after stringent washing of the wells, identifies DNA bound to MPO using a peroxidase-labeled anti-DNA monoclonal antibody. Indeed, using this procedure, I found a number of SVV patient sera that were positive for circulating MPO-DNA complexes. The sera from healthy donors (n = 3) and the sera from multiple sclerosis (MS) patients (n = 5) were completely negative in this assay. While the sera from SVV patients in remission (n = 9) only showed slight reactivity in this set-up, sera from patients in partial remission (n = 5) showed medium reactivity and from patients with active disease (n = 5) were highly positive (**Figure 4.25**). This showed that circulating nucleosomes in SVV patients were derived – at least in part – from NETs, since they displayed neutrophil granular markers, in these case the autoantigen MPO, attached to them.

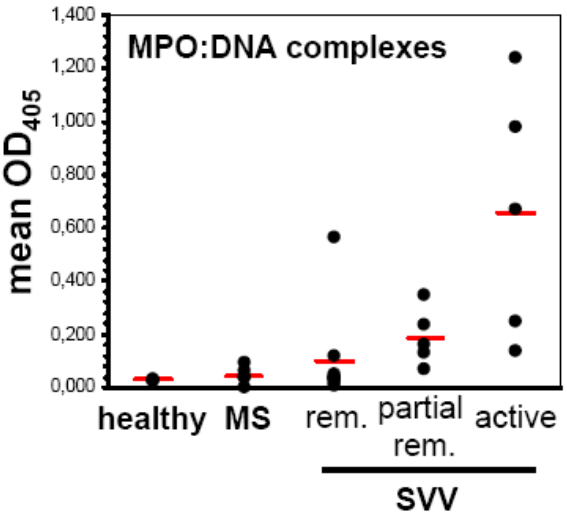

Figure 4.25 – MPO-DNA complexes circulating in the sera of SVV patients. Sera were incubated on anti-MPO coated microtiter plates and DNA attached to MPO was identified using peroxidase-labeled anti-DNA monoclonal antibody. Averaged values from duplicate measurements at OD at 405 nm are shown. Red horizontal bars represent the average OD of each group. Sera from healthy donors (n = 3) and from multiple sclerosis (MS) patients (n = 5) were negative, while patients with SVV with remission (n = 9) were marginally positive, with partial remission (n = 5) showed medium reactivity and with active disease (n = 5) were highly positive.

5 Discussion

5.1 Proteolytic control of inflammation by PR3 and NE

Chronic inflammatory and autoimmune diseases are often perpetuated by continuous neutrophil infiltration and activation. According to the current view, the role of neutrophil serine proteases (NSPs) in these diseases is mainly associated with proteolytic tissue degradation after their release from activated or dying neutrophils. However, recent observations suggest that NSPs such as CG may contribute to non-infectious diseases in a more complex manner, namely as specific regulators of inflammation (Pham, 2006). In the present study, I demonstrated that PR3 and NE cooperatively fulfill an important pro-inflammatory role during neutrophilic inflammation. PR3 and NE directly enhanced neutrophil activation by degrading oxidative-burst suppressing PGRN. These findings support the use of specific serine protease inhibitors as anti-inflammatory agents (Kessenbrock et al., 2008).

Much attention has been paid to the degradation of extracellular matrix components by NSPs. Therefore, I expected that ablation of both PR3 and NE would potentially cause impaired neutrophil extravasation and interstitial migration. Surprisingly, I found that the proteases are principally dispensable for these processes, as PR3/NE-depleted neutrophils migrated normally through a dense, three-dimensional collagen matrix *in vitro* (**Figure 4.4**) and demonstrated regular extravasation *in vivo* when phorbol-esters (croton oil) were applied (**Figure 4.3**). This agrees with recent findings that neutrophils preferentially and readily cross the barrier of the endothelial basement membrane through regions of low matrix density in the absence of NE (Wang et al., 2006).

Regarding these data, it was striking to find that PR3 and NE were required for the inflammatory response to locally formed ICs in the skin (**Figure 4.5** and **4.6**). This suggested that the enzymes may be specifically involved in the response of neutrophils to ICs. Indeed, it turned out in the following experiments that even isolated PR3/NE-deficient neutrophils were significantly hampered to perform an oxidative burst after IC-stimulation *in vitro* (**Figure 4.8A**), showing that the proteases

directly enhanced the activation of neutrophils also in the absence of extracellular matrix. However, when receptor-mediated signal transduction was "bypassed" by means of phorbol ester (PMA), neutrophils from PR3/NE-deficient mice performed a normal oxidative burst (**Figure 4.8B**) indicating that the function of the phagocyte oxidase (phox) complex was not altered in the absence of PR3 and NE. These findings substantiated a novel paradigm that all three serine proteases of azurophilic granules (CG, PR3 and NE) potentiate a positive autocrine feedback on neutrophil activation, *e.g.* after their release in response to IC encounter.

In contrast to CG, the highly related proteases PR3 and NE cooperated in the effacement of anti-inflammatory progranulin (PGRN) leading to enhanced neutrophil activation. Previous studies already demonstrated that PGRN can be a potent inhibitor of the adhesion-dependent oxidative burst of neutrophils *in vitro*, which can be degraded by NE (Zhu et al., 2002). Here, I showed that PR3 and NE play an equally important role in the regulation of PGRN function. NE single-deficient neutrophils were sufficiently able to degrade PGRN. Only in the absence of both PR3 and NE, PGRN-degradation was significantly impaired resulting in the accumulation of anti-inflammatory PGRN during neutrophil activation *in vitro* (**Figure 4.15**) and neutrophilic inflammation *in vivo* (**Figure 4.17**). This clearly showed that PR3 has to be regarded as an important PGRN-degrading enzyme and it also highlighted the similarity and – in this case even – redundancy of PR3 and NE in their physiological functions.

PGRN was previously demonstrated to be a crucial modulator of inflammation and the wound healing process (He et al., 2003; Zhu et al., 2002), but role of PGRN in non-infectious inflammatory models *in vivo* was still unclear. In my work, I firstly provided *in vivo* evidence for the crucial function of PGRN as an inflammation-suppressing mediator, since administration of recombinant PGRN potently inhibited the neutrophil influx to sites of IC formation (**Figure 4.16**). Hence, the cooperative degradation of PGRN by PR3 and NE appears to be a decisive step for the establishment of neutrophilic inflammation.

The molecular mechanism of PGRN function is not yet completely understood, but it seems to interfere with integrin (CD11b/CD18) outside-in signaling by blocking the function of pyk2 and thus dampens adhesion-related oxidative burst even when added after the initial lag phase of oxidase activation (Zhu et al., 2002). PGRN is produced

by neutrophils and pre-stored in highly mobile secretory granules (Lin et al., 2007). It was recently shown that PGRN can bind to heparan-sulfated proteoglycans (Gonzalez et al., 2003), which are abundant components of the endothelial basement membrane (EBM) and various cell surfaces including those of neutrophils. Also PR3 and NE are known to interact with heparan-sulfates on the outer membrane of neutrophils, where the enzymes seem to be protected against protease inhibitors (Campbell et al., 2000; Owen et al., 1995; Campbell and Owen, 2007). These circumstantial observations support the notion that PGRN cleavage by PR3/NE takes place at the pericellular microenvironment of the neutrophil cell surface.

Impaired outside-in signaling most likely reduced the oxidative burst in PR3/NE-deficient neutrophils adhering to ICs. In support of this hypothesis, I excluded an altered response to TNFα priming and reduced adhesion to immobilized ICs (**Figure 4.9**). MPO content and processing was not changed either in PR3/NE-null neutrophils (**Figure 4.2A**) and hence the inhibitory effect of MPO on phox activity as previously discussed (Locksley et al., 1983; Rosen and Klebanoff, 1976) does not appear to be stronger in neutrophils that are lacking PR3/NE. As there was no difference in the "lag phase" of the oxidative burst, initial IC-triggered receptor activation was probably not affected by either PRGN or PR3/NE. My concept is consistent with all these observations and takes into account that PGRN unfolds its suppressing effects in the second phase, when additional membrane receptors, endogenous PGRN and some PR3/NE from highly mobile intracellular pools are translocated to the cellular surface. The decline and cessation of ROS production suggested that outside-in signaling was not sustained and that active oxidase complexes were no longer replenished in the absence of PR3 and NE. The current state of findings, however, does not permit to exclude other potential mechanisms like an accelerated disassembly of the active oxidase complex.

During cutaneous inflammation, PGRN is provided by multiple sources including skin cells and neutrophils themselves, which produce and release PGRN as they infiltrate the tissue (He et al., 2003; Lin et al., 2007). Thus, PGRN represents a prominent factor to control extravascular neutrophil function during skin inflammation. Proteolytic processing of PGRN was previously shown to generate granulin (GRN) peptides that accumulated in inflammatory exudates, *e.g.* during casein-induced peritonitis (Couto et al., 1992). In contrast to the precursor PGRN, these GRN

peptides might be pro-inflammatory and induce the release of neutrophil attracting IL-8 from epithelial cells (Zhu et al., 2002). In the absence of PR3 and NE, neutrophils are no longer able to provide the switch from inflammation-suppressing PGRN to pro-inflammatory GRN peptides. The activation of neutrophils by ICs is a decisive event in the cascade of reactions during the reverse, passive Arthus reaction. IC-activated neutrophils are known to release cytokines and chemokines and thus establish an inflammatory milieu. I hypothesize that the local persistence of PGRN dampens neutrophil activation and release of ROS as well as other inflammatory mediators in response to ICs, which results in diminished recruitment of further neutrophils as observed in PR3/NE-lacking mice. Hence, defective PGRN-degradation can account for the impaired inflammation in the absence of PR3 and NE (illustrated in **Figure 5.1**).

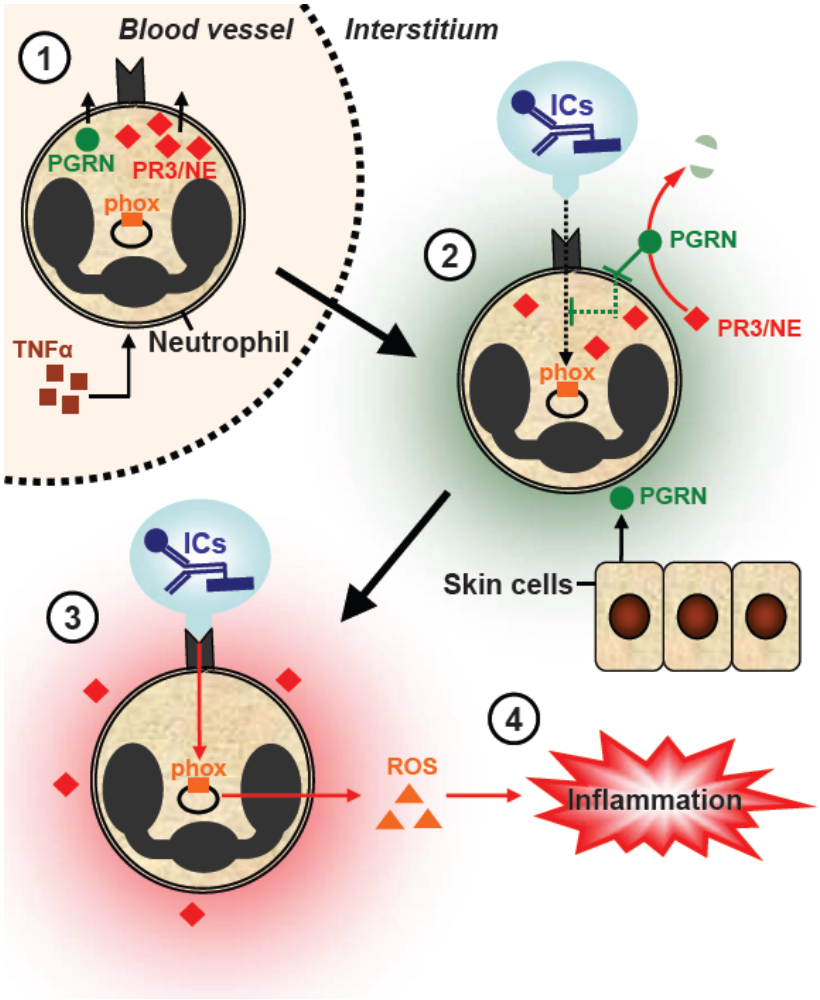

Figure 5.1 – Proposed function of PR3 and NE in IC-mediated inflammation. TNF-α–primed neutrophils extravasate from blood vessels, translocate PR3/NE to the cellular surface, and discharge PGRN to the pericellular environment (**1**). During transmigration of interstitial tissues (**2**), neutrophil activation is initially suppressed by relatively high pericellular levels of antiinflammatory PGRN (green shading), which is also produced locally by keratinocytes and epithelial cells of the skin. Until IC depots are reached, neutrophil activation is inhibited by PGRN. Surface receptors (e.g., Mac-1) recognize ICs, which results in signal transduction (black dotted arrow) and activation of the phox. The molecular pathway of PGRN-mediated inhibition is not completely understood, but it may interfere with integrin signaling after IC encounter (green dotted line inside the cell). Adherence of neutrophils to ICs (**3**) further increases pericellular PR3 and NE activity. PR3 and NE cooperatively degrade PGRN in the early stage of neutrophilic activation to facilitate optimal neutrophil activation (red shading), resulting in sustained integrin signaling (red arrow) and robust production of ROS by the phox system. Subsequently, neutrophils release ROS together with other proinflammatory mediators and chemotactic agents, thereby enhancing the recruitment of further neutrophils and establishing inflammation (**4**). In the absence of PR3/NE, the switch from inflammation-suppressing (**2**) to inflammation-enhancing (**3**) conditions is substantially delayed, resulting in diminished inflammation in response to ICs (**4**).

Interestingly, PGRN was recently identified as a key factor in dementia. Mutations in the PGRN gene on chromosome 17 and the associated haploinsufficiency of PGRN in the brain was linked with the development of a frontotemporal form of dementia in humans (Baker et al., 2006; Cruts et al., 2006). These findings were mainly explained by PGRN working as a neuronal survival factor (Baker et al., 2006). However, since PGRN is an important suppressor of inflammation in the periphery, the role of PGRN in dementia may also be linked with neuroinflammation (Ahmed et al., 2007). Hypothetically, lowered levels of the anti-inflammatory factor PGRN in the brain may cause subtle but chronic inflammatory conditions that lead to dementia as a long-term consequence. In this context, my findings of PR3/NE-mediated shedding of PGRN might also be important for dementia and certain neuroinflammatory conditions.

NSPs are strongly implicated as effector molecules in a large number of destructive diseases such as lung emphysema or the autoimmune blistering skin disease bullous pemphigoid (Liu et al., 2000a; Liu et al., 2000b; Shapiro, 2002; Shapiro et al., 2003). Normally, PR3/NE activity is tightly controlled by high plasma levels of α1-antitrypsin. This balance between proteases and protease-inhibitors is disrupted in patients with genetic α1-antitrypsin deficiency, which represents a high risk factor for the development of lung emphysema and certain autoimmune disorders (Stoller and Aboussouan, 2005). The pathogenic effects of NSPs in these diseases have so far been associated with tissue destruction by the proteases after their release from dying neutrophils. Our findings show that PR3 and NE are already involved in much earlier events of the inflammatory process, since the enzymes directly regulate cellular activation of infiltrating neutrophils by degrading inflammation-suppressing PGRN. This concept is further supported by previous studies showing increased inflammation in mice lacking serine protease inhibitors such as SERPINB1 or SLPI (Benarafa et al., 2007; Ashcroft et al., 2000). Blocking PR3/NE activity using specific inhibitors therefore represents a promising therapeutic strategy to treat chronic, non-infectious inflammation. Serine protease inhibitors as anti-inflammatory agents can interfere with the disease process at two different stages, since they attenuate both early events of neutrophil activation as well as the proteolytic tissue injury caused by released NSPs.

5.2 Autoimmunity against PR3 in small-vessel vasculitis

Autoimmune diseases are one of the leading causes of death among young and middle aged women in the United States (Cooper and Stroehla, 2003). In many of these diseases, self-reactive antibodies are directly associated with the autoinflammatory disorder. For instance, anti-neutrophil cytoplasm autoantibodies (ANCAs) specifically occur in patients with small-vessel vasculitis (SVV), where they are directed against granular proteins of neutrophil granulocytes, namely against PR3 in Wegener´s granulomatosis (WG) and MPO in microscopic polyangiitis (MPA) (Bosch et al., 2006). The levels of circulating ANCAs are most prominent in the generalized stage of the disease, which mostly affects the glomeruli of the kidneys (glomerulonephritis). If left untreated in patients, SVV rapidly progresses and is lethal within months. The pathogenic effect of ANCAs was recently supported by animal models of the diseases (Pfister et al., 2004; Xiao et al., 2002). The widely accepted concept that ANCAs activate tumor necrosis factor α (TNFα)-primed neutrophils relates to their pathogenicity (Falk et al., 1990), however, it does not explain the mechanism that drives the sustained and progressive autoimmune response against the two neutrophil antigens PR3 and MPO.

Here, I investigated whether a recently discovered, alternative cell death program of neutrophils, called NETosis (Brinkmann et al., 2004), is implicated in ANCA-associated autoimmunity. In this work, I found several lines of evidence that support a role of NETs, which consist of extracellular chromatin fibers displaying the autoantigens PR3 and MPO, in the autoimmunity against self proteins of neutrophil granulocytes.

NETosis appears to be distinct from apoptosis and necrosis and was recently shown to depend critically on the production of ROS (Fuchs et al., 2007). As ANCAs are known to bind to PR3 or MPO on the neutrophil cell surface and thereby trigger profound ROS formation in neutrophils (Falk et al., 1990), I wondered whether ANCA-activation of neutrophils may result in NETosis. To this end, isolated human neutrophils from the peripheral blood of healthy donors were primed with TNFα and were incubated with purified IgG from SVV patients and from healthy donors as

negative controls according to a widely used procedure established previously (Falk et al., 1990). As shown in **Figure 4.18**, I indeed observed that ANCA, but not IgG from healthy individuals, trigger the formation of NETs by TNFα-primed neutrophils. This strongly suggested that NETosis might play a role in ANCA-associated vasculitis.

In their seminal study in 2004, Brinkmann and colleagues have found that neutrophil elastase (NE) is an abundant component of the extracellular chromatin fibers of NETs (Brinkmann et al., 2004). Since both autoantigens MPO and PR3 are stored in the same cytoplasmic compartments of neutrophils as NE, namely the azurophilic granula, I next asked whether PR3 and MPO were also components of NETs. By immunofluorescence, large amounts of both PR3 and MPO were detected clearly co-localizing with the extracellular chromatin/DNA of NETs (**Figure 4.19**). Importantly, the targeted epitopes were readily accessible also when PR3 was bound on NETs (**Figure 4.21**). These data strongly support the notion that NETosis may be an adequate source of antigen to nourish the autoimmune response against these – normally intracellular – self proteins.

A strikingly high proportion of autoantibodies developed in autoimmune diseases such as systemic lupus erythematosus (SLE) are directed against nucleic acid-binding proteins (Marshak-Rothstein, 2006). A number of subsequent studies linked this observation with the capacity of RNA and DNA to activate toll-like receptors (TLRs) in B cells, dendritic cells or macrophages (Lau et al., 2005; Leadbetter et al., 2002; Means et al., 2005; Vollmer et al., 2005). Therefore, the high amount of extracellular DNA present in NETs is potentially immunostimulatory, as it may activate the TLR9 pathway in immune cells and thereby drive the immune response against the NET-associated autoantigens PR3 and MPO.

In support of this view, I also found that an antimicrobial peptide of neutrophils, called LL37, was formed and released during NET formation and was enriched around chromatin fibers (**Figure 4.19**). LL37 was recently shown to be the key factor in converting self-DNA into an activator of dendritic cells in psoriasis, an autoimmune disease of the skin (Lande et al., 2007). Consequently, I suggest that the self-chromatin of NETs in conjunction with LL37 acts similarly on dendritic cells and B cells in SVV. Clearly, the combination of ANCA, the respective autoantigens attached with TLR-activating chromatin must be regarded as a potentially immunogenic composition.

Most importantly, I sought to find *in vivo* evidence for the occurrence of NETosis in patients with autoimmune vasculitis. I focused my attention to patients with non-infectious ANCA-associated glomerulonephritis, a clinical manifestation of both forms of the disease Wegener´s granulomatosis and microscopic polyangiitis. In collaboration with Dr. Volker Brinkmann from the Max Planck Institute of Infectious Biology in Berlin, we analyzed needle biopsies from affected kidneys of five patients with Wegener´s disease and two patients with microscopic polyangiitis by *in situ* immunofluorescence microscopy. Using a combination of antibodies for histone protein, MPO or NE and DNA dyes, we were able to discriminate NETs from DNA released in the course of necrosis. Indeed, structures of different sizes composed of extracellular chromatin and granular proteins were found in the kidney biopsies (**Figure 4.21**). These NETs displaying the targeted autoantigens were especially abundant in cases with severe glomerulonephritis lesions and strong neutrophil infiltration. Importantly, also the immunostimulatory peptide LL37 was present in the inflamed kidney, where it was located to neutrophil-enriched sites and partially colocalized with NETs (**Figure 4.23**). Chromatin fibers of NETs in conjunction with disease specific autoantigens were mainly localized in close proximity to infiltrated neutrophils in affected glomeruli. These findings showed that NETosis indeed occurs in SVV patients even in the absence of infection, as glomerulonephritis is known as a non-infectious inflammation of the kidney. My *in vitro* data strongly suggests that the anti-PR3 and anti-MPO ANCAs actually stimulated the neutrophils to form NETs in these patients.

In the kidney tissue, a number of DNAses are expressed that swiftly degrade extracellular DNA depositions that derive from NETs or necrotic cells during inflammation. Therefore, it was surprising to find – in some areas – abundant NET deposition in the inflamed kidney. Presumably, much larger amounts of NETs are produced and immediately degraded by DNAses present in the kidney and are thus not detectable anymore. The degradation of chromatin by DNAses results in production of smaller nucleosomes consisting of DNA and histone proteins. Strikingly, in a previous study, strongly increased levels of circulating nucleosomes were detected in sera from patients with ANCA-associated vasculitis (Holdenrieder et al., 2006). My results suggest that the circulating nucleosomes may – at least in part – derive from ANCA-induced NETs. As I observed NET formation in the affected kidney, I assumed that some of the NET-derived nucleosomes may locate into the

urine due to leakiness of the inflamed kidney. I detected NET formation especially in association with strong neutrophil infiltration, which happens particularly during the active phase of the disease. In line with this notion, I found increased nucleosome levels in the urine samples from one untreated patient with active disease and one patient in partial remission, in remission (n = 6) were negative (**Figure 4.24**). I also found MPO activity attached to circulating nucleosomes in an untreated SVV patient (**Figure 4.24B**) and increased MPO:DNA complexes circulating in the sera of SVV patients especially during active disease (**Figure 4.25**). These observations showed that the circulating nucleosomes in SVV patients were most likely derived from NETosis, since they displayed granular markers attached to them.

I hypothesize that ANCAs stimulate neutrophils during the active phase of disease to release NETs. These NETs display large amounts of the targeted autoantigens PR3 and MPO in connection with TLR9 activating chromatin. The uptake of these immunostimulatory complexes by immune cells such as B cells or dendritic cells might be mediated by LL37 (Lande et al., 2007). Somwhere in the patient body, autoreactive B cells are activated by the circulating autoantigen:DNA complexes in an TLR-dependent manner and therefore produce more of the pathogenic autoantibodies. This results in a vicious circle driving the autoimmune response in patients with SVV (**Figure 5.2**).

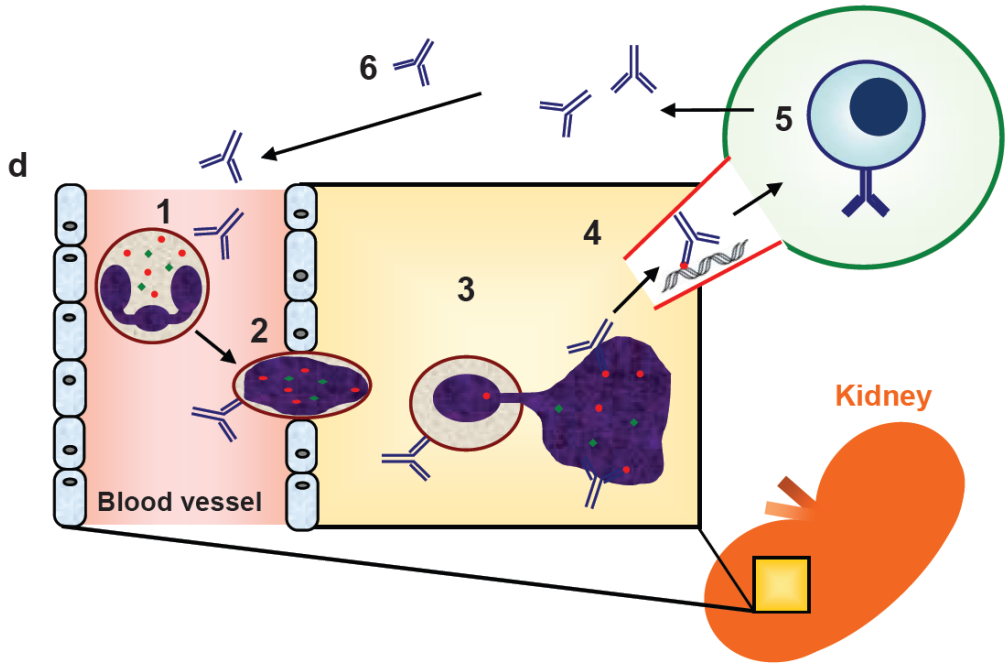

Figure 5.2 – Hypothetical scheme depicting the proposed *circulus vitiosus* in patients with small-vessel vasculitits. (**1**) ANCA bind to MPO/PR3 on the cell surface to induce neutrophil activation. (**2**) This leads to oxidative burst, local adhesion and extravasation of neutrophils within capillary loops of glomeruli, which subsequently results in perivascular inflammation in the kidney. (**3**) Inside the glomerulus, ANCA-activated neutrophils release NETs decorated with the target autoantigens (red circles) and with immunostimulatory LL37 (green diamonds) (**4**) Renal inflammation causes leakiness of the glomerulus resulting in dissemination of ANCA-NET immune complexes to the regional lymph nodes and the blood stream. (**5**) Small amounts of ANCA-NET immune complexes may suffice to drive autoantibody production by autoreactive B cells via FcR involvement plus chromatin-TLR9 activation. (**6**) Further production of circulating ANCAs closes the vicious circle in patients with SVV (**1**).

In summary, these studies showed for the first time that NETs occur in an autoinflammatory disorder in the absence of microbial infection, namely triggered by autoreactive antibodies that activate neutrophils. NETs are the result of an unusual cell death program and are suited to enhance and perpetuate the pre-existing autoimmune response and may also contribute to the initial break of tolerance against neutrophil autoantigens. It would be interesting to analyze the current *in vivo* mouse models of the diseases for the production of NETs. According to my hypothesis, pattern recognition of self DNA by toll-like receptors might be a crucial event in the disease course of SVV. Thus, another interesting experiment would be to interfere

with TLR9 signaling genetically or pharmacologically in the established mouse models of SVV. Further study is required to find out whether suppression of NET formation, for instance using ROS scavengers (Fuchs et al., 2007), can abrogate chronic, humoral autoimmunity versus PR3 and MPO and, therefore, may be suitable for therapy to help patients suffering from ANCA-associated SVV.

6 Literature

Reference List

Adkison,A.M., Raptis,S.Z., Kelley,D.G., and Pham,C.T. (2002). Dipeptidyl peptidase I activates neutrophil-derived serine proteases and regulates the development of acute experimental arthritis. J. Clin. Invest *109*, 363-371.

Ahmed,Z., Mackenzie,I.R., Hutton,M.L., and Dickson,D.W. (2007). Progranulin in frontotemporal lobar degeneration and neuroinflammation. J. Neuroinflammation *4*.

Arthus,M. and Breton,M. (1903). Cutaneous lesions produced by injections of horse serum in a rabbit anaphylactised by and for this serum. Comptes Rendus des Seances de la Societe de Biologie et de Ses Filiales *55*, 1478-1480.

Ashcroft,G.S., Lei,K.J., Jin,W.W., Longenecker,G., Kulkarni,A.B., Greenwell-Wild,T., Hale-Donze,H., McGrady,G., Song,X.Y., and Wahl,S.M. (2000). Secretory leukocyte protease inhibitor mediates non-redundant functions necessary for normal wound healing. Nat. Med. *6*, 1147-1153.

Baker,M., Mackenzie,I.R., Pickering-Brown,S.M., Gass,J., Rademakers,R., Lindholm,C., Snowden,J., Adamson,J., Sadovnick,A.D., Rollinson,S., Cannon,A., Dwosh,E., Neary,D., Melquist,S., Richardson,A., Dickson,D., Berger,Z., Eriksen,J., Robinson,T., Zehr,C., Dickey,C.A., Crook,R., McGowan,E., Mann,D., Boeve,B., Feldman,H., and Hutton,M. (2006). Mutations in progranulin cause tau-negative frontotemporal dementia linked to chromosome 17. Nature *442*, 916-919.

Bateman,A., Belcourt,D., Bennett,H., Lazure,C., and Solomon,S. (1990). Granulins, a novel class of peptide from leukocytes. Biochem. Biophys. Res. Commun. *173*, 1161-1168.

Belaaouaj,A., Kim,K.S., and Shapiro,S.D. (2000). Degradation of outer membrane protein A in Escherichia coli killing by neutrophil elastase. Science *289*, 1185-1188.

Belaaouaj,A., McCarthy,R., Baumann,M., Gao,Z., Ley,T.J., Abraham,S.N., and Shapiro,S.D. (1998). Mice lacking neutrophil elastase reveal impaired host defense against gram negative bacterial sepsis. Nat. Med. *4*, 615-618.

Belorgey,D. and Bieth,J.G. (1995). Dna Binds Neutrophil Elastase and Mucus Proteinase-Inhibitor and Impairs Their Functional-Activity. Febs Letters *361*, 265-268.

Benarafa,C., Priebe,G.P., and Remold-O'Donnell,E. (2007). The neutrophil serine protease inhibitor serpinb1 preserves lung defense functions in Pseudomonas aeruginosa infection. J. Exp. Med. *204*, 1901-1909.

Bories,D., Raynal,M.C., Solomon,D.H., Darzynkiewicz,Z., and Cayre,Y.E. (1989). Down-regulation of a serine protease, myeloblastin, causes growth arrest and differentiation of promyelocytic leukemia cells. Cell *59*, 959-968.

Bosch,X., Guilabert,A., and Font,J. (2006). Antineutrophil cytoplasmic antibodies. Lancet *368*, 404-418.

Brinkmann,V., Reichard,U., Goosmann,C., Fauler,B., Uhlemann,Y., Weiss,D.S., Weinrauch,Y., and Zychlinsky,A. (2004). Neutrophil extracellular traps kill bacteria. Science *303*, 1532-1535..

Brinkmann,V. and Zychlinsky,A. (2007). Beneficial suicide: why neutrophils die to make NETs. Nat. Rev. Microb. *5*, 577-582.

Campbell,E.J., Campbell,M.A., and Owen,C.A. (2000). Bioactive proteinase 3 on the cell surface of human neutrophils: Quantification, catalytic activity, and susceptibility to inhibition. J. Immunol. *165*, 3366-3374.

Campbell,E.J. and Owen,C.A. (2007). The sulfate groups of chondroitin sulfate- and heparan sulfate-containing proteoglycans in neutrophil plasma membranes are novel binding sites for human leukocyte elastase and cathepsin G. J. Biol. Chem. *282*, 14645-14654.

Carden,D.L. and Korthuis,R.J. (1996). Protease inhibition attenuates microvascular dysfunction in postischemic skeletal muscle. American Journal of Physiology-Heart and Circulatory Physiology *40*, H1947-H1952.

Cooper,G.S. and Stroehla,B.C. (2003). The epidemiology of autoimmune diseases. Autoimmunity Rev. *2*, 119-125.

Couto,M.A., Harwig,S.S., Cullor,J.S., Hughes,J.P., and Lehrer,R.I. (1992). eNAP-2, a novel cysteine-rich bactericidal peptide from equine leukocytes. Infect. Immun. *60*, 5042-5047.

Cruts,M., Gijselinck,I., van der Zee,J., Engelborghs,S., Wils,H., Pirici,D., Rademakers,R., Vandenberghe,R., Dermaut,B., Martin,J.J., van Duijn,C., Peeters,K., Sciot,R., Santens,P., De Pooter,T., Mattheijssens,M., Van den Broeck,M., Cuijt,I., Vennekens,K., De Deyn,P.P., Kumar-Singh,S., and Van Broeckhoven,C. (2006). Null mutations in progranulin cause ubiquitin-positive frontotemporal dementia linked to chromosome 17q21. Nature *442*, 920-924.

El Ouriaghli,F., Fujiwara,H., Melenhorst,J.J., Sconocchia,G., Hensel,N., and Barrett,A.J. (2003). Neutrophil elastase enzymatically antagonizes the in vitro action of G-CSF: implications for the regulation of granulopoiesis. Blood *101*, 1752-1758.

Falk,R.J., Terrell,R.S., Charles,L.A., and Jennette,J.C. (1990). Anti-neutrophil cytoplasmic autoantibodies induce neutrophils to degranulate and produce oxygen radicals in vitro. Proc. Natl. Acad. Sci. U. S. A *87*, 4115-4119.

Fleming,T.J., Fleming,M.L., and Malek,T.R. (1993). Selective Expression of Ly-6G on Myeloid Lineage Cells in Mouse Bone-Marrow - Rb6-8C5 Mab to Granulocyte-

Differentiation Antigen (Gr-1) Detects Members of the Ly-6 Family. J. Immunol. *151*, 2399-2408.

Fuchs,T.A., Abed,U., Goosmann,C., Hurwitz,R., Schulze,I., Wahn,V., Weinrauch,Y., Brinkmann,V., and Zychlinsky,A. (2007). Novel cell death program leads to neutrophil extracellular traps. J. Cell Biol. *176*, 231-241.

Gonzalez,E.M., Mongiat,M., Slater,S.J., Baffa,R., and Iozzo,R.V. (2003). A novel interaction between perlecan protein core and progranulin - Potential effects on tumor growth. J. Biol. Chem. *278*, 38113-38116.

Harper,L., Ren,Y., Savill,J., Adu,D., and Savage,C.O.S. (2000). Antineutrophil cytoplasmic antibodies induce reactive oxygen-dependent dysregulation of primed neutrophil apoptosis and clearance by macrophages. Am. J. Pathol. *157*, 211-220.

He,Z. and Bateman,A. (2003). Progranulin (granulin-epithelin precursor, PC-cell-derived growth factor, acrogranin) mediates tissue repair and tumorigenesis. J. Mol. Med. *81*, 600-612.

He,Z., Ong,C.H., Halper,J., and Bateman,A. (2003). Progranulin is a mediator of the wound response. Nat. Med. *9*, 225-229.

Heeringa,P., Huugen,D., and Tervaert,J.W.C. (2005). Anti-neutrophil cytoplasmic autoantibodies and leukocyte-endothelial interactions: a sticky connection? Trends Immunol. *26*, 561-564.

Hestdal,K., Ruscetti,F.W., Ihle,J.N., Jacobsen,S.E.W., Dubois,C.M., Kopp,W.C., Longo,D.L., and Keller,J.R. (1991). Characterization and Regulation of Rb6-8C5 Antigen Expression on Murine Bone-Marrow Cells. J. Immunol. *147*, 22-28.

Hirche,T.O., Atkinson,J.J., Bahr,S., and Belaaouaj,A. (2004). Deficiency in neutrophil elastase does not impair neutrophil recruitment to inflamed sites. Am. J. Resp. Cell .Mol. Biol. *30*, 576-584.

Holdenrieder,S., Eichhorn,P., Beuers,U., Samtleben,W., Schoenermarck,U., Zachoval,R., Nagel,D., and Stieber,P. (2006). Nudeosomal DNA fragments in autoimmune diseases. Circulating Nucleic Acids in Plasma and Serum Iv *1075*, 318-327.

Jancar,S. and Sanchez,C.M. (2005). Immune complex-mediated tissue injury: a multistep paradigm. Trends Immunol. *26*, 48-55.

Janeway,C.A. and Medzhitov,R. (2002). Innate immune recognition. Ann. Rev. Immunol. *20*, 197-216.

Jenne,D.E., Tschopp,J., Ludemann,J., Utecht,B., and Gross,W.L. (1990). Wegener Autoantigen Decoded. Nature *346*, 520.

Kallenberg,C.G.M., Heeringa,P., and Stegeman,C.A. (2006). Mechanisms of Disease: pathogenesis and treatment of ANCA-associated vasculitides. Nat. Clin. Prac. Rheumatol. *2*, 661-670.

Kaufmann,S.H.E. (2008). Immunology's foundation: the 100-year anniversary of the Nobel Prize to Paul Ehrlich and Elie Metchnikoff. Nat. Immunol. *9*, 705-712.

Kessenbrock,K., Frohlich,L., Sixt,M., Lammermann,T., Pfister,H., Bateman,A., Belaaouaj,A., Ring,J., Ollert,M., Fassler,R., and Jenne,D.E. (2008). Proteinase 3 and neutrophil elastase enhance inflammation in mice by inactivating antiinflammatory progranulin. J. Clin. Invest. *118*, 2438-2447.

Klebanoff,S.J. (2005). Myeloperoxidase: friend and foe. J. Leuk. Biol. *77*, 598-625.

Kocher,M., Edberg,J.C., Fleit,H.B., and Kimberly,R.P. (1998). Antineutrophil cytoplasmic antibodies preferentially engage Fc gamma RIIIb on human neutrophils. J. Immunol. *161*, 6909-6914.

Laemmli,U.K. (1970). Cleavage of Structural Proteins During Assembly of Head of Bacteriophage-T4. Nature *227*, 680-&.

Lande,R., Gregorio,J., Facchinetti,V., Chatterjee,B., Wang,Y.H., Homey,B., Cao,W., Wang,Y.H., Su,B., Nestle,F.O., Zal,T., Mellman,I., Schroder,J.M., Liu,Y.J., and Gilliet,M. (2007). Plasmacytoid dendritic cells sense self-DNA coupled with antimicrobial peptide. Nature *449*, 564-5U6.

Lau,C.M., Broughton,C., Tabor,A.S., Akira,S., Flavell,R.A., Mamula,M.J., Christensen,S.R., Shlomchik,M.J., Viglianti,G.A., Rifkin,I.R., and Marshak-Rothstein,A. (2005). RNA-associated autoantigens activate B cells by combined B cell antigen receptor/Toll-like receptor 7 engagement. J. Exp. Med. *202*, 1171-1177.

Leadbetter,E.A., Rifkin,I.R., Hohlbaum,A.M., Beaudette,B.C., Shlomchik,M.J., and Marshak-Rothstein,A. (2002). Chromatin-IgG complexes activate B cells by dual engagement of IgM and Toll-like receptors. Nature *416*, 603-607.

Lin,W.L., Zehr,C., Lewis,J., and Dickson,D.W. (2007). Progranulin is located in secretory granules and vesicles of neutrophils and macrophages by immunogold electron microscopy. Faseb Journal *21*, A22.

Liu,Z., Shapiro,S.D., Zhou,X.Y., Twining,S.S., Senior,R.M., Giudice,G.J., Fairley,J.A., and Diaz,L.A. (2000a). A critical role for neutrophil elastase in experimental bullous pemphigoid. J. Clin. Invest. *105*, 113-123.

Liu,Z., Zhou,X.Y., Shapiro,S.D., Shipley,J.M., Twining,S.S., Diaz,L.A., Senior,R.M., and Werb,Z. (2000b). The serpin alpha 1-proteinase inhibitor is a critical substrate for gelatinase B/MMP-9 in vivo. Cell *102*, 647-655.

Locksley,R.M., Wilson,C.B., and Klebanoff,S.J. (1983). Increased Respiratory Burst in Myeloperoxidase-Deficient Monocytes. Blood *62*, 902-909.

Lowell,C.A., Fumagalli,L., and Berton,G. (1996). Deficiency of Src family kinases p59/61(hck) and p58(c-fgr) results in defective adhesion-dependent neutrophil functions. J. Cell Biol. *133*, 895-910.

Marshak-Rothstein,A. (2006). Toll-like receptors in systemic autoimmune disease. Nat. Rev. Immunol. *6*, 823-835.

Marshak-Rothstein,A. and Rifkin,I.R. (2007). Immunologically active autoantigens: The role of Toll-like receptors in the development of chronic inflammatory disease. Ann. Rev. Immunol. *25*, 419-441.

Mayadas,T.N. and Cullere,X. (2005). Neutrophil beta(2) integrins: moderators of life or death decisions. Trends Immunol. *26*, 388-395.

Means,T.K., Latz,E., Hayashi,F., Murali,M.R., Golenbock,D.T., and Luster,A.D. (2005). Human lupus autoantibody-DNA complexes activate DCs through cooperation of CD32 and TLR9. J. Clin. Invest. *115*, 407-417.

Meyer,T.S. and Lamberts,B.L. (1965). Use of Coomassie Brilliant Blue R250 for Electrophoresis of Microgram Quantities of Parotid Saliva Proteins on Acrylamide-Gel Strips. Biochim. Biophys. Acta *107*, 144-&.

Murao,S., Stevens,F.J., Ito,A., and Huberman,E. (1988). Myeloperoxidase - A Myeloid Cell Nuclear Antigen with Dna-Binding Properties. Proceedings of the Nat. Ac. Sci.USA *85*, 1232-1236.

Nathan,C. (2002). Points of control in inflammation. Nature *420*, 846-852.

Nathan,C. (2006). Neutrophils and immunity: challenges and opportunities. Nat. Rev. Immunol. *6*, 173-182.

Owen,C.A., Campbell,M.A., Sannes,P.L., Boukedes,S.S., and Campbell,E.J. (1995). Cell Surface-Bound Elastase and Cathepsin-G on Human Neutrophils - A Novel, Nonoxidative Mechanism by Which Neutrophils Focus and Preserve Catalytic Activity of Serine Proteinases. J. Cell Biol. *131*, 775-789.

Pfister,H., Ollert,M., Frohlich,L.F., Quintanilla-Martinez,L., Colby,T.V., Specks,U., and Jenne,D.E. (2004). Antineutrophil cytoplasmic autoantibodies against the murine homolog of proteinase 3 (Wegener autoantigen) are pathogenic in vivo. Blood *104*, 1411-1418.

Pham,C.T. (2006). Neutrophil serine proteases: specific regulators of inflammation. Nat. Rev. Immunol. *6*, 541-550.

Porges,A.J., Redecha,P.B., Kimberly,W.T., Csernok,E., Gross,W.L., and Kimberly,R.P. (1994). Antineutrophil Cytoplasmic Antibodies Engage and Activate Human Neutrophils Via Fc-Gamma-Riia. J. Immunol. *153*, 1271-1280.

Raptis,S.Z., Shapiro,S.D., Simmons,P.M., Cheng,A.M., and Pham,C.T. (2005). Serine protease cathepsin G regulates adhesion-dependent neutrophil effector functions by modulating integrin clustering. Immunity *22*, 679-691.

Ravetch,J.V. (1994). Fc receptors: rubor redux. Cell *78*, 553-560.

Reeves,E.P., Lu,H., Jacobs,H.L., Messina,C.G., Bolsover,S., Gabella,G., Potma,E.O., Warley,A., Roes,J., and Segal,A.W. (2002). Killing activity of neutrophils is mediated through activation of proteases by K+ flux. Nature *416*, 291-297.

Rosen,H. and Klebanoff,S.J. (1976). Chemiluminescence and Superoxide Production by Myeloperoxidase-Deficient Leukocytes. J. Clin. Invest. *58*, 50-60.

Sanger,F., Air,G.M., Barrell,B.G., Brown,N.L., Coulson,A.R., Fiddes,J.C., Hutchison,C.A., Slocombe,P.M., and Smith,M. (1977). Nucleotide-Sequence of Bacteriophage Phichi174 Dna. Nature *265*, 687-695.

Segal,A.W. (2005). How neutrophils kill microbes. Annu. Rev. Immunol. *23*, 197-223.

Shapiro,S.D. (2002). Neutrophil elastase - Path clearer, pathogen killer, or just pathologic? Am. J. Resp. Cell Mol. Biol. *26*, 266-268.

Shapiro,S.D., Goldstein,N.M., Houghton,A.M., Kobayashi,D.K., Kelley,D., and Belaaouaj,A. (2003). Neutrophil elastase contributes to cigarette smoke-induced emphysema in mice. Am. J. Pathol. *163*, 2329-2335.

Singer,A.J. and Clark,R.A.F. (1999). Mechanisms of disease - Cutaneous wound healing. New Eng. J. Med. *341*, 738-746.

Skold,S., Rosberg,B., Gullberg,U., and Olofsson,T. (1999). A secreted proform of neutrophil proteinase 3 regulates the proliferation of granulopoietic progenitor cells. Blood *93*, 849-856.

Sorensen,O.E., Follin,P., Johnsen,A.H., Calafat,J., Tjabringa,G.S., Hiemstra,P.S., and Borregaard,N. (2001). Human cathelicidin, hCAP-18, is processed to the antimicrobial peptide LL-37 by extracellular cleavage with proteinase 3. Blood *97*, 3951-3959.

Springer,T.A. (1994). Traffic Signals for Lymphocyte Recirculation and Leukocyte Emigration - the Multistep Paradigm. Cell *76*, 301-314.

Stoller,J.K. and Aboussouan,L.S. (2005). alpha 1-antitrypsin deficiency. Lancet *365*, 2225-2236.

Tkalcevic,J., Novelli,M., Phylactides,M., Iredale,J.P., Segal,A.W., and Roes,J. (2000). Impaired immunity and enhanced resistance to endotoxin in the absence of neutrophil elastase and cathepsin G. Immunity *12*, 201-210.

Vollmer,J., Tluk,S., Schmitz,C., Hamm,S., Jurk,M., Forsbach,A., Akira,S., Kelly,K.M., Reeves,W.H., Bauer,S., and Krieg,A.M. (2005). Immune stimulation mediated by autoantigen binding sites within small nuclear RNAs involves Toll-like receptors 7 and 8. J. Exp. Med. *202*, 1575-1585.

Wang,S., Voisin,M.B., Larbi,K.Y., Dangerfield,J., Scheiermann,C., Tran,M., Maxwell,P.H., Sorokin,L., and Nourshargh,S. (2006). Venular basement membranes contain specific matrix protein low expression regions that act as exit points for emigrating neutrophils. J. Exp. Med. *203*, 1519-1532.

Weinrauch,Y., Drujan,D., Shapiro,S.D., Weiss,J., and Zychlinsky,A. (2002). Neutrophil elastase targets virulence factors of enterobacteria. Nature *417*, 91-94.

Weiss,S.J. (1989). Tissue Destruction by Neutrophils. New Engl. J. Med. *320*, 365-376.

Wiesner,O., Russell,K.A., Lee,A.S., Jenne,D.E., Trimarchi,M., Gregorini,G., and Specks,U. (2004). Antineutrophil cytoplasmic antibodies reacting with human neutrophil elastase as a diagnostic marker for cocaine-induced midline destructive lesions but not autoimmune vasculitis. Arthritis and Rheumatism *50*, 2954-2965.

Xiao,H., Heeringa,P., Hu,P., Liu,Z., Zhao,M., Aratani,Y., Maeda,N., Falk,R.J., and Jennette,J.C. (2002). Antineutrophil cytoplasmic autoantibodies specific for myeloperoxidase cause glomerulonephritis and vasculitis in mice. J. Clin. Invest *110*, 955-963.

Yamada,K.M. and Miyamoto,S. (1995). Integrin Transmembrane Signaling and Cytoskeletal Control. Curr. Opin. Cell Biol. *7*, 681-689.

Young,R.E., Thompson,R.D., Larbi,K.Y., La,M., Roberts,C.E., Shapiro,S.D., Perretti,M., and Nourshargh,S. (2004). Neutrophil elastase (NE)-deficient mice demonstrate a nonredundant role for NE in neutrophil migration, generation of proinflammatory mediators, and phagocytosis in response to zymosan particles in vivo. J. Immunol. *172*, 4493-4502.

Zhu,J., Nathan,C., Jin,W., Sim,D., Ashcroft,G.S., Wahl,S.M., Lacomis,L., Erdjument-Bromage,H., Tempst,P., Wright,C.D., and Ding,A. (2002). Conversion of proepithelin to epithelins: roles of SLPI and elastase in host defense and wound repair. Cell *111*, 867-878.

7 Abbreviations and Initialisms

AAPV-pNa	Alanine-alanine-proline-valine-p-nitroanilide
ABTS	2,2'-azino-bis(3-ethylbenzthiazoline-6-sulphonic acid)
ADN	Adipsin (also known as complement factor D)
AKH	Adipokinetic hormone
ANCA	Anti-neutrophil cytoplasm autoantibodies
ATP	Adenosinetriphosphate
BB	Blocking buffer
bp	basepair
BSA	Bovine serum albumin
CD	Cluster of differentiation
CG	Cathepsin G
CGD	Chronic granulomatous disease
DHR	Dihydrorhodamine
DIC	Differential interference contrast
DNA	Desoxyribonucleic acid
dNTP	Desoxy-nucleotide-triphosphate
DTNB	5-5′-Dithiobis-2-nitrobenzoic acid
EBM	Endothelial basement membrane
ECL	Enhanced chemiluminescence
EDTA	Ethylen-diamine-tetra-acetate
ELISA	Enzyme linked immunosorbent assay
EtBr	Ethidiumbromide
FACS	Fluorescence activated cell sorting
F-actin	Filamentous actin
FcγR	Fc gamma receptor
FITC	Fluorescein-5-isothiocyanate
GRN	Granulin
H&E	Hematoxylin and eosin
HPF	High power field
hr	hour

HRP	Horseradish peroxidase
i.p.	Intra-peritoneal
i.v.	intravenous
IC	Immune complex
Ig	Immunoglobulin
IL	Interleukin
kb	Kilobase
kD	Kilo Dalton
LN	Laminin
LPS	Lipopolysaccharide
M	Molar
MPA	Microscopic polyangiitis
MPO	Myeloperoxidase
NE	Neutrophil elastase
NET	Neutrophil extracellular trap
nm	Nanometer
NSP	Neutrophil serine protease
OD	Optical density
OVA	Ovalbumin
PBS	Phosphate buffered saline
PCR	Polymerase chain reaction
PFA	Para-formaldehyde
PGRN	Progranulin
Phox	Phagocyte oxidase
PKC	Protein kinase C
PMA	Phorbol 12-myristate 13-acetate
PMN	Polymorphonuclear cell
PMSF	phenylmethanesulphonylfluoride
PR3	Proteinase 3
RNA	Ribonucleinic acid
ROS	Reactive oxygen species
RPA	Reverse, passive Arthus reaction
rpm	Rounds per minute
RT	Room temperature
SD	Standard deviation

SDS-PAGE	sodium dodecyl sulphate polyacrylamide gel electrophoresis
SEM	Standard error of the mean
SN	supernatant
SVV	Small-vessel vasculitis
TLR	Toll-like receptor
TMB	3.3', 5.5'-tetramethylbenzidine
TNFα	Tumor necrosis factor alpha
U	Unit
UV	Ultraviolett
WB	Western blot
WG	Wegener´s granulomatosis
WT	wildtype

8 Curriculum vitae

Kai Kessenbrock
Curriculum vitae
Born October 25, 1978, in Bad Neuenahr near Bonn, Germany

Full name	Kai Alexander Ulrich Kessenbrock
Address	Pfälzer-Wald-Str. 67 81539 München Germany *Phone* +49-89-8578-3589 Kessenbrock@neuro.mpg.de
Languages	German, English, French, Latin (basic)

Education and scientific career

06/98	Abitur, *Peter-Joerres-Gymnasium*, Ahrweiler (Rheinland-Pfalz)
09/98 - 09/99	Zivildienst (alternative service), *Klinik Niederrhein*, Bad Neuenahr
10/99 - 03/01	"Vordiplom" in Biology, *University of Bonn*
04/01 - 10/03	Diploma in Molecular Biology, *University of Heidelberg*
01/02 - 06/02	Research practical at the *Institute of Genetics, University of Heidelberg* in the group of Dr. Martin Blüthner at the department of Prof. Ekkehard Bautz about "Epitope mapping of autoantigens"
07/02 - 12/02	Research practical at the *Biochemie-Zentrum Heidelberg (BZH)* in the laboratory of Prof. Irmgard Sinning supervised by Dr. Matthew Groves about "Recombinant protein expression and X-ray crystallography"
01/03 - 10/03	Diploma thesis about "Characterization of the ribosomal P proteins as autoantigens in Systemic Lupus Erythematodes" carried out at *Pharmacia Diagnostics* (Freiburg im Breisgau, Germany) and *Institute of Genetics* in Heidelberg (Grade A; "sehr gut")
02/04 - present	Ph.D. thesis at the *Max Planck Institute of Neurobiology, Department Neuroimmunology* in Munich about "Neutrophil serine proteases as triggers of inflammation and targets of autoimmunity"

Grants and scholarships

02/04 - present	Ph.D. thesis supported by the DFG (SFB 571: Autoimmune reactions: from manifestations and mechanisms to therapy)
11/07	Travel grant from the *Böhringer Ingelheim Fonds* for a short-term visit (one month) of Prof. Zena Werb´s laboratory at the University of California, San Francsisco (UCSF), USA.
10/08 - 10/11	Post Doctoral Fellowship from the *Susan G. Komen for the Cure* foundation

Awards

03/07	Best scientific work presentation at the 24th winter school on

	proteinases and their inhibitors in Tiers, Italy, 2007.
10/07	Travel Award for the *5th General Meeting of the International Proteolysis Society* in Patras, Greece, 2007 (http://www.ips2007patras.gr/).

Other skills and personal interests

Sport	- Football (Soccer), Basketball, Tennis, Fitness - Outdoor activities like hiking and mountainbiking - Chess
Computer	Proficient in use of PC and Macintosh computer software including statistical, bioinformatical and graphical software
Cultural	Theatre, Opera, Museum, Cinema
Traveling	Visiting friends in different countries and cities including Berlin, Paris, London, Oxford, Stockholm, Madrid, San Francisco, etc.

9 Publications and Meetings

9.1 Presentations at international conferences

Poster presentations:

- Mahler M, **Kessenbrock K**, Raats J, Blüthner M. Epitope-fine mapping of the major C-terminal epitope of the ribosomal P proteins. *6th Dresden Symposium on Autoantibodies*, Dresden, Germany (2002). Abstract published in "*From Proteomics to Molecular Epidemiology: Relevance of Autoantibodies*" Karsten Conrad, Marvin Fritzler, Ulrich Sack, Yehuda Shoenfeld (Eds.) Pabst science publishers (2002).
- **Kessenbrock K**, Fritzler MJ, Mahler M. Structural analysis of the major ribosomal P epitope C22. *9th International Workshop on Autoantibodies and Autoimmunity*, Gainesville, Florida, USA (2005).

Oral presentations:

- Proteinase 3 and neutrophil elastase as triggers of inflammation. *24th International winter school on proteinases and their inhibitors* in Tiers, Italy, 2007. **(Best talk award)**
- Proteinase 3 and neutrophil elastase enhance inflammation by inactivating anti-inflammatory progranulin. *5th General Meeting of the International Proteolysis Society* in Patras, Greece, 2007 **(Abstract selected for oral presentation)**
- Neutrophil serine proteases as triggers of inflammation and targets of autoimmunity. Informal seminar at the *Immunology Graduate Program,* University of California, San Francisco (UCSF), USA, November 2007.
- Autoantibody-mediated release of neutrophil extracellular traps in patients with small-vessel vasculitis. *25th International winter school on proteinases and their inhibitors* in Tiers, Italy, 2008

9.2 Publications in peer-reviewed journals

- Mahler M, **Kessenbrock K**, Raats J, Williams R, Fritzler MJ, Bluthner M. Characterization of the human autoimmune response to the major C-terminal epitope of the ribosomal P proteins. *J. Mol. Med.* **81**:194-204 (2003).
- Mahler M, **Kessenbrock K**, Raats J, Fritzler MJ. Technical and clinical evaluation of anti-ribosomal P protein immunoassays. *J. Clin. Lab. Anal.* **18**:215-23 (2004).
- Mahler M, **Kessenbrock K**, Szmyrka M, Takasaki,Y, Garcia-De La Torre I, Shoenfeld Y, Hiepe F, Shun-le C, von Muhlen CA, Locht H, Hopfl P, Wiik A, Reeves W, Fritzler MJ. International multicenter evaluation of autoantibodies to ribosomal P proteins. *Clin. Vaccine Immunol.* **13**:77-83 (2006).
- **Kessenbrock K**, Fritzler MJ, Groves M, Eissfeller P, von Mühlen CA, Höpfl P, Mahler M. Diverse humoral autoimmunity to the ribosomal P proteins in systemic lupus erythematosus and hepatitis C virus infection. *J. Mol. Med.* **85**, 953-959 (2007). **Ω**
- **Kessenbrock K**, Raijmakers R, Fritzler MJ, Mahler M. Synthetic peptides: The future of patient management in systemic rheumatic diseases? *Curr. Med. Chem.* **14**, 2831-2838 (2007). (Review) **Ω**
- **Kessenbrock K,** Fröhlich L, Sixt M, Lämmermann T, Bateman A, Belaaouaj A, Ring J, Ollert M, Fässler R, Jenne DE. Proteinase 3 and neutrophil elastase enhance inflammation by inactivating antiinflammatory progranulin. *J. Clin. Invest.* **118**, 2438-2447 (2008). **Ω**
  Also see editorials: "In this issue" *J. Clin. Invest.* **118**, 2367 (2008) and "Research Highlights" *Nat. Rev. Immunol.* **8,** 572 (2008).
- Riedl J*, Crevenna AH*, **Kessenbrock K**, Yu JH, Neukirchen D, Bista M, Bradke F, Jenne DE, Holak TA, Werb Z, Sixt M, Wedlich-Soldner R. Lifeact – a novel versatile marker for the visualization of F-actin. *Nat. Meth.* **5**, 605-607 (2008). **Ω**

Manuscripts in preparation:

- **Kessenbrock K,** Brinkmann V, Zychlinsky A, Jenne DE. Autoantibody-induced formation of Neutrophil Extracellular Traps in patients with autoimmune small-vessel vasculitis. In revision *Nat. Med.* **Ω**
- **Kessenbrock K** and Werb Z. The roles of matrix metalloproteinases in the tumor stroma. Invited review for *Cell*, due in December 2008.

Ω these publications resulted from this Ph. D. thesis.

9.3 Editorials and press releases

Parts of the results of this Ph.D. thesis were selected for editorials and press releases:

Web pages and online journals:

http://www.neuro.mpg.de/news_events/download/0806_Jenne_D.pdf

http://www.scienceticker.info/2008/06/24/abwehrzellen-bringen-sich-in-stimmung/

http://www.schattenblick.de/infopool/medizin/fakten/mz2fo848.html

http://www.scinexx.de/wissen-aktuell-8419-2008-06-25.html

from:

MaxPlanckForschung
2/2008 | B20396F
DAS WISSENSCHAFTSMAGAZIN DER MAX-PLANCK-GESELLSCHAFT

BLICKPUNKT

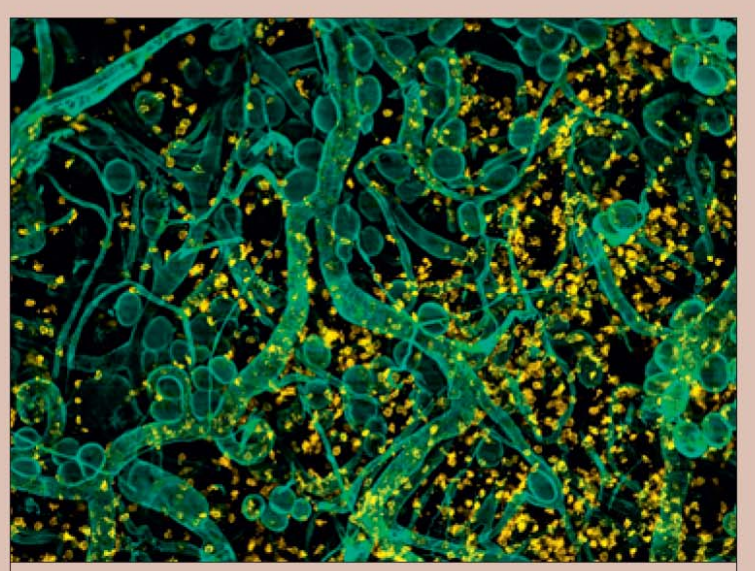

Zersetzende Zellen: Am Ort einer Entzündung wandern neutrophile Granulozyten (gelb gefärbt) aus den Blutgefäßen (blau gefärbt) in das Gewebe ein. Diese neutrophilen Granulozyten stellen die größte Gruppe der weißen Blutkörperchen und bilden im Zug von Abwehrreaktionen des Immunsystems die vorderste Verteidigungslinie: Sie setzen Enzyme frei, die Proteine spalten und auf diese Weise eingedrungene Krankheitserreger zersetzen und unschädlich machen. Ein internationales Team um Dieter Jenne und Kai Kessenbrock vom Martinsrieder Max-Planck-Institut für Neurobiologie hat jetzt herausgefunden, dass Granulozyten auch bei chronischen, nicht durch Infektionen ausgelösten Entzündungen sowie bei Autoimmun-Erkrankungen eine möglicherweise entscheidende Rolle spielen. Denn zwei der von ihnen freigesetzten Enzyme spalten auch ein körpereigenes, entzündungshemmendes Eiweiß und fördern damit chronische Entzündungen, die – etwa bei rheumatischen Erkrankungen – das umgebende Gewebe zerstören. Man hofft, über diese Befunde zu Medikamenten zu gelangen, die den schädigenden Einfluss der neutrophilen Granulozyten bei chronisch-entzündlichen Prozessen unterbinden.

Foto: Max-Planck-Institut für Neurobiologie

MAX-PLANCK-GESELLSCHAFT

from:

nature REVIEWS IMMUNOLOGY

INFLAMMATION

A crucial cut

The neutrophil-derived serine proteases proteinase-3 (encoded by *PRTN3*) and neutrophil elastase (encoded by *ELA2*) are implicated in antibacterial defence, but they also contribute to tissue damage and non-infectious chronic inflammation. A recent study in *The Journal of Clinical Investigation* describes how these enzymes cooperate in the cleavage of the anti-inflammatory factor progranulin, thereby inactivating it and promoting neutrophil activation and inflammation.

The generation of mice lacking both proteinase-3 and neutrophil elastase enabled the authors to explore for the first time the biological relevance of these closely related enzymes. $Prtn3^{-/-}Ela2^{-/-}$ mice developed normal neutrophil populations and, surprisingly, given that these enzymes have been implicated in facilitating cell movement by degrading extracellular matrix components, neutrophil chemotaxis and migration also proved to be unaffected. However, neutrophil infiltration in response to immune-complex deposition (a common occurrence in autoimmune disorders and chronic inflammation) was severely reduced in $Prtn3^{-/-}Ela2^{-/-}$ mice compared with $Ela2^{-/-}$ and wild-type mice. In addition, $Prtn3^{-/-}Ela2^{-/-}$ neutrophils showed impaired production of reactive oxygen species that was induced by tumour-necrosis factor and immune complexes, suggesting a role for these proteases in neutrophil activation.

These observations led the authors to measure the levels of progranulin, a known inhibitor of neutrophil oxidative burst. Importantly, the intact, inhibitory form of progranulin was only found in the supernatants of immune-complex-stimulated $Prtn3^{-/-}Ela2^{-/-}$ neutrophils and not wild-type neutrophils, suggesting that proteinase-3 and neutrophil elastase normally cleave progranulin. The observations that exposure of wild-type neutrophils to recombinant progranulin inhibited their activation; that $Prtn3^{-/-}Ela2^{-/-}$ neutrophils failed to degrade progranulin *in vitro* and *in vivo*; and that treatment of inflammatory lesions with recombinant progranulin reduced neutrophil accumulation in both wild-type and $Prtn3^{-/-}Ela2^{-/-}$ mice are all consistent with an important role for serine-protease-mediated progranulin degradation in neutrophilic inflammation.

So, by eliminating a crucial inhibitory factor, serine proteases pave the way for neutrophil activation, and this supports the potential application of specific serine protease inhibitors as anti-inflammatory agents.

Lucy Bird

ORIGINAL RESEARCH PAPER Kessenbrock, K. *et al.* Proteinase 3 and neutrophil elastase enhance inflammation in mice by inactivating antiinflammatory progranulin. *J. Clin. Invest.* **118**, 2438–2447 (2008)

p572 | doi:10.1038/nri2387

from:

The Journal of Clinical Investigation http://www.jci.org Volume 118 Number 7 July 2008

In this issue

A noninfectious proinflammatory role for neutrophils

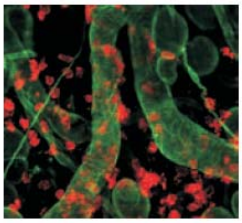

Although neutrophils are best known as one of the first types of cell to respond to invading microorganisms, they also contribute to noninfectious chronic inflammation. One mechanism by which neutrophils mediate host defense is by internalizing microorganisms and degrading them using neutrophil serine proteases (NSPs), but whether NSPs have a role in noninfectious chronic inflammation has not been clearly determined. However, using mice lacking two very similar NSPs, proteinase 3 (PR3) and neutrophil elastase (NE), Kessenbrock and colleagues have now shown that these two NSPs have a crucial role in noninfectious inflammation induced by the subcutaneous formation of antigen-antibody immune complexes (ICs) (pages 2438–2447). When compared with littermate controls, mice lacking NE and PR3 exhibited reduced neutrophil infiltration to subcutaneous sites of IC formation. This was not a generalized defect in neutrophil extravasation to sites of noninfectious inflammation, as neutrophil infiltration in response to application of phorbol esters to the skin was not impaired. Further analysis indicated that NE and PR3 cleaved the antiinflammatory molecule progranulin (PGRN) both in vitro and in vivo and that PGRN administration to wild-type mice inhibited neutrophil infiltration to subcutaneous sites of IC formation. These data led the authors to conclude that NE and PR3 mediate local proinflammatory effects by degrading, and thereby inactivating, PGRN.